17RPT03 DIG-AC
A digital traceability chain for AC voltage and current

Activity A6.1.8

Deliverable D8: Good Practice Guide on traceability of digital dynamic measurements of AC voltage and current

Leader
GUM

Contributors
FER, CEM, CMI, INRIM, IPQ, JV, Metrosert, NPL, PTB TUBITAK, UMA

Due date
May 2022

Delivered
May 2022

Version 2
September 2022

This project 17RPT03 DIG-AC has received funding from the EMPIR programme co-financed by the Participating States and from the European Union's Horizon 2020 research and innovation programme.

The authors

Javier Díaz de Aguilar, Yolanda A. Sanmamed, David Peral
Centro Español de Metrología (CEM), Spain

Martin Šíra
Cesky Metrologicky Institut (CMI)

Damir Ilić
Sveučilište u Zagrebu, Fakultet elektrotehnike i računarstva, Primarni elektromagnetski laboratorij (FER-PEL), Croatia

Witold Rzodkiewicz, Patryk Bruszewski, Grzegorz Sadkowski
Główny Urząd Miar (GUM), Poland

Andrea Sosso
Istituto Nazionale di Ricerca Metrologica (INRIM), Italy

Vitor Cabral, Luís Ribeiro
Instituto Português da Qualidade (IPQ), Portugal

Helge Malmbekk
Justervesenet (JV), Norway

Andrei Pokatilov
Eesti metroloogia keskasutus (Metrosert), Estonia

Jane Ireland, Patrick Reuvekamp, Jonathan Williams
National Physical Laboratory (NPL), United Kingdom

Ralf Behr, Jonas Herick
Physikalisch-Technische Bundesanstalt (PTB), Germany

Tezgül Coşkun Öztürk, Mehedin Arifoviç, Naylan Kanatoğlu
Türkiye Bilimsel ve Teknolojik Araştırma Kurumu (TUBITAK), Turkey

José Ramón Salinas
Universidad de Málaga (UMA), Spain

Table of Contents

Abstract

This Good Practice Guide is intended for both National and Industrial Metrology Laboratories who wish to invest in the development of a quantum standard for alternating voltage based on the Josephson effect. Dynamic electrical measurements are critical in many applications where the RMS (root mean square) value of an electrical signal does not provide the required information and the signal needs to be sampled and processed. At present, NMIs and calibration laboratories provide traceability with high accuracy using thermal converters, but this is limited to AC magnitudes deduced from RMS values. Therefore, the most accurate commercial calibration equipment is also limited to RMS values. Several research projects have developed AC quantum standards to provide traceability for dynamic measurements within some European NMIs. It is now necessary to establish the traceability chain for dynamic electrical measurements to a wider group of NMIs and calibration laboratories. The text in this Good Practice Guide is supported by a comprehensive list of references to material already published in scientific literature.

Foreword

This Good Practice Guide was prepared by the authors withing the 17RPT03 DIG-AC EMPIR project and can be accessed on the project website: https://digac.gum.gov.pl/.

The project 17RPT03 DIG-AC has received funding from the EMPIR programme co-financed by the Participating States and from the European Union's Horizon 2020 research and innovation programme.

1. INTRODUCTION

Josephson junction arrays have been in use as a primary standard for voltage metrology for over 30 years. A number of review articles have been written which summarise the main aspects of the design of junction arrays and their associated measurement systems to form a practical quantum standard of voltage. The development of non-hysteretic junctions paved the way for quantum metrology of dynamic voltages using either programmable arrays of Josephson junctions arranged in a binary sequence or linear arrays of Josephson junctions with a pulse train bias. This Good Practice Guide gives a detailed description of the components and systems required to realise a practical AC quantum voltage standard. It refers extensively to material already available in scientific literature and complements this with practical details and illustrations.

The Table of Contents shows the Sections of this Good Practice Guide. The references are given separately at the end of each Section.

2. REQUIREMENTS FOR DIGITIZER SELECTION AND THE BEST QUANTUM-BASED SYSTEM VERIFICATION APPROACH FOR TESTING DİGİTİZERS

2.1. AC Voltage, Basic Requirements

AC Voltage in LF field is defined to be in the range of 1 mV to 1000 V at a single frequency in the band of 10 Hz to 1 MHz. Best specification of the state-of-the-art electronic instruments (thermal converters not considered) widely used for AC voltage measurements are 24 µV/V (Fluke 5790A), and 43 µV/V (Fluke 5720A). To provide traceability for this range using a digitizer, it is necessary to have basic specifications as:

Range*: 100 mV to 1 V_{rms} @ DC to 1 MHz
Uncertainty: ≤ 25 µV/V @ 1 V, 1 kHz

*For higher voltages (up to 1000 V), digitizer will be combined with suitable dividers developed in the scope of QuADC and other projects. For measurements at low voltages (1 mV to 100 mV) digitizer alone or combined with special amplifiers can be used.

2.2. Parameters used in the selection of digitizers for voltage measurements

Basic parameters required to specify digitizers used for voltage measurements are listed below.

Input Range

Input range, or vertical range, is the peak-to-peak voltage span that a digitizer can measure at the input connector. The simplest interface is to have a single input with a fixed input range matching the ADC of the digitizer. Single fixed input range shifts design work from the digitizer manufacturer (general purpose design) to the end user who needs to care for correct amplification/attenuation by himself (metrology purpose design).

Input Impedance

Input Impedance is defined as the effective resistance and capacitance seen at the input to the digitizer. In general, the higher the input impedance of the digitizer, the less the digitizer will disturb (load) the signal (device) being measured.

Dynamic Range/Resolution

The dynamic range is defined as the ratio between the largest and smallest values that a digitizer can reliably measure. Resolution determines the dynamic range of the digitizer. However, all real digitizers introduce some noise and distortion reducing the ideal number of quantized levels. Effective number of bits (ENOB) is a quality measure of the dynamic performance of a digitizer. ENOB specifies the resolution of an ideal ADC that would have the same resolution as the digitizer being specified.

Frequency Response/Bandwidth

Bandwidth describes the highest frequency sine wave that can be digitized with attenuation to 70.7 % of its original amplitude, also known as the -3 dB point. For sine waves, a bandwidth of greater four to five times the maximum frequency is generally adequate.

Sample Rate

Sample rate is the rate at which the analog-to-digital converter (ADC) in the digitizer is clocked to digitize the incoming signal. According to the Nyquist theorem, to avoid aliasing, the sample rate of a digitizer needs to be at least twice as fast as the highest frequency component in the signal being measured. To

accurately digitize the incoming signal, it is recommended the digitizer's real-time sample rate should be at least three to four times the digitizer's bandwidth.

Accuracy / Uncertainty

Accuracy is the total error with which the digitizer can convert a known voltage, including the effects of quantization error, gain error, offset error, and nonlinearities. Accuracy of digitizers is often specified in time domain and includes static parameters as Gain, Offset, INL and DNL.

Synchronization/Trigger Capabilities

Triggers synchronize data acquisition with external events. Effective use of a digitizer requires great flexibility in device triggering. If digitizer contains more than one channel or multiple single-channel digitizers are used, they should be able to share common triggers and a common clock.

Internal Memory Size

Memory size is important in determining the amount of time a digitizer can sample an analog waveform without interruption. Memory, sample rate and acquisition time of a digitizer are related as:

Acquisition Memory = Time Span x Required Sample Rate.

Other way to increase uninterrupted acquisition is to use digitizers with fast bus technology like PCI Express and PXI Express which are able to sustain multi-GSa/s rates.

Larger memory lets sample at a high rate for a longer period of time to capture more points. More points in signal processing enable averaging which results in lower noise and improved resolution.

Software Compatibility/Drivers

Digitizers should include driver software that supports user operating system and programming language, especially LabVIEW, LabWindows, Matlab and other common software used in metrology applications.

Common Mode Rejection Ability (CMRR)

Common-Mode Rejection Ratio (CMRR) is a measure of the capability of an instrument to reject a signal that is common to both input leads; CMMR / dB = 20 log (Differential Gain / Common Mode Gain). It decreases as frequency of the signal increases. Higher CMRRs are preferable.

In Table 2.1 optimum parameters for a digitizer to be used for AC voltage measurements (as given above) are summarized.

Table 2.1. *Summary of the parameters and their values for a digitizer to be used for AC voltage measurement.*

Parameter	Value
Input Range	1 V_{rms}
Input Impedance	≥1 MΩ
Resolution	≥20 Bits
Bandwidth	5 MHz
Sample Rate	15 MSa/s
Accuracy (Uncertainty)	0.0025 %
Trigger/Clock	Ext Trigger, Ext Clock
Internal Memory	≥1 MB
CMRR	≥100 dB
Software	LabVIEW, LabWindows

2.3. List of available digitizers

List of currently available (and known) digitizers are given in Table 2.2, with information about the resolution, sample rate and available platform.

Table 2.2. *List of available digitizers.*

Manufacturer	Model	Resolution	Sample rate	Platform
Keysight (Agilent/HP)	3458A	28-Bit (DCV)	150 kSa/s (DCV)	Standalone
National Instruments	5922	24-Bit (Max)	15 MSa/s (Max)	PXI
Applicos	WFD22	22-Bit	1 MSa/s	ATX
Zurich Instruments	MF-DIG	16-24-Bit	60 MSa/s	Standalone*
Adlink	PXI-9527	24-Bit	432 kSa/s	PXI
Keithley	DMM7510	18-Bit	1 MSa/s	Standalone
Spectrum GmbH	MX.4963	16-Bit	50 MSa/s	PXI
Astronix Test Systems	PXIe-1803	16-Bit	180 MSa/s	PXIe
VX Instruments	PXD(e)721x	16-Bit	100 MSa/s	PXIe

*Option to ZI Lock-in Amplifier

2.4. List of the test parameters of digitizers for voltage

Most common specifications used to define digitisers for voltage measurements are as follows:

- Input Range
- Input Impedance
- Dynamic Range/Resolution
- Frequency Response/Bandwidth
- Sample Rate
- Accuracy / Uncertainty
- Synchronization/Trigger Capabilities
- Internal Memory Size
- Software Compatibility/Drivers
- Common Mode Rejection Ability (CMRR)

Resolution, sample rate, memory size and software compatibility are rather design parameters used by manufacturer to specify product. On the other hand, input range, input impedance, dynamic range and frequency response are critical when digitisers are used to measure AC voltage. These specifications are expressed by various parameters which should be tested to determine how digitiser is suitable for AC measurements. In Table 2.3. specifications and parameters related to are listed. Parameters describing step response of the digitisers are omitted.

Table 2.3. *Parameters which should be tested to determine how digitiser is suitable for AC measurements.*

Parameter	Test	Test System
Input Range	• Static Offset • Static Gain • Static Gain Drift (Temperature) • Integral non-linearity (INL) • Differential non-linearity (DNL) • Static Gain Stability	PJVS (Static) JAWS (Histogram)
Input Impedance	• Input Impedance	Impedance Analyzer
Dynamic Range	• Signal-to-noise ratio with distortion/ Effective number of bits SINAD/ENOB • Total Harmonic Distortion (THD) • Spurious Free Dynamic Range (SFDR)	JAWS
Frequency Response	• Bandwidth • Dynamic gain, Flatness • Dynamic gain, Level dependence • Dynamic gain, Stability • CMRR • Crosstalk (for 2-ch digitizers):	JAWS PJVS (≤100 kHz)
Synchronization/Trigger Capabilities	• Phase (for 2-ch digitizers)	JAWS

2.5. Test methods for digitizers parameters

Reference [1] extensively describes methods for the testing of the digitiser parameters. Similar methodology is presented in [2] aiming testing of ADCs which are critical part of each digitiser. In Table 2.4 parameters list, related tests and their citing in [1] and [2] are presented.

Table 2.4. *Parameters list, tests and citing in [1] and [2].*

Parameter	Test	Method
Input Range	Static Offset	[1], 6.1, p. 83 [2], 7.4.1 p. 44
	Static Gain	[1], 6.1, p. 83 [2], 7.4.1 p. 44
	Static Gain Drift (Temperature)	Perform static gain test at different environmental temperatures
	Integral non-linearity (INL)	[1], 7.1.2, p. 85 [2], 8.2.1 p. 46
	Differential non-linearity (DNL)	[1], 7.3.2, p. 86 [2], 8.4.1 p. 47

	Static Gain Stability	Repeat static gain test during a specific period*
Impedance	Input Impedance	[1], Chapter 5.1, p. 81 [2], Chapter 7.2.1 p. 44
Dynamic Range	SINAD/ENOB	[1], Chapter 8.1, p. 105 [2], Chapter 9.2, p. 65
	Total Harmonic Distortion (THD)	[1], Chapter 7.7, p. 91 [2], Chapter 8.8, p. 51
	Spurious Free Dynamic Range (SFDR)	[1], Chapter 8.8, p. 112 [2], Chapter 8.8.2, p. 56
Frequency Response	Bandwidth	[1], Chapter 10.1, p. 127 [2], Chapter 11.1, p. 76
	Dynamic gain, Flatness	[1], Chapter 10.2, p. 127 [2], Chapter 11.2, p. 78
	Dynamic gain, Level dependence	[1], Chapter 10.3, p. 128 [2], Chapter 11.3, p. 78
	Dynamic gain, Stability	Repeat dynamic gain test during a specific period*
	CMRR	[1], Chapter 15.2, p. 140 [2], Chapter 14.4.2, p. 96
	Crosstalk (for 2-ch digitizers):	[1], Chapter 11.1, p. 133
Synchronization/Trigger Capabilities		

2.6. Digitizer evaluation

Overview of digitizer evaluation is given in Table 2.5. The meanings of used abbreviations are following:

Input Imp. Input Impedance
Res. Resolution
B Bandwidth
SR Sample Rate
IM Internal Memory
Trig. Trigger
Note: For all models the software NI LabVIEW is applicable.

Table 2.5. *Evaluation of digitizers.*

Model	Input Range	Input Imp.	Res.	B	SR	Trig. / Clock	IM	Other
Adlink PXI-9527	Selectable: ±(0.3 to 40) V	50 Ω/1 MΩ	24 Bit	130 kHz	432 kSa/s (24Bit)	Ext Trig. PXI Clock	2048 S	PXI, 2 ch
Applicos WFD22	Selectable: ±(0.4 to 10) V	1 MΩ	22 Bit	1 MHz	1 MSa/s	Ext Trig. Ext Clock	32 MSa	ATX
Applicos WFD20	Selectable: ±(0.5 to 8) V	1 MΩ	20 Bit	2 MHz	2 MSa/s	Ext Trig. Ext Clock	4 MSa	ATX
Applicos WFD16	Selectable: ±(0.5 to 8) V	50 Ω/1 MΩ	16 Bit	100 MHz	180 MSa/s	Ext Trig. Ext Clock	8 MSa	ATX
Astronix PXIe-1803	Selectable: ±(0.5 to 30) V	50Ω/1MΩ	16 Bit	175 MHz	180 MSa/s	Ext Trig. Ext Clock	64 MSa	PXIe, 2 ch
Keithley DMM7510	Selectable: ±(0.1 to 1000) V	10GΩ/10MΩ	18 Bit	600 kHz	1 MSa/s	Ext Trig. Ext Clock	8 MSa	Standalone
Keysight 3458A	Selectable: ±(0.1–1000) V	10GΩ	28 Bit	150 kHz	1 MSa/s	Ext Trig. Ext Clock(m)	48 kSa	Standalone
NI 5922	Selectable: ±(2, 10) V	50Ω/1MΩ	24 Bit	6 MHz	15 MSa/s	Ext Trig. Ext Clock	64 MSa/ch	PXI, 2 ch
NI 9225	300 V	1MΩ	24 Bit	25 kHz	50 kSa/s	--	--	NI CompactRio
Spectrum MX.4963	Selectable: ±(0.2 to 10) V	50Ω/1MΩ	16 Bit	30 MHz	50 MSa/s	Ext Trig. Ext Clock	64 MSa/ch	Standalone, 4 ch
Tasler LTT24	Selectable: ±(0.3 to 50) V	50Ω/1MΩ	24 Bit	1.7 MHz	4 MSa/s	Ext Trig. Ext Clock	32 MSa/ch	Standalone, 4 ch
VX Instruments PXD(e)721x	Selectable: ±(0.25 to 60) V	50Ω/1MΩ	16 Bit	100 MHz	100 MSa/s	Ext Trig. PXI Clock	2 MSa	PXIe, 2 ch
Zurich Instr. MF-DIG	Selectable: ±(0.001 to 3) V	50Ω/1MΩ	24 Bit	7 MHz	60 MSa/s	Ext Trig. Ext Clock	2.5 MSa/ch	Standalone 2 ch

Useful notes for selection of the digitizers:

Resolution – Sample rate

Two most important specifications of the digitizer are resolution and sample rate. While resolution determines the precision of the amplitude measurements, sample rate determines the bandwidth. These two parameters are not independent, increasing the resolution causes decreasing the bandwidth. In the case both specifications cannot be satisfied, depending on the application trade-offs can be made. Digitizers for measurement of low distorted AC voltage can be adjusted to sample at a rate only slightly higher than twice the frequency of the signal. On the other hand, for measurement of the distorted signals (harmonics) sample rate should be set to twice of the largest frequency component of the interest.

Accuracy – Resolution

Resolution and Accuracy are terms that are often interchanged when the performance of a digitizer is discussed. Resolution does not imply but only indicates what the theoretical accuracy can be.
The accuracy of the digitizer determines how close the actual digital output is to the theoretically expected digital output for a given analog input. In other words, how close a digitizer comes to meeting its theoretical resolution. If specified by manufacturer accuracy of a digitizer is often defined in time domain, where specifications are static (DC). Despite these figures still can be used at low frequencies (up to several kilohertz, depending on the bandwidth of the digitizer), accuracy at higher frequencies should be related to dynamic parameters.

Resolution – Dynamic range

High-resolution digitizer is preferred when small signals are measured. As an example, with a vertical range of 1 V, the 8 bit digitizer cannot ideally resolve voltage differences smaller than 3.92 mV; while a 16 bit digitizer, with 65656 discrete levels, can ideally resolve voltage differences as small as 15 µV.
Digitizers intended to be used in the scope of this project should have minimum 10:1 dynamic ratio. If such a digitizer with full scale of 1 V is used to measure Fluke 5720A calibrator whose AC voltage specification at 100 mV @ 1 kHz is 135 µV/V, targeted error is $135 \times 10^{-6} \times 100\ mV = 13.5\ \mu V$. In that case digitizer needs to resolve 13.5 µV out of 1 V, which would require 17 bit ENOB. This probably will not be enough if digitizer does not also have the good noise floor.

Measurement Conditions – Dynamic range

It is very important to match the amplitude of the test signal to digitizer range. For example, if 1.4 V is applied to a 3 V & 16 bit digitizer, loss in ENOB will be 1 bit. For the best accuracy, amplitude of the reference system should be equal or higher than digitizer range. The similar situation is when digitizer is going to be used with auxiliary equipment like shunts, dividers or external amplifiers; for best accuracy the range in which the auxiliary equipment will be used should match the digitizer range.

ADC Architecture

Digitizers based on integrating analog-to-digital converters (IADC) provide high resolution with good noise rejection. The main disadvantage is they are slow and can be used at low frequencies (up to hundreds Hz), making them ideal for LF power applications. On the other hand, Delta-Sigma (ΔΣ) type ADCs provides high resolution with relatively wide bandwidth. It is possible to combine different types of digitizers to cover frequency band of interest.

Isolation and CMRR

Common mode rejection of the digitizer gets important when used to measure outputs of shunts or voltage dividers. When high CMRR is required digitizer with differential inputs or platform powered with battery is recommended.

2.7. Recommendation of the digitizers for evaluation

According to the parameters of the digitizers specified by their manufacturers, we can classify them into 3 groups:

1. National Instruments 5922, Tasler LTT24, Applicos WFD20/22, Zurich Inst. MF-DIG. This group has the best resolution – bandwidth performances and seems to be most suitable for evaluation during the project.
2. Astronix PXIe-1803, Applicos WFD16, VX Instruments PXD(e)721x, Spectrum MX.4963 This group has fair resolution and large bandwidth. Those digitizers whose bandwidth can be traded for resolution may be interesting for evaluation.
3. Keysight 3458A, Keithley 7510. These digitizers are ideal for low frequency applications. Although extensively studied for almost three decades (3458A) it is desirable to have it included for evaluation during the project.

2.8. Using Quantum Voltage Standards in digitiser testing

Quantum voltage standards are intrinsic standards, based on Josephson Effect, and generate voltages that are defined only by fundamental constants (namely *e* and *h*). They have been used and constantly improved over the last 40 years, and greatly increased the accuracy of the electrical measurements. Early Josephson standards, also named conventional, are suitable only for DC voltage measurements due to hysteretic behaviour of their junctions. However, recent improvements of the arrays led to the new types of quantum standards which can be used for AC measurements, as well: Programmable Josephson Voltage Standard (PJVS) and pulse driven, also known as Josephson Arbitrary Waveform Synthesizer (JAWS).

Programmable Josephson Voltage Standard

PJVS are based on using binary-divided arrays of damped Josephson junctions which can produce stable DC voltages, or stepwise AC waveforms. As the steps of the generated waveform are intrinsic, quantum voltages, PJVS is an ideal digital-to-analogue converter (DAC) [3]. Accuracy of rms value and frequency range of PJVS is limited due to the transition time between steps, as well due to the transients. Recent developed PJVSs can produce DC voltages up to 10 V amplitude, and 7 V_{rms} AC stepwise AC waveforms used up to several kilohertz by differential sampling [4], and possibly up to 100 kHz by sub-sampling [5].

PJVS is very suitable for DC static tests of the digitisers like gain, INL, DNL, and for dynamic tests using fast settling features of PJVS [6-10].

Josephson Arbitrary Waveform Synthesizer (JAWS)

In JAWS, RF excitation of the array is performed by periodic streams of pulses instead of sinewaves [10]. The time integral of each junction's voltage pulse is quantized in units of *h*/*2e*. So, the arrays behave as perfect pulse quantisers and can generate arbitrary voltage waveforms that are accurate and predictable. Recent developed JAWS can produce rms voltages up to 3 V for the frequencies up to 1 MHz. As JAWS can produce complex signals it is very suitable for dynamic tests and frequency response of the digitisers up to 1 MHz [15]. In addition, JAWS can be used for testing static parameters of the digitisers with statistical method (histogram). Furthermore, it still can be used as DC reference for calibration of the static parameters of the digitisers. State of the art of PJVS and JAWS are summarized in Table 2.6.

Table 2.6. *State of the art of PJVS and JAWS.*

Parameter	Programmable Josephson Voltage Standard (PJVS)	Josephson Arbitrary Waveform Synthesizer (JAWS)
Voltage Range	±10 V, 7 V_{rms}	1 V_{rms} (PTB) 3 V_{rms} (NIST)
Frequency	DC to 100 kHz*	DC to 1 MHz
Accuracy	DC: ±10 V, $\Delta V/V_{10V} = 1\times10^{-10}$ AC: $\Delta V/V = 5\times10^{-7}$ @ V ≤ 7.1 V_{rms} ≤ 1 kHz, 1 min meas. time** Limit of calibrator, otherwise 1×10^{-8}	Best; 12 nV/V @ 250 Hz
SFDR	-	120 dBc
Synchronization	Yes	Yes
Advantages	• Relatively high output • Suitable for differential sampling	• Arbitrary signals • Very high signal purity • Suitable as Synthesizer
Drawbacks	• AC_{rms} not calculable	

* Differential sampling up to 10 kHz and sub-sampling up to 100 kHz

** Fluke 5720A ACV calibration

Table 2.7 provides a cross-section of the parameters of the digitiser and the quantum voltage standards suitable for their testing. Rows marked with yellow colour show parameters which need to be measured due to the calculation of uncertainty. Rows marked with green colour show parameters which need to be measured for the determination of corrections that will be applied on the measured values.

Table 2.7. *Overview of the digitizer parameters and possibilities of quantum voltage standards to be used for their measurements; other explanations are given in the text above.*

Parameter	PJVS	JAWS
Static Offset	√	√ (2)
Static Gain	√	√ (2)
Static Gain Drift (Temperature)	√	√ (2)
Integral non-linearity (INL)	√	√ (2)
Differential non-linearity (DNL)	√	√ (2)
Static Gain Stability	√	√ (2)
SINAD/ENOB	√ (1)	√
Total Harmonic Distortion (THD)	√ (1)	√
Spurious Free Dynamic Range (SFDR)	√ (1)	√
Bandwidth	√ (1)	√
Dynamic gain, Flatness	√ (1)	√
Dynamic gain, Level dependence	√ (1)	√
Dynamic gain, Stability	√ (1)	√
CMRR	√ (1)	√
Crosstalk (for 2-ch digitisers)	√ (1)	√

(1) up to 100 kHz using sub-sampling technique
(2) either in DC mode or using statistical method

2.9. Conclusion

Table 2.7 gives the information about the **parameters of the digitiser and the quantum voltage standards suitable for their testing**. Important rows are marked with **yellow** colour, meaning that these parameters need to be measured due to the calculation of uncertainty, while rows marked with **green** colour pointed parameters which need to be measured for the determination of corrections that will be applied on the measured values. Both these groups of parameters are important and have priority in the plans for verification. However, it does not mean that other parameters cannot be measured, as appropriate, or are of interest for testing, comparison of results, or gathering experience.

Based also on the (i) recommendation given in section 8 of the deliverable D1, (ii) existing equipment available to the partners nowadays, and (iii) that new digitiser Fluke 8588A came just recently on the market and possibly would be important for NMIs, DIs and calibration laboratories, the conclusion of the partners is that the following 3 digitisers would be of the highest interest to be validate in WP4. These are:

1. National Instruments 5922
2. Keysight (Agilent, HP) 3458A
3. Fluke 8588A

However, it does not mean that other digitisers cannot be tested and validated, as appropriate, or are of interest for testing, comparison of results, or gathering experience.

2.10. References

[1] IEEE Standard for Digitizing Waveform Recorders

[2] IEEE Standard for Terminology and Test Methods for Analog-to-Digital Converters

[3] C. A. Hamilton, C. J. Burroughs, and R. L. Kautz: “Josephson D/A converter with fundamental accuracy”, IEEE Trans. Instrum. Meas., vol. 44, pp. 223–225, 1995.

[4] R. Behr, L. Palafox, G. Ramm, H. Moser, and J. Melcher: “Direct comparison of Josephson waveforms using an AC quantum voltmeter”, IEEE Trans. Instrum. Meas., vol. 56, no. 2, pp. 235–238, Apr. 2007.

[5] W. G. K. Ihlenfeld, R.P. Landim: “Investigations on extending the frequency range of PJVS based AC voltage calibrations by coherent subsampling”, Conference on Precision Electromagnetic Measurements, Ottawa, Canada, July 2016.

[6] W. G. K. Ihlenfeld, E. Mohns, R. Behr, J. Williams, P. Patel, G. Ramm, and H. Bachmair: “Characterization of a high resolution analog-to-digital converter with a Josephson AC voltage source”, IEEE Trans. Instrum. Meas., vol. 54, no. 2, pp. 649–652, Apr. 2005.

[7] R. Iuzzolino, L. Palafox, W. G. K. Ihlenfeld, E. Mohns, and C. Brendel: “Design and characterization of a sampling system based on Σ–Δ analog-to-digital converters for electrical metrology”, IEEE Trans. Instrum. Meas., vol. 58, no. 4, pp. 786–790, Apr. 2009.

[8] F. Overney, A. Rufenacht, J.-P. Braun, B. Jeanneret, P. S. Wright: “Characterization of Metrological Grade Analog-to-Digital Converters Using a Programmable Josephson Voltage Standard”, IEEE Trans. Instrum. Meas., vol. 60, no. 7, pp. 2172–2177, July 2011.

[9] G. Rietveld, D. Zhao, C. Kramer, E. Houtzager, O. Kristensen, C. de Leffe, and T. Lippert: “Characterization of a wideband digitizer for power measurements up to 1 MHz”, IEEE Trans. Instrum. Meas., vol. 60, no. 7, pp. 2195–2201, July 2011.

[10] S. P. Benz, and C. A. Hamilton: “A pulse-driven programmable Josephson voltage standard”, Appl. Phys. Lett., vol. 68, pp. 3171–3173, 1996.

[11] P. D. Dresselhaus, M. M. Elsbury, D. Olaya, C. J. Burroughs, and S. P. Benz: “10 volt programmable Josephson voltage standard circuits using NbSi-barrier junctions”, IEEE Trans. Appl. Supercond., vol. 21, no. 3, pp. 693–696, June 2011.

[12] J. Lee, R. Behr, L. Palafox, M. Schubert, M. Starkloff, and A. C. Böck: “An ac quantum voltmeter based on a 10 V programmable Josephson array”, Metrologia, vol. 50, pp. 612–622, 2013.

[13] N. Flowers-Jacobs, A. Rüfenacht, A. E. Fox, S. B. Waltman, J. Brevik, and S. P. Benz: “Three Volt Pulse-Driven Josephson Arbitrary Waveform Synthesizer”, Conference on Precision Electromagnetic Measurements, Paris, France, July 2018.

[14] O. F. Kieler, R. Behr, R. Wendisch, S. Bauer, L. Palafox, and J. Kohlmann: “Towards a 1 V Josephson Arbitrary Waveform Synthesizer”, IEEE Applied Superconductivity, vol. 25, issue 3, June 2015.

[15] M. Šíra, O. Kieler, R. Behr: “A Novel Method for Calibration of ADC Using JAWS”, IEEE Trans. Instrum. Meas., vol. 68, issue 6, June 2019.

3. SCALING GUIDELINES FOR TRACEABLE DYNAMIC SGNALS

3.1. Introduction

The aim of this work is to provide a practical guideline for implementing measurement systems employing digital techniques in step-up and step-down procedures involving electrical current and voltage and starting with a Josephson standard as the fundamental reference. The main target addressed by this guide is clearly represented by researcher's techniques working in National Metrological Institutes (NMIs), considering in particular the needs for steering toward digital techniques in European NMIs.

The discussion starts with an overview of the state-of-the-art of scaling techniques, analysed as a common starting point for building a new quantum traceable and digital-ready European traceability chain. How to move from a measurement system based on traditional scaling methodologies toward digital-based solutions is the topic of the second section, where a main part is devoted to issues related to the digitizer selection. The field of digital scaling is still open and various solutions have been proposed in the literature; a discussion on the various possibilities for implementing a practical solution considering these proposals is presented in the subsequent section, then a solution based on integration of analog scaling techniques with digitizers is suggested as the most viable option. In the last section, some specific uncertainty contributions that arise switching to digital are presented and analysed in detail in relation with the analog to digital conversion architectures.

Brand and model names may be used in the following for identification purposes. Such use is intended to represent a generic class of instruments and implies neither endorsement by the authors nor assurance that the equipment is the best available.

3.2. Scaling techniques currently in use

Scaling methods are widely used in NMIs to cover the wide ranges of calibration services offered. Implementing a new digital based scaling method starting form already used techniques has several advantages, like better integration of previous know-how; smoother process; reuse of instrumentation; cost savings.

An overview of the scaling techniques, both upward and downward, currently used by the DIG-AC project participating institutes was presented in [1] and provides information to completely describe the state of art in Europe. Overall, nine NMI&DIs, including the main institutes in Europe, contributed to this analysis that presents a synthetic overview of the techniques adopted in the laboratories of: FER, INRIM, CEM, Metrosert, PTB, TUBITAK, IPQ, and NPL. The methods used in these NMI&DIs to scale AC voltage and currents over the whole of range of calibration values were summarized in this report.

To summarize the outcome, noticeably, with just a few laboratories starting research on digitally based methods, in all institutes involved only techniques based on classical thermal standards are used on a regular basis for AC measurements of voltage and currents and over all ranges. Exceptions exist when lower accuracy calibrations are considered. The methods developed for scaling are then always built around the thermal converter, to extend its operating range. To that aim, solutions used by different institutes may vary.

Exploiting the capability of a commercial multi-range commercial semiconductor thermal converter (Fluke 792A) is a viable option, provided a suitable calibration service is available, as does GUM with PTB. Otherwise, the exploitation of converters with increasing but partly overlapping ranges, makes it possible to implement a voltage step-up procedure, as done for instance by PTB, CEM, IPQ, NPL and INRIM. However, resistive techniques are the most widely used for voltage scaling: with resistive dividers in step-down setups as performed, e.g., by FER, Metrosert, CEM and NPL; with range

extenders in step-up procedures, as in the case of: PTB, TUBITAK, GUM, IPQ, INRIM. Solutions based on active circuits and dedicated amplifiers are adopted in a few cases. With regard to ranges, the lowest value is typically down to a millivolt, but it can be as high as hundreds of millivolts for some institutes. Greater uniformity is observed in high values, always upper bounded to one kilovolt. Uncertainties vary significantly with value and signal frequency: best results reported, close to 1 kHz and 1 V, are some μV/V (CEM, NPL) and below 1 μV/V (INRIM); at the lower and upper boundaries and frequencies above 100 kHz, figures in excess of 100 μV/V are typical (TUBITAK, PTB).

For current scaling, thermal converters are generally used in voltage mode, with two possibilities to implement current-voltage conversion: shunts used, for instance, by FER, PTB, Metrosert; or transconductance amplifiers, adopted, e.g., by NRIM and CEM. In current calibrations the lowest frequency value of 10 Hz is the same in all laboratories whereas the highest frequency is generally 10 kHz (FER, GUM, Metrosert), but can be as high as 100 kHz in some cases (NPL, IPQ). Measurement range extends from about 10 μA up to 20 A typically, with the exception of CEM that reports 100 A and PTB that goes up to 160 A. Uncertainties vary from about 20 μA/A, close to 10 mA and with frequencies around 1 kHz, up to several hundred μA/A at the upper range values.

3.3. Moving toward digital based scaling methods

The very successful results of the application of a purely digital solution, namely the extremely high intrinsic linearity of AD converters, to scaling DC quantities suggest, quite naturally, the possibility of its extension to the AC regime. But technical limitations change the landscape in AC, where the performances of ADCs degrade as frequency increase, according to the law: “more speed means less resolution” [2]. This general rule holds true for all conversion technologies and in particular for the two most widely used in metrological labs: integrating and sigma-delta. Besides this main classes one has to choose among the several options for the core element of the system: the digitizer.

3.3.1. Selecting digital scaling range

A fundamental issue in programming digital based scaling setups is the definition of the proper range of values over which scaling is required or useful or advisable, based on customers’ needs, economic and technical issues. In that regard, it is preferable to subdivide voltage and current, since they necessarily involve different measurement methods, then consider for both upscaling and downscaling methods, to highlight specific issues with measurements at small and high values of the range. Balancing all terms, like technical complexities and values typically required for calibrations, it seems advisable to consider the range form 10 mV to 100 V as the best compromise for a digital scaling in voltage calibrations. This subdivision is somewhat less defined with currents, due to the “shift” of the typical reference point down to a very low value within the range, leaving little room for the downscaling interval. However, an analysis to evaluate the relevant parameters as done for voltage gives for current the 10 mA to 1 A range as the preferred solution, in implementing digital based scaling for most NMI calibration needs.

3.3.2. Selecting the digitizer

A detailed report is available, published as DIG-AC deliverable, to discuss how to select the digitizer that best suits the needs of a digital traceability chain [3]. Considering the previous selection of voltage ranges it is shown there that the operating range for such a digitizer is required to be 100 mV to 1 V_{rms}. About frequency, taking into account that AC voltage in LF field is defined to be in the range of 1 mV to 1000 V at a single frequency in the band of 10 Hz to 1 MHz one can derive a suitable bandwidth of the digitizer to be from DC to 1 MHz.

Resolution, sample rate, memory size and software compatibility are design parameters that may be used by manufacturer to specify product. On the other hand, input range, input impedance, dynamic range and frequency response are critical when digitisers are used to measure AC voltage. These specifications are expressed by various parameters which should be tested in order to determine how digitiser is suitable for AC measurements.

Most common specifications used to define digitisers for voltage measurements are listed here:

- Input Range/Impedance/Common Mode Rejection Ratio (CMRR)
- Dynamic Range/Resolution
- Frequency Response/Bandwidth/Sample Rate
- Accuracy/Uncertainty
- Synchronization/Trigger Capabilities
- Internal Memory Size
- Software Compatibility/Drivers

On the other side, several tests are defined in normative documents [4],[5], that allow to characterize all aspects of a digitizer, if required by special needs, when typical specifications are not sufficient. Test parameters that may be relevant for the applications discussed here include:

- Static Offset
- Static Gain
- Static Gain Drift (Temperature)
- Integral non-linearity (INL)
- Differential non-linearity (DNL)
- Static Gain Stability
- Input Impedance
- Signal-to-noise ratio with distortion/ Effective number of bits SINAD/ENOB
- Total Harmonic Distortion (THD)
- Spurious Free Dynamic Range (SFDR)
- Bandwidth
- Dynamic gain, Flatness
- Dynamic gain, Level dependence
- Dynamic gain, Stability
- CMRR
- Crosstalk (for 2-ch digitisers): · Phase (for 2-ch digitisers)

Very specific requirements are set on the digitizer by the peculiarities of signals at the output of quantum voltage standards. Quantum voltage standards are intrinsic standards, based on the Josephson Effect, which generate voltages linked to fundamental constants. Recent types of quantum standards can be used for AC measurements. They are: Programmable Josephson Voltage Standard (PJVS) and pulse driven, also known as Josephson Arbitrary Waveform Synthesizer (JAWS).

PJVS are based using binary-divided arrays of damped Josephson junctions which can produce bias selectable stable DC voltages, or stepwise AC waveforms. As the steps of the generated waveform are intrinsic, quantum voltages, PJVS is an ideal digital-to-analogue converter (DAC) [6]. Accuracy of rms value and frequency range of PJVS is limited due to the transition time between steps, as well due to the transients. Recent developed PJVSs can produce DC voltages up to 10 V amplitude, and 7 V rms AC stepwise AC waveforms used up to several kilohertz by differential sampling [7], and possibly up to 100 kHz by sub-sampling [8]. PJVS is very suitable for DC static tests of the digitisers like gain, INL, DNL, and for dynamic tests using fast settling features of PJVS [9]-[12].

In JAWS, rf excitation of the array is performed by periodic streams of pulses instead of sinewaves [13]. The time integral of each junction's voltage pulse is quantized in units of h/2e. So, the arrays behave as perfect pulse quantisers and can generate arbitrary voltage waveforms that are accurate and predictable. Recent developed JAWS can produce rms voltages up to 3 V for the frequencies up to 1 MHz. As JAWS can produce complex signals it is very suitable for dynamic tests and frequency response of the digitisers up to 1 MHz [15]. In addition, JAWS can be used for testing static parameters of the digitisers with statistical method (histogram) [15]. Furthermore, it still can be used as DC reference for calibration of the static parameters of the digitisers.

Obviously, to make it worthwhile to calibrate a digitizer against a quantum standard, the converter must be the highest quality available.

To summarize, from the previous analysis, one can derive the following selection of candidates for analog-to-digital conversion in a digital quantum traceable AC metrological measurement system. Based on conversion architecture, we can classify them into 3 groups:

- **Best for low frequency applications** - Keysight 3458A, Keithley 7510
- **Best resolution-bandwidth** - National Instruments 5922, Tasler LTT24, Applicos WFD20/22, Zurich Inst. MF-DIG
- **Bandwidth/resolution trade-off** - Astronix PXIe-1803, Applicos WFD16, VX Instruments PXD(e)721x, Spectrum MX.4963hundred µA/A at the upper range values.

3.4. Configurations for digital based scaling systems

The idea of using direct digital techniques has been very successfully applied in the DC regime already several years ago. The method is based on the possibility, shown in [16], of taking advantage of some particular Digital Volt Meters (DVM's) characteristics like short term stability, resolution and linearity and use them as high accuracy standards, to replace the traditional ones like resistance bridges and resistive dividers in many applications as DC voltage reference comparison, resistance comparison and step-up, as well as evaluation of attenuation/amplification ratios.

A preliminary survey among DIG-AC project participants, showed that a rather small part of calibrations is based on sampling and almost none on digital techniques for voltage/current scaling. This is in general a quite surprising outcome, considering the central role of digital instrumentation in measurements, yet the idea supporting DIG-AC, namely that research in electrical quantum standards should focus on the development of digital-ready techniques is further motivated by this result. Besides this, it is clear that integration of analog and digital techniques can be considered the best way to cover the relevant calibration ranges. In setting up a new digital-based scaling then laboratories still have several options to consider. We'll describe some possibilities presented in the literature that are suited for the purpose.

The results published by PTB researchers for scaling in power calibrations [17] are particularly interesting since they involve the two quantities discussed here: voltage and current. In this setup, these are both obtained from accurate DACs; for voltage, scaling is done by means of an amplifier, whose output amplitude is traceable being measured by a DVM, followed by a high accuracy transformer rising final amplitude to 120 V; similarly for current, conversion is made by means of a transconductance amplifier, followed by a precision current transformer yielding 5 A at the output. The uncertainties obtained with this system is of the order of a few parts in 10^{-6} for both voltage and current.

Otherwise, a remarkably ambitious target was set for quantum-traceable voltage scaling in QuADC project [18]. The plan was to scale quantum waveforms up to 1 kV using voltage dividers or amplifiers, making it possible to connect the divider output directly with a Josephson based digitizing system (to be developed as part of the project). Traceability of higher voltage waveforms the Josephson volt was foreseen, with uncertainties ranging from 5 µV/V at 1 kV (50 Hz) to 25 µV/V at 120 V (100 kHz). A new prototype divider using the split guard technique has been constructed and a buffer amplifier was developed at CMI to support voltage dividers operation by minimizing loading effects. The target was not fully attained, however, also due to the complexity of the quantum part of the setup for sampling and digitizing voltage signals using a real-time feedback loop that involves a Josephson array.

An interesting example of DVM and traditional dividers integration is provided by a method developed at Metrosert where the DVM and the divider are considered as a "black box" and calibrated together, with the divider connected directly to the DVM inputs to improve repeatability. With this method, both step-up and step-down scaling are feasible, and AC voltage calibrations attaining 50 µV/V accuracies up to 5 kHz frequencies were demonstrated.

The approach tackled in [19] allows to calibrate currents with traceability to a quantum standard by means of a shunt resistor, with stable results up to 1 kHz. The shunt can be taken as scaling element here; by means of three different resistors the ranges: 20 mA, 200 mA and 2 A can be covered and the output of commercial calibrators that generate currents up to the typical value of 2.2 A can be calibrated.

From the previous analysis of methods available for scaling, it seems clear that the most viable and straightforward way to implement a digital-based scaling setup for AC signals is to adopt traditional analog, scaling techniques and integrate with digitizers operating in the highest accuracy ranges. As reported in [1] these are primarily: thermal-converter based, and voltage-divider based.

3.5. Selection of divider for wide range scaling the digitizer

High quality voltage scaling devices, which are wide band, linear time invariant, insensitive to environment conditions and have low level dependence, are necessary to scale up quantum waveform measurement accuracy. Traceability and ratio measurement uncertainty is another issue that should be taken into account while evaluating the dividers.

The lowest uncertainty is obtained in DC Voltage metrology where resistive voltage dividers are used to scale up and down [1]. Such dividers are almost insensitive to environment conditions while the divider architecture is the main constraint for the accuracy of the ratio. Generally, two terminal dividers consisting of one terminal for input and one terminal for output take traceability from another divider or another measuring and/or sourcing standard, so such dividers cannot be a primary standard [2]. The exception is a divider based on Hamon] resistance which also has two terminals but is based on adjusting the input resistors to be equal to 10 or 100 times of output resistor where just two ratios are available [3].

The dividers called absolute dividers [4] consist of equal successive resistance sections connected serially and have corresponding terminals. Divider ratio is based on adjusting/measuring successive resistance sections compared to output resistance. Dividers of this architecture do not take any traceability from other device and are primary voltage scaling devices for DC voltage metrology. Their calibration uncertainty is 0.2 µV/V range if power coefficients are omitted. Kelvin Varley type dividers [5] consist of cascaded absolute dividers that are originally designed for comparisons of voltage standards. They have poor performance at high voltages as their calibration is made at low voltages and power coefficient cannot be neglected. Primary dividers used for DC Voltage scaling have very large output resistance, more than 10 kΩ. The AC-DC difference of the divider [6] is measured and it is large even at frequencies below 50 Hz more over is not flat, so these dividers are not suitable for use in AC voltage or waveform scaling measurements.

The current AC voltage scale is based on Thermal Transfer Techniques (TTT) and DC voltage calibration described in detail in [7]. Range resistors connected serially to TVC have low AC-DC difference. Combining these resistors with cage AC-DC current shunts [8], which also have low AC-DC difference, is another opportunity to construct a ratio device for waveform measurements. Such a divider is two terminal devices, its DC ratio is nominally far away from primary devices so direct comparison to a reference divider is not sensible. Its DC voltage ratio measurement uncertainty is about 1.5 µV/V and its AC-DC Difference measurement uncertainty may change from 5.0 µV/V to 6.5 µV/V in the frequency range 10 Hz to 100 kHz [9]. After all AC ratio measurement uncertainty of such divider varies from 5.2 µV/V to 6.6 µV/V. The problem of this divider is its sensitivity to environment conditions. A divider consisting of a range resistor and a shunt with ratio 131.92 V/V is tested in a temperature chamber and the temperature of the environment is set 18 °C, 23 °C and 28 °C respectively. Temperature coefficient of ratio is measured to be about 47 (µV/V)/°C. This coefficient is too large the divider to be used in laboratory environment where temperature varies +/- 1°C.

Two terminal dividers are used extensively in electrical power metrology [10]. These dividers have low phase shift and low AC-DC difference that makes possible to achieve low calibration uncertainty at AC Voltage.[10] Their output is fixed, and their ratios are nominally different from primary ratio devices so direct comparison to a reference DC divider is not possible. Its DC voltage ratio measurement uncertainty is nearly 1.5 µV/V, and its AC-DC difference measurement uncertainty will change from 5.0 µV/V to 6.5 µV/V in the 10 Hz to 100 kHz frequency range [9]. Also, their sensitivity to environment conditions is expected to be low.

Inductive Voltage Dividers (IVD) are suitable to be used as ratio devices for AC Voltage metrology [11, 12, 13]. These dividers consist of equal successive inductance sections connected serially. Because of

their architecture these dividers do not take traceability from any other standard. The core inside IVD has a saturation coefficient which is dependent to the core material. Taking into account saturation coefficient (0.35 V/Hz) the maximum voltage level at power frequencies is around 20 V. Recently dividers that go up to 1000 V at 40 Hz to 1 kHz range are presented [14]. The errors of these dividers are often declared in ppm of input giving very low figures, but when calculated relative to the output voltage the ratio uncertainty is about 1 µV/V @ 40 Hz to 7 µV/V @ 1 kHz and still can compete with ratio uncertainty obtained by TTTs. Another question is how these dividers behave under multi-harmonic waveforms. Their classical calibration is based on locking the system to a single frequency. Now, IVD response to harmonics is being investigated in TÜBİTAK UME by applying harmonically related 5 tones with amplitude and phase relation as in previous Q-Wave comparison [15].

Recently, new types of dividers with architecture similar to absolute divider are being investigated [16, 17, 18]. Divider with ratio 5 V/V (50 V / 10 V) and improved AC-DC difference up to 1 kHz (<3 ppm) [19] is manufactured by TÜBİTAK UME. Its DC ratio is measured with 0.2 µV/V uncertainty and power coefficient (level dependence) is measured to be less than 0.5 µV/V at DC. It has been observed that variation of temperature or humidity (of 10 °C and 40 % rh) does not influence noticeable change in divider performance up to 10 kHz [19]. Dividers with the same architecture and resistive elements and with ratios 10 V/V (100 V / 10 V) and 100 V/V (400 V / 4 V) are manufactured. Measurements with AC measurement Standard show that AC-DC difference is flat and less than 10 ppm up to 1 kHz and 100 Hz respectively for the dividers with ratios 10 V/V and 100 V/V.

A two-terminal divider with nominal ratio 101 V/V (190 V / 1.88 V) is also manufactured. The divider architecture is similar to those presented in [18]. Measurement results indicate that AC-DC difference is flat and less than 10 ppm up to 10 kHz.

3.6. Integration of digital voltmeters and dividers for scaling

In order study application of two digital voltmeters in the sampling mode for the voltage ratio measurement, a setup consisting of two sampling multimeters 8588A and a set of precision resistive voltage dividers was composed. For measurements in a step-up procedure the dividers can be designed with the output voltages of two adjacent dividers to be within 50 % of the full scale of the input range of the digitizer. In audio and higher frequencies, the resistive voltage dividers with the low phase angle errors are commonly used Error: Reference source not found. In the current study, the voltage dividers from the sampling wattmeter measurement setup were applied. As for the phase displacement characterization, the divider and the digitizer are calibrated as a single voltage channel and the connections between the digitizers and the dividers are kept as short as possible to improve the repeatability of the measurements. The correction due to linearity of the multimeters can be characterized by applying the same input voltages to the inputs of the multimeters. In the case of using of the external voltage dividers, their parameters like the power and the voltage level dependences can be separately characterized and included in the measurement uncertainty analysis. The step-up procedure for determination of the voltage ratio is shown in Fig. 3.1.

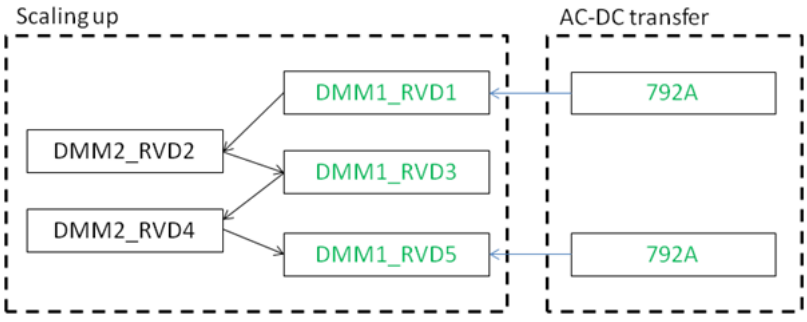

Fig. 3.1. *Step-up procedure for determination of voltage ratio*

The measurement starts from 12 V level by calibrating of the sampling multimeter DMM1 with the voltage divider RVD1 against the AC-DC transfer standard Fluke 792A, see Fig. 3.2.

After that, the AC-DC transfer standard was replaced by the next voltage divider RVD2 with the nominal input voltage of 24 V connected to the sampling multimeter DMM2. In the next steps, the voltage dividers were connected to the multimeters DMM1 and DMM2 to reach the voltage level of 220 V, where each pair of the divider and the multimeter is considered as a separate voltage channel. The AC-DC transfer at the RVD5 level was performed to check the accuracy of the scaling-up procedure. The schematic diagram and the photograph of the measurement setup applied for comparisons of two voltage channels are shown in Fig. 3.3.

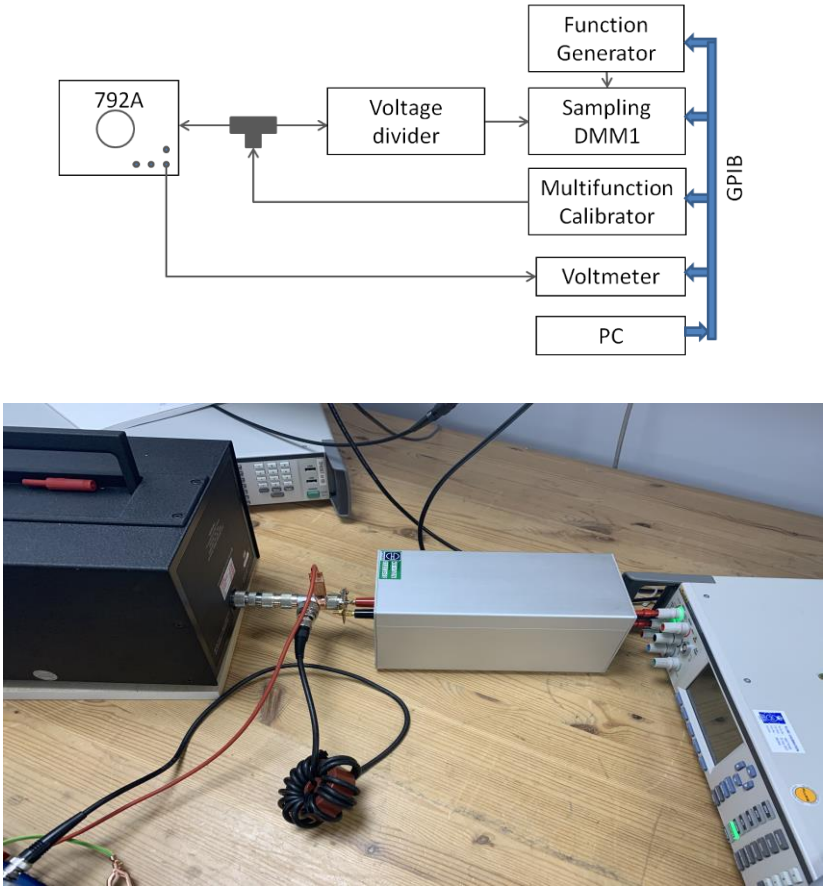

Fig. 3.2. *Schematic diagram and photograph of the measurement setup used for calibration of the first voltage divider RVD1 connected to the DMM1 and in control measurement with RVD5.*

The ratio of the *i*-th voltage channel consisting of a DMM and a voltage divider can be described by:

$$r_i = \frac{U_i}{U_j} \tag{3.1}$$

where:

U_i- input voltage applied to the *i*-th voltage channel,
U_j- output voltage of a DMM, j = 1, 2.

The *i*-th ratio r_i can be expressed by a product of a number of the ratios $\frac{r_{i+1}}{r_i}$ multiplied by the ratio r_1:

$$r_j = \prod_{i=1}^{j-1} \frac{r_{i+1}}{r_i} r_1 \tag{3.2}$$

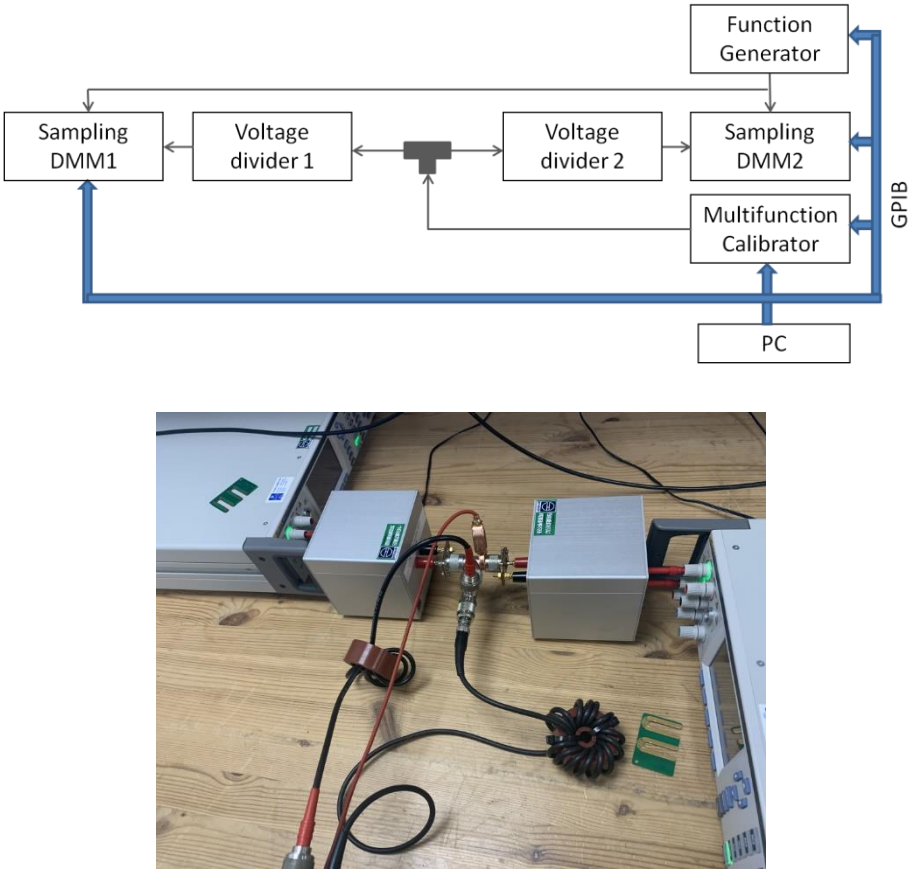

Fig. 3.3. *Schematic diagram and photograph of the measurement setup used for comparison of voltage channels*

Using (3.1) and (3.2), the voltage level of 220 V U_{220_scale} obtained by the scaling up process can be related to the starting point of the procedure:

$$U_{220_{scale}} = \frac{r_2}{r_1}\frac{r_3}{r_2}\frac{r_4}{r_3}\frac{r_5}{r_4} U_{12_{ACDC}} \frac{U'_{r5@ACDC}}{U'_{r1@ACDC}} \tag{3.3}$$

or

$$U_{220_{scale}} = \frac{U'_{r1@1.0FS}}{U''_{r2@0.5FS}} \frac{U''_{r2@1.0FS}}{U'_{r3@0.5FS}} \frac{U'_{r3@1.0FS}}{U''_{r4@0.5FS}} \frac{U''_{r4@1.0FS}}{U'_{r5@0.5FS}} k^2 U_{12_{ACDC}} \frac{U'_{r5@ACDC}}{U'_{r1@ACDC}} \tag{3.4}$$

where:
U' and U'' - output voltages of the multimeters 1 and 2 connected to a divider r_i,
FS – full-scale output of the voltage divider (0.8 V),
U_{12_ACDC} – voltage level of 12 V calibrated against the AC-DC transfer standard.

The correction *k* due to the linearity of the multimeters was measured by applying the same input voltages to the inputs of the multimeters:

$$k = \frac{U''_{1.0FS}}{U''_{0.5FS}} \frac{U'_{0.5FS}}{U'_{1.0FS}} \tag{3.5}$$

The results for the voltage level of 220 V obtained from the voltage of 12 V by four ratio measurements in the scaling up procedure were compared to the 220 V level calibrated directly against the AC-DC transfer standard, see Fig. 3.4. The measurement results are within ±5 μV/V up to 5 kHz well within the measurement uncertainty of (50 to 60) μV/V.

The major uncertainty components are due to the AC-DC transfer at the levels of 12 V and 220 V, the voltage coefficients of the dividers, the linearity of the multimeters. The voltage dependences of the

dividers were taken into account as the uncertainty components considering that the repeatability in the voltage coefficients measurements should be further improved.

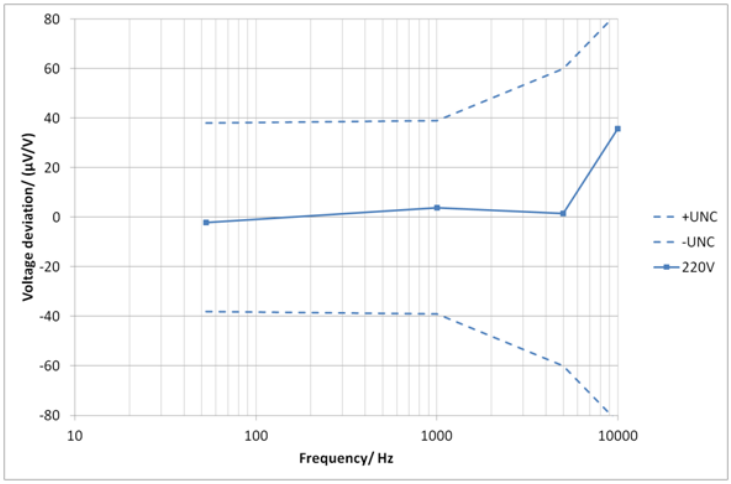

Fig. 3.4. *Deviation in the voltage level obtained by the scaling up procedure against the same voltage level calibrated directly by the AC-DC transfer standard*

In the scaling down process, the voltage divider RVD3 with the ratio r = 70 was calibrated against the AC-DC transfer standard at the input voltage level of 8 V with the output of the voltage divider measured by the calibrated multimeter 8588A in the digitizing mode at the 100 mV range. After that, the same range of the multimeter was calibrated at the 10 mV level by applying 0.8 V in parallel with the AC-DC transfer standard.

The measurement results were confirmed by the interlaboratory comparison between Metrosert and PTB where the multimeter 8588A served as a transfer standard, see Fig. 3.5.

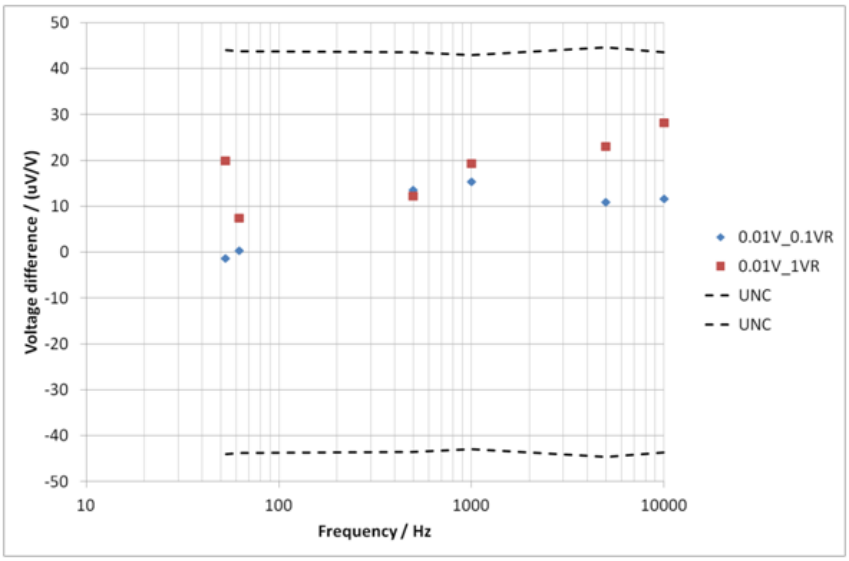

Fig. 3.5. *Voltage differences at the voltage value of 10 mV between Metrosert and PTB*

3.7. A digital counterpart of thermal converters

In the digital based current step-up method proposed the same current is provided to two combinations of shunt-digitiser connected in series. Each shunt and digitiser are connected, in turn, in parallel; the shunt-digitizer under test and the standard shunt-digitiser. An example of the setup is shown in Fig. 3.6 where each digitiser samples the output voltage of the shunts independently and simultaneously.

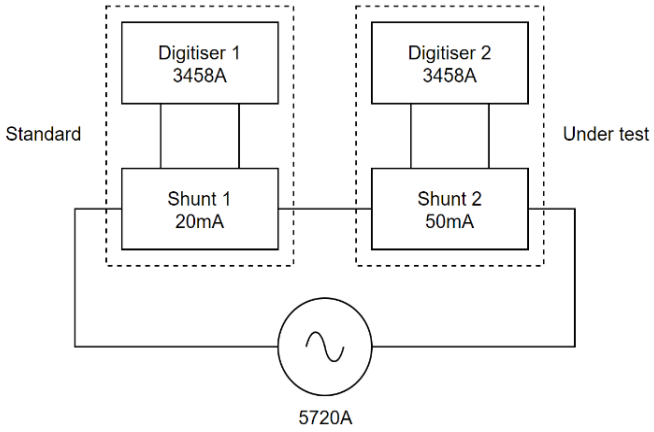

Fig. 3.6. *Setup of the digital current step up*

Comparing the output of the digitisers and knowing the correction of the standard shunt-digitiser, the correction of the shunt-digitizer under test can be calculated. If this process is repeated with shunts for higher currents, a complete digital traceability chain can be established.

Some experimental results for a current step-up in five steps from 20 mA up to 1 A, and nine frequencies from 10 Hz up to 10 kHz are going to be presented here. The equipment includes two digitisers Keysight 3458A and a current source Fluke 5720A in voltage mode (Fig. 3.7). Further information regarding noise reduction, shielding and guarding can be found in [25].

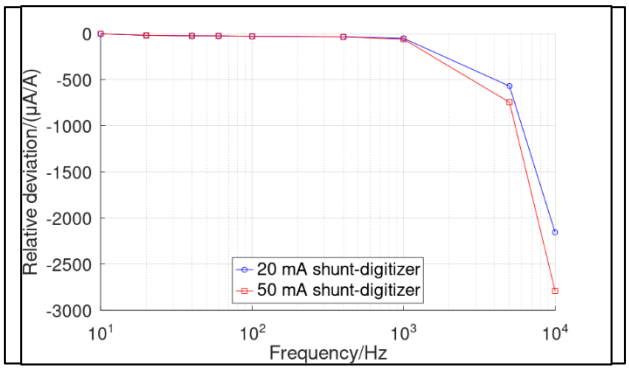

Fig. 3.7. *Frequency response normalized with 10 Hz response for the 20 mA to 50 mA step up*

For the first step-up (20 mA to 50 mA), Fig. 3.7 represents the shunt-digitiser frequency responses. The values in μA/A have been represented as a relative deviation from the values at 10 Hz. Responses represented here includes, therefore, the contribution of both, shunts and digitisers.

Fig. 3.7 shows that the normalized frequency response has a moderately constant value up to 1 kHz. For higher frequencies, the differences are much bigger. This frequency response is mainly due to the input impedance of the digitizer [29]. Also, at higher frequencies the aperture time must be lower meaning lower accuracy and higher noise on the measurements. In order to validate the new digital traceability chain, the shunt AC-DC difference obtained by thermal and digital methods is compared. Note that in the digital-based step-up of shunts proposed, DC measurements are not required, however, these are taken here to compare them with thermal method measurements.

The first step consists in removing the digitizer influence. To this end, two sets of measurements are needed: one with the configuration shown in Fig. 3.6 and another swapping the digitisers. The next procedure is followed:

1. The same AC current is applied to the standard shunt-digitiser and shunt-digitiser under test. The output of both digitisers is recorded.

2. The same DC current is applied to the standard shunt-digitiser and shunt-digitiser under test. The output of both digitisers is recorded again.

3. AC-DC differences for each digitiser are calculated (δ_s and δ_t, where sub index *s* refers to the standard equipment and *t* to the equipment under test).

The process is repeated swapping the digitisers, so new AC-DC differences for each digitiser (δ'_s and δ'_t) are calculated.

In these circumstances it can be shown that the subtraction of the difference AC-DC between the shunt under test and the standard shunt $(s_t - s_s)$ can be obtained from the following expression, where the digitiser influence has been removed.

$$s_t - s_s = \frac{(\delta_s + \delta'_s) - (\delta_t + \delta'_t)}{2} \tag{3.6}$$

This value will be compared to the one obtained by thermal converter characterization from historical data. Values from both, classical and digital approaches, are shown in Table 3.1 together with the differences of both techniques. Blank spaces indicate no historical results available.

Table 3.1. *AC-DC difference between shunts for the equivalent historical results of a thermal-converters-based realization of AC current, the digital step up measured in this paper and the differences between both techniques.*

	Thermal converters step up $(s_t - s_s)$/(μA/A)					Digital step up $(s_t - s_s)$/(μA/A)					Techniques difference (μA/A)				
Step up /mA	20	50	100	200	500	20	50	100	200	500	20	50	100	200	500
f / Hz	50	100	200	500	1000	50	100	200	500	1000	50	100	200	500	1000
10	-2.2	-1.8	-2.0	-2.4	-1.7	-0.3	0.6	0.5	1.2	1.7	1.9	2.4	2.5	3.7	3.4
20	-0.6	-0.7	-0.1	-0.9	0.0	-0.2	0.6	0.7	1.4	0.5	0.4	1.4	0.8	2.3	0.5
40	-0.6	0.0	-0.5	0.0		-0.5	0.5	1.1	1.4	1.0	0.0	0.5	1.6	1.5	
60	0.0	-0.1	0.0	-1.3		-0.2	0.0	0.5	0.9	1.4	-0.2	0.1	0.5	2.2	
100	0.1	-0.1	-0.1	0.3		0.2	0.4	0.7	1.1	0.5	0.1	0.5	0.9	0.8	
400	0.8	0.2	0.2	0.2		-0.8	0.9	2.0	0.3	0.3	-1.6	0.8	1.8	0.1	
1 000	0.0	0.2	0.0	-0.1	0.0	-1.9	-0.6	-0.8	0.5	0.4	-1.9	-0.9	-0.8	0.6	0.5
5 000	0.7	0.9	0.1	-1.4		-20.2	4.9	5.7	-2.1	5.7	-20.9	4.1	5.7	-0.6	
10 000	-0.7	1.4	-0.1	-1.3	-0.6	-69.4	12.7	17.1	-4.2	12.5	-68.7	11.3	17.2	-2.9	13.1

For the thermal converter step-up approach, Table 3.1 shows very small AC-DC differences, as expected.

In the case of the digital step up, AC-DC difference between shunts is also very low for the whole current range when the frequency is lower than 1 kHz. Regarding 5 kHz and 10 kHz, some differences are also very low, however, this does not occur for all the step ups.

Regarding frequencies up to 1 kHz for all step-ups, the data from the difference of both techniques shows small differences. This means that, knowing the digitiser error from a quantum calibration, comparable results to thermal converter can be achieved with the benefit of not performing DC measurements and taking dynamic measurements.

These promising results would allow laboratories to establish a digital traceability chain for AC current, permitting high accuracy dissemination for complex waveforms that vary with time or have a decent amount of harmonic content. At the same time this digital chain would simplify and reduce the amount of time needed for calibrations.

3.8. Uncertainty issues in digital scaling methods

3.8.1. Input impedance

The typical impedance of a signal source can be below the ohm range, but the situation can be very different if a voltage signal is derived from the output of a divider. In such case, the impedance at input node can be as high as 100 Ω and even higher. This represents an issue if the input impedance of the sampler is taken into account.

First, the finite input resistance of the sampling device act as a load on the divider, effectively modifying the divider ratio. This contribution is strongly dependent on the specific sampler adopted: in integrating-type DVMs (e.g., Keysight 3458) the very high input impedance in the operating range of interest makes this contribution negligible, while in sigma-delta based instruments values are typically around 1 MΩ as in National Instruments PXI-5922. Considering the output resistance of the divider to be 100 Ω, the change in the ratio is of the order of 10^{-4}, thus cannot be neglected. The correction for loading of the ratio value cannot be calculated yet, since the input resistance of the sampling device is not defined by a device with standard-grade stability, its value cannot be guaranteed over time and with varying operating conditions, e.g., with changes in temperature.

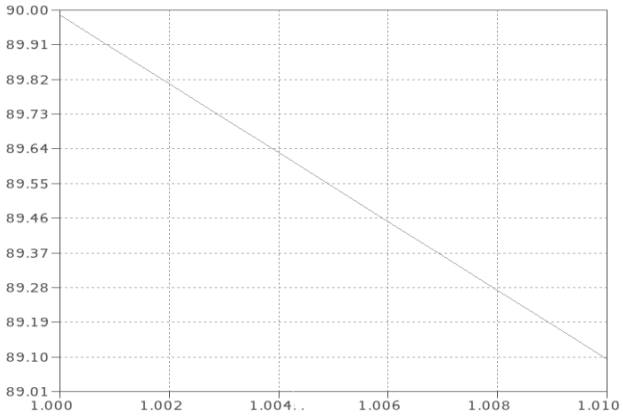

Fig. 3.8. *Deviation from nominal value of the ratio for a 10:1 voltage divider with 100 Ω output resistance when loaded by a 1 MΩ resistor over a 1% change of the load resistor x-axis: resistance/MΩ, y-axis: ppm deviation*

A recent paper [21] addressing the issue of the temperature influence of various operating parameters of a Keysight 3458A reports variations of parameters on the order of percent for a temperature variation of few Kelvins. If such input resistance changes in the order of percent, the ratio of a divider with 100 Ω output impedance is affected at the ppm level, a non-negligible amount, if quantum standard accuracy level is targeted.

3.8.2. Digitisers limitations with PJVS staircase signals

Two main high resolution ADC technologies are available and typically in use in NMIs primary voltage laboratories for the measurement of sampled signals: integrating and, more recently, sigma-delta. Integrating, dual slope, ADCs have been adopted since long for high accuracy Digital Volt Meters (DVM) that are capable of resolutions up to 28 bits, which is a value still unsurpassed by other technologies, but suffer from limited bandwidth causing problems when frequencies in excess of a few kilohertz are measured. The adoption of sigma-delta ADC tackles this issue, being a technology capable of a very high sampling frequency together with high resolution [3]. However, known limitations of sigma-delta ADCs in processing input signals with discontinuities must be considered with the stepped output of a PJVS and addressed for proper performances.

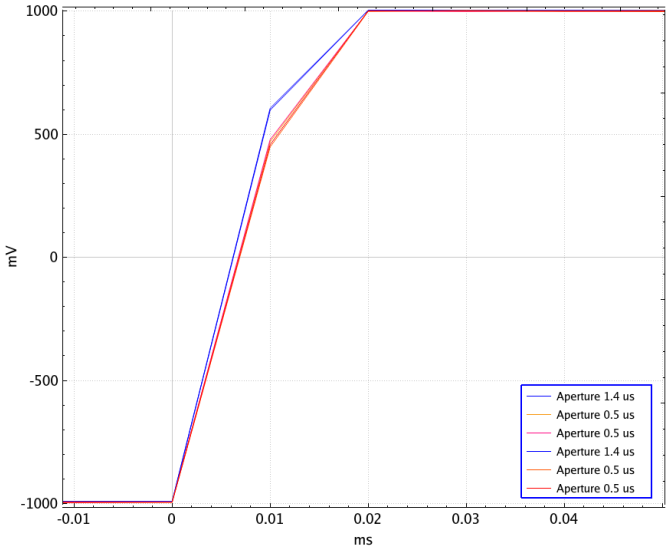

Fig. 3.9. *Step response of an Keysight 3458 multimeter at different aperture times. It can be seen the effect of aperture time on step response*

To test performances of digitizers of both types, one can apply a square wave from an arbitrary waveform generator. The generator connected, e.g., to a Keysight 3458 multimeter operated in high resolution digitizing DCV mode, with apertures: 0.5 µs and 1.4 µs. The results, plotted in Fig. 3.9, clearly show an exponential decay response with a total duration of about 20 µs, perfectly matching the specifications provided by the manufacturer, reporting a 20 µs settling time to obtain an error below 0.01 % of the step height in measurement. Owing to the 100 kSa/s sampling rate (the maximum available), the number of points where the response is steeper is just a few, making it difficult to evaluate the time response with accuracy. It is however clear that aperture time affects the time constant appreciably. The effect on frequency response can be seen as well in the noise of the acquired samples in Fig. 3.10.

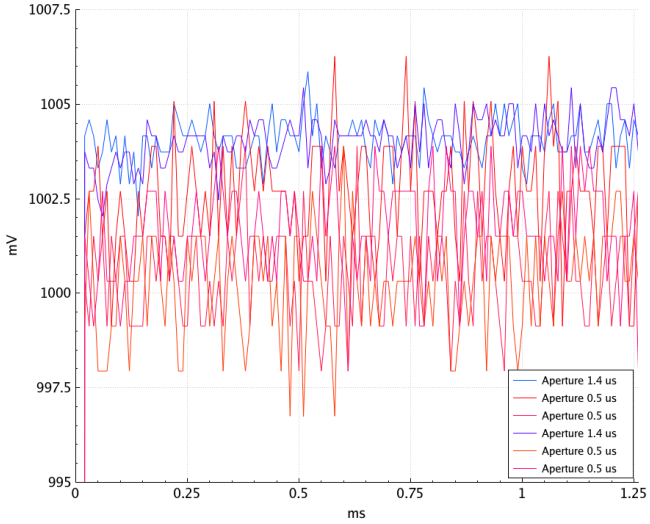

Fig. 3.10. *Samples of a constant input measured with an Keysight 3458 multimeter at different aperture times. It can be seen the effect of aperture time on noise*

The significant increment in the measurement noise observed shows that a suitable value of the aperture has to be found by a trade-off between speed and signal to noise ratio. Regarding speed, it should be noted that decay error is a relevant uncertainty contribution and the error considered in the DVM specifications is not sufficient for application to a Josephson voltage standard. Considering that amplitudes up to 100 mV are present at the sampler input [7], such error amounts to 10 µV; to reduce

tenfold this value, 25 µs are necessary, thus 30 µs is a reasonable estimate of the minimum duration for a voltage step to provide proper accuracy. Assuming a staircase signal generated by a PJVS with 20 steps per period, this constraint translates into a 1.5 kHz maximum frequency.

Several alternative technologies suitable for the application to the AC voltage standard are currently available, yet sigma-delta ADCs are typically considered as the most viable alternative to integrating converters for several reasons. They provide both high sample rate and bandwidth, along with high resolution [24] there are instruments available in the market that provide analog to digital conversion based on sigma delta technology with an input front-end for impedance adapting, range scaling, etc., as well as a convenient computer interface for the acquisition of the digital stream and operating parameters setup. A significant drawback of sigma-delta ADCs, however, lies in the much higher complexity of their structure that makes the determination of the quantization noise and effective resolution different from typical conversion technologies. Additionally, owing to the internal digital filter processing, they are very idiosyncratic towards abrupt changes in the input signal, a feature well known in general applications, where it becomes a problem in multiplexed signal circuits [23], as well as in metrological literature, due to the voltage steps in signals at PJVSs output Error: Reference source not found. The motivations for this behaviour are several and involve both technical and mathematical issues that are beyond the scope of this document. A possible solution was proposed in [22], to compensate for the frequency dependence, with significant improvements. In any case, the correction has no effect on the problems related to the step response of the converter. In circuit design, the adoption of low-latency sigma delta ADCs is proposed for such problems [23], but instruments based on sigma-delta converters chips are missing information on this subject neither report the chip used, so it is in general, not possible to determine, from manufacturer's specifications, the best sampler for this task.

The problem is widely discussed in programmable Josephson standard literature, where it is observed as oscillations in the digital output values, before and after the step transition. The widely adopted approach is based on the empirical determination of the samples with detectable ringing near the transition. Once the number of affected samples in known, they can be easily removed from readings in calibrations. Throwing away data for about 7 µs, is sufficient to observe a value consistent with theoretical calculations and stable, i.e., not changing if data are removed for longer durations.

Compared with an integrating converter, the time required by a sigma-delta ADC seems better, however in the latter a rule for the calculation of the time response in simple form is missing, making it difficult to define a general law for processing data.

Such behaviour is intrinsically related to the filtering in all sigma-delta ADCs and can be easily observed with instruments of this kind by applying a step signal at the input. Fig. 3.11 shows the results of such test with a 24 sigma-delta data acquisition module (National Instruments NI 9239, CompactDAQ).

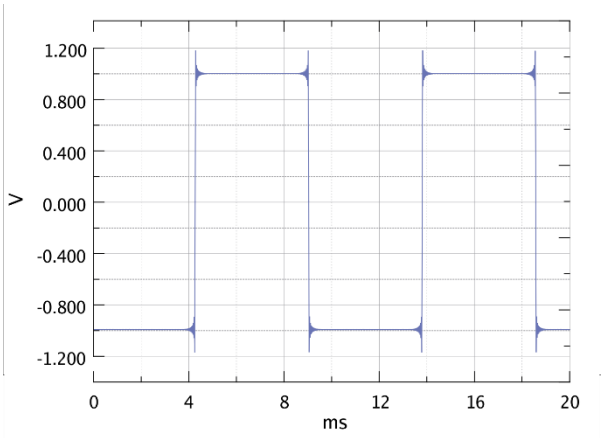

Fig. 3.11. *Values of samples read at 50 kSa/s with a National Instruments NI 9239, CompactDAQ, 24 bit sigma-delta data acquisition module with a 100 Hz 2 V peak-to-peak square wave applied at the input*

The ringing seen at every transition has an overshoot that amounts to approximately 20 % of the step amplitude and decays to an apparently negligible value after about 500 µs (Fig. 3.12). It should be noted, however, that the digital output timing is determined by the data rate (50 kSa/s in this case), thus both time and frequency response must be properly rescaled according to the value set for the data rate.

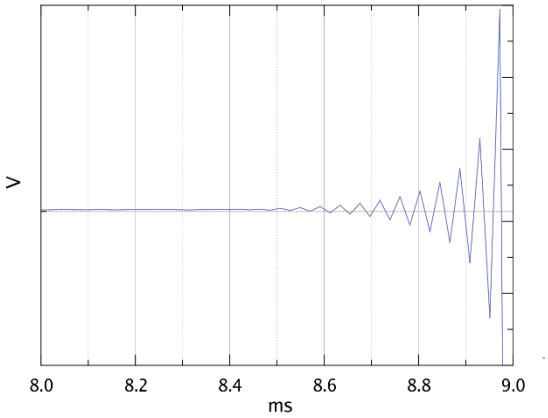

Fig. 3.12. *Plot of the oscillations near the step transition in Fig 3.11*

A suitable choice to assess consistently the duration of the decay would be to define it corresponds to a value such that the oscillations become lower than the least significant bit of the converter. This obviously implies that the higher the accuracy of the converter, the longer the wait time before reliable data will be required.

3.8.3. Phase accuracy in dividers and shunts

This section summarizes the work performed on characterisation of the phase displacement of dividers and shunts in systems with two digital voltmeters. In measurement standards of electrical power based on a sampling wattmeter, voltage dividers and current shunts are usually employed to convert the input quantities to the voltage level of around of 1 V. To reduce the loading effect caused by the input impedance, a transducer and a digitizer can be calibrated as a single channel. If the phase angle error of a transducer is sought, then the measurement result should be calculated for no loading conditions by correcting for the input impedance of a digitizer.

In phase characterization of the voltage dividers, the scaling-up procedure is very similar to determination of the voltage ratio shown in Fig. 3.2, except the AC-DC transfer standard is not required and the procedure starts from the phase difference measurements between two digitizers. The schematic diagram and the photograph of the setup used in the scaling-up procedure are shown in Fig. 3.3.

The precision voltage dividers are constructed from foil resistors, capacitive voltage guards and capacitors in parallel with the resistors. The phase response of the divider's changes with the voltage level and with the heat dissipation in the resistive elements [26].

As the voltage levels during the step-up process vary from 50 % to 100 % of the nominal ratings of the dividers, the power and voltage dependences of the voltage dividers should be considered.

The power dependence of a voltage divider can be determined from a warm-up measurement [26]. The divider under test (DUT) is connected to the previously warmed-up reference divider. For the particular design considered above, in the audio frequency range the highest observed power dependence is shown in Fig. 3.13. At frequencies up 10 kHz, the power dependence is below a few microradians, and it can be taken as an uncertainty component in the step-up procedure.

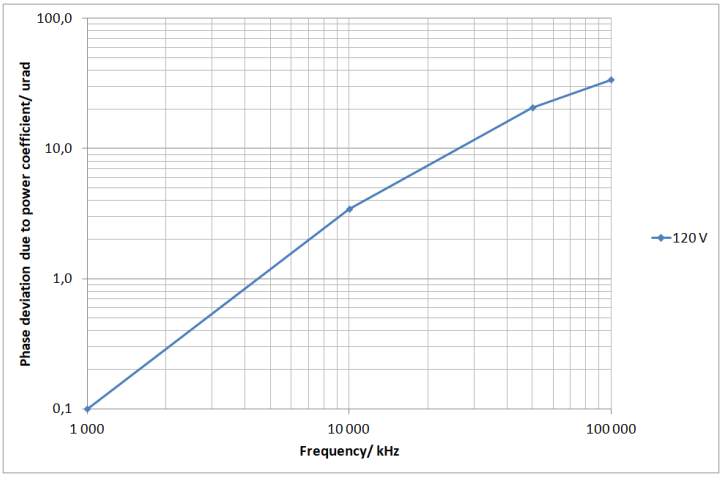

Fig. 3.13. *Phase deviation due to power dependence for the 120 V voltage divider*

The voltage level dependence of the DUT can be determined against a reference voltage divider with the known voltage level dependence. For this purpose, the voltage dividers with no capacitive components were constructed as described in [26, 27]. To reduce dielectric losses in resistors, a foil resistor without the isolation cover was used. The level dependence was measured by rapid switching between voltage levels, much faster than the thermal stabilisation of the divider. The voltage level dependence measurements at 10 kHz for the 120 V divider are shown in Fig. 3.14. In Table 3.2 the corrections due to voltage dependence to the step-up procedure are given.

Table 3.2. *Corrections due to voltage level dependence for step-up procedure in µrad.*

	Voltage divider								
f, Hz	1.6V	5V	12 V	24 V	56 V	120 V	240 V	560 V	1000 V
53	-0.7	-1.6	-1.3	-1.6	-1.6	0.5	-2.1	-4.7	-3.5
1000	0.1	-0.9	-0.5	-0.6	-0.8	3.8	-22.4	-14.4	-38.8
5000	0.7	-0.2	-0.3	-0.5	-0.7	20.9	-87.7	-62.4	-197.0
10000	-3.1	0.0	0.4	-0.5	-0.6	41.8	-171.2	-119.2	-380.8

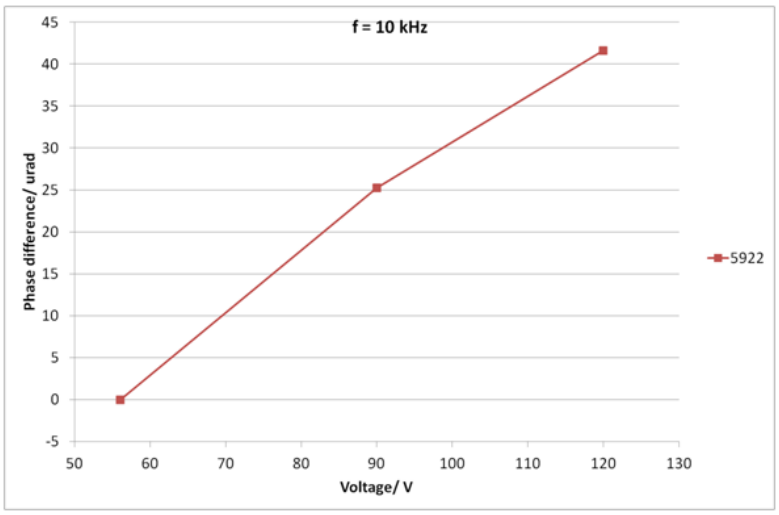

Fig. 3.14. *Voltage level dependence measurements for the 120 V divider at 10 kHz*

The phase angle error of a current shunt can be estimated from its circuit model, see Fig. 3.15(a). If a current shunt is connected to a digitizer the circuit model becomes as shown in Fig. 3.15(b) [28]. The impedance components of the models can be measured by an LCR meter and a capacitance bridge. The measurement uncertainties of the calculated phase angle errors can be estimated by the Monte Carlo method.

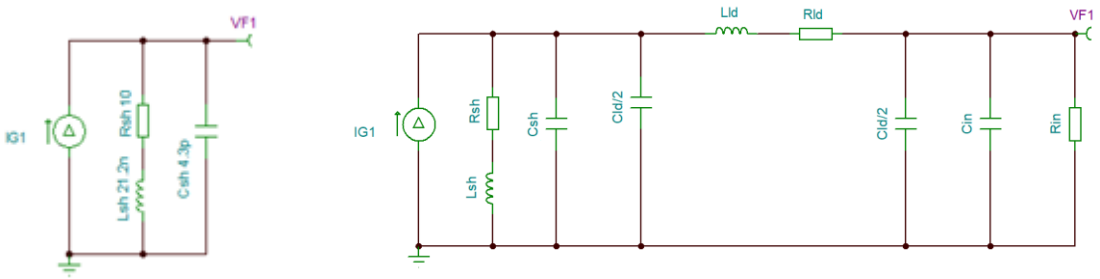

(a) (b)

Fig. 3.15. *Circuit diagram of a standalone shunt (a) and a shunt connected to a digitizer (b)*

To check the calculated phase angle errors, two current shunts with nominal values of 10 Ω and 20 Ω were constructed and measured in a system consisting of two digitizers, see Fig. 3.16. The difference of the calculated phase angle errors (time constants) of two shunts in a good agreement with the measurement results, see Fig. 3.17.

(a) (b)

Fig. 3.16. *Schematic diagram (a) and photograph (b) of the measurement setup for phase difference measurement*

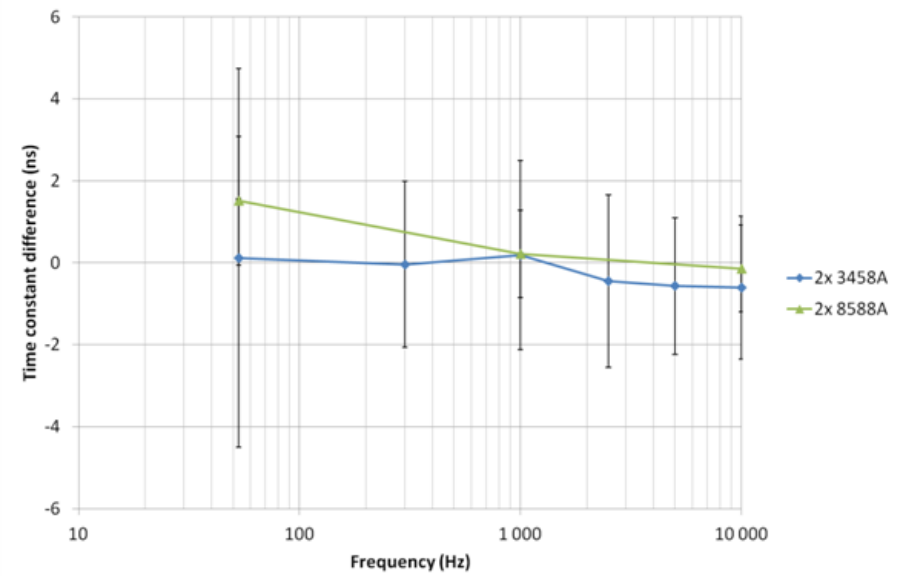

Fig. 3.17. *Time constant differences of two shunts, deviation of measured results from the modelled values*

The step-up procedure starts from the comparison of an unknown current shunt to the reference shunt connected in accordance with the diagram shown in Fig. 3.16(a). The step-up procedure continues to the next nominal values, with the output voltages of the shunts being within 50 % of the full scale of the input range of the digitizer in each step, see Fig. 3.18.

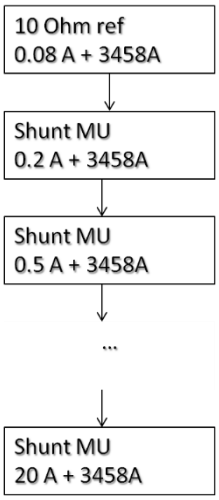

Fig. 3.18. *Step-up procedure in the phase angle measurement*

If the phase angle error of a standalone current shunt is sought, then the measurement result should be calculated for no loading conditions by correcting for the input impedance of a digitizer. For digitizers with the high input impedance the loading correction is negligible as compared to the measurement uncertainty for the shunts with impedances below 1 Ω. For example, the calculated phase errors (time constants) for the 10 Ω reference shunt with and without a multimeter 3458A serving as a load are shown in Fig. 3.19.

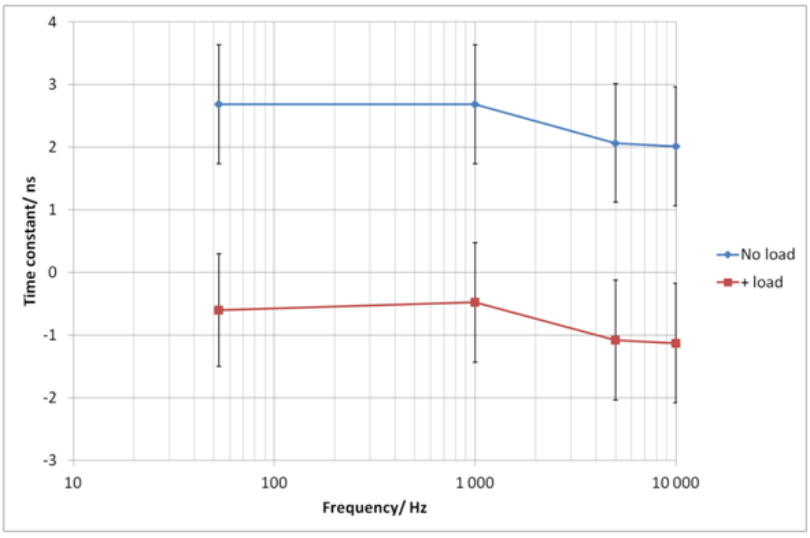

Fig. 3.19. *Calculated time constants for the reference shunt with and without a load*

3.8.4. Stability of digitizers vs. time, temperature and frequency

Since most instruments operate under dynamic condition, where signals vary with time, their calibration should be performed in such dynamic conditions.

This section shows the experimental work where two digital multimeters Keysight 3458A (DMM1 and DMM2) have been employed working in DCV sampling mode using an AC input signal. Both DMMs were placed inside a climatic chamber. The 0.8 V, 1 kHz, AC signal was provided by a Fluke 5720

multifunction calibrator. Measurements were carried out twice (temperature increasing from 20 ºC to 26 ºC and temperature decreasing from 26 ºC to 20 ºC). More details are depicted in Fig. 3.20.

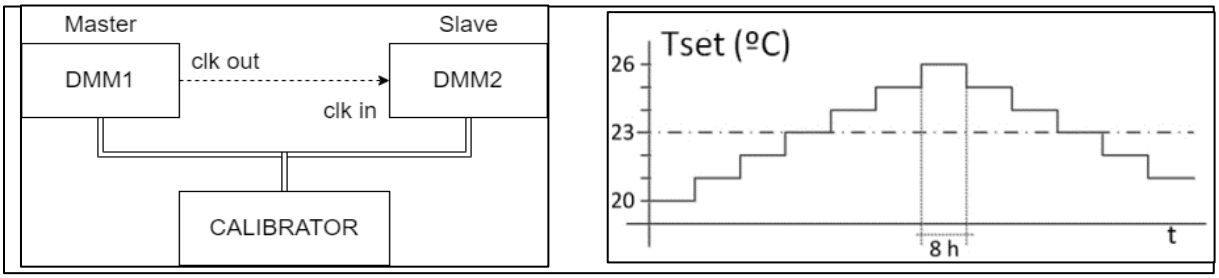

Fig. 3.20. *Details of the temperature coefficient evaluation setup*

DMM gain error (δg) is defined as:

$$\delta g(T_a) = \frac{V_M - V_R}{V_R} 10^6 \tag{3.6}$$

Where V_M is the average of the acquired samples and V_R is the AC source reference voltage.$\delta g(T_a)$ is plotted for different temperatures in Fig. 3.21: for DMM1 on the left and for DMM2 on the right.

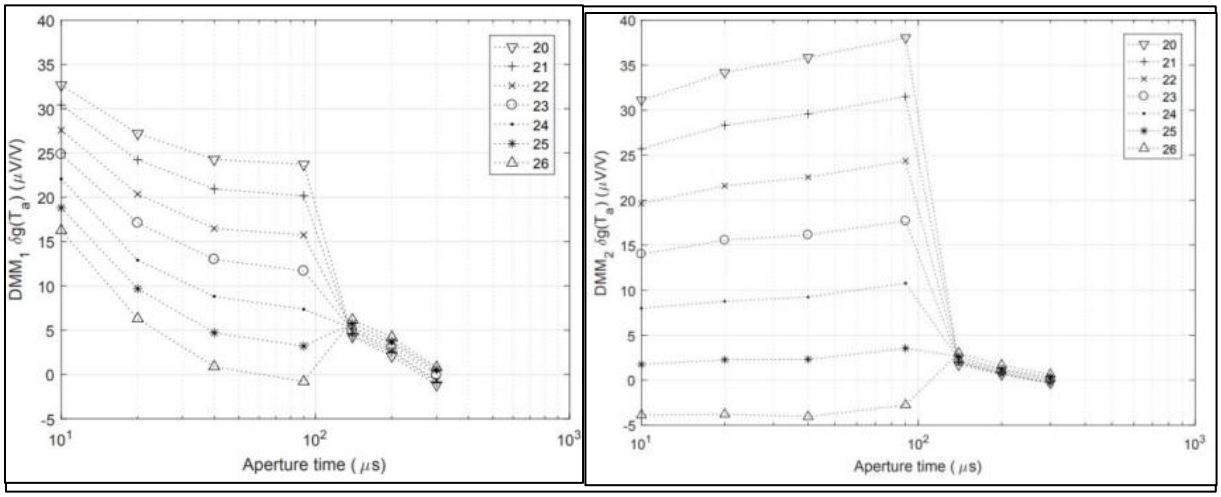

Fig. 3.21. *Gain error curves for the set-point temperatures for DMM1 (left) and DMM2 (right)*

After data processing, an estimation of temperature coefficients for each DMM has been done for each aperture time. Table 3.3 presents mean temperature coefficients for DMM1 together with standard deviations. DMM1-up represents an increasing temperature test and DMM1-down a down-decreasing temperature test.

Table 3.3. *Temperature coefficients for DMM1 in (μV/V)/°C*

T_a/μs	DMM1-up	DMM1-down	Mean	Std
10	-2.39	-2.81	-2.60	0.21
20	-3.22	-3.49	-3.35	0.14
40	-3.50	-3.84	-3.67	0.17
90	-3.76	-4.07	-3.91	0.16
140	0.33	0.06	0.20	0.13
200	0.42	0.27	0.42	0.08
300	0.36	0.31	0.33	0.02

From Fig. 3.21 two different temperature coefficients arise, depending on the aperture times considered. For the high accuracy stage ($T_a > 100$ µs) the temperature influence is negligible, whereas in the high-speed stage ($T_a < 100$ µs) temperature influence is important and should be considered in the metrological grade DMM characterization.

Differences in both DMM are not negligible when $T_a < 100$ µs. Therefore, every DMM should be characterized when these aperture times are used. This behaviour is a consequence of the ADC switch between 10 kΩ and 50 kΩ inputs at 100 µs.

Temperature coefficients when applying a DC signal was digitized [31] are similar to those obtained in this work.

Table 3.3 shows no significant difference so that the AC source stability can be evaluated.

A similar behaviour to that found employing a DC voltage reference [31] has been achieved and similar temperature coefficients are obtained.

As expected, two different temperature coefficients are found, depending on the aperture times considered being higher or lower than 100 µs. Temperature influence is important and should be considered in metrological grade DMM characterization when $T_a < 100$ µs.

For $T_a < 100$ µs, every DMM should be studied when used in metrological grade characterization. Temperature gradient direction is not important.

3.9. Conclusions

It is now generally accepted that Electrical Metrology will face in the future the expanding needs of a digital world. A survey carried out among the participants of DIG-AC European project, showed that a rather small part of AC calibrations is based on sampling and almost none on digital techniques for voltage/current scaling. Nevertheless, research on this topic has been quite active in recent years and some interesting results have been published involving scaling of both voltage and current based on digital methods.

The adoption of intrinsically digital techniques for scaling the electrical standards of voltage and current has proven very successful for DC signals, raising interest in their application also to the AC and, more generally, to time-dependent regimes.

Digital techniques for upscaling and downscaling the operating range of an AC quantum standard were considered and a suitable interval of operating values was defined, depending on the signal frequency. From the analysis of the solutions adopted, the integration of high accuracy ADCs available in modern precision DVM along with traditional, divider-based, methods offer the best solution to exploit digital techniques for scaling quantum standards.

This guide summarizes the knowledge advancements attained within the DIG-AC project in the field of scaling AC electrical signals to extend digital techniques over the relevant ranges of calibrations and traceability to quantum standards of AC signals. The results reported here provide a fundamental tool to coordinate the future developments for a digital-ready and quantum accurate European metrological network.

3.10. References

[1] A. Sosso, *et al*: ”Overview of scaling methods in use”, DIG-AC Project, Internal Report, October 2021.
[2] Hewlett Packard Journal, April 1989, Volume 40, Number 2.
[3] TÜBİTAK UME, “Report on the selection of three digitisers and their parameters that meet the necessary requirements for digital traceability chain”, 17RPT03 DIG-AC Project – Report D1

[4] "IEEE Standard for Terminology and Test Methods for Analog-to-Digital Converters," in IEEE Std 1241-2010 (Revision of IEEE Std 1241-2000), pp.1-139, 14 Jan. 2011.
[5] "IEEE Standard for Digitizing Waveform Recorders," in IEEE Std 1057-2017 (Revision of IEEE Std 1057-2007) - Redline , vol., no., pp.1-313, 26 Jan. 2018.
[6] C. A. Hamilton, C. J. Burroughs, and R. L. Kautz: “Josephson D/A converter with fundamental accuracy”, IEEE Trans. Instrum. Meas., vol. 44, pp. 223–225, 1995.
[7] R. Behr, L. Palafox, G. Ramm, H. Moser, and J. Melcher: “Direct comparison of Josephson waveforms using an AC quantum voltmeter”, IEEE Trans. Instrum. Meas., vol. 56, no. 2, pp. 235–238, Apr. 2007.
[8] W. G. K. Ihlenfeld, R.P. Landim: “Investigations on extending the frequency range of PJVS based AC voltage calibrations by coherent subsampling”, Conference on Precision Electromagnetic Measurements, Ottawa, Canada, July 2016.
[9] W. G. K. Ihlenfeld, E. Mohns, R. Behr, J. Williams, P. Patel, G. Ramm, and H. Bachmair: “Characterization of a high resolution analog-to-digital converter with a Josephson AC voltage source”, IEEE Trans. Instrum. Meas., vol. 54, no. 2, pp. 649–652, Apr. 2005.
[10] R. Iuzzolino, L. Palafox, W. G. K. Ihlenfeld, E. Mohns, and C. Brendel: “Design and characterization of a sampling system based on Σ–Δ analog-to-digital converters for electrical metrology”, IEEE Trans. Instrum. Meas., vol. 58, no. 4, pp. 786–790, Apr. 2009.
[11] F. Overney, A. Rufenacht, J.-P. Braun, B. Jeanneret, P. S. Wright: “Characterization of Metrological Grade Analog-to-Digital Converters Using a Programmable Josephson Voltage Standard”, IEEE Trans. Instrum. Meas., vol. 60, no. 7, pp. 2172–2177, July 2011.
[12] G. Rietveld, D. Zhao, C. Kramer, E. Houtzager, O. Kristensen, C. de Leffe, and T. Lippert: “Characterization of a wideband digitizer for power measurements up to 1 MHz”, IEEE Trans. Instrum. Meas., vol. 60, no. 7, pp. 2195–2201, July 2011.
[13] S. P. Benz, and C. A. Hamilton: “A pulse-driven programmable Josephson voltage standard”, Appl. Phys. Lett., vol. 68, pp. 3171–3173, 1996.
[14] N. Flowers-Jacobs, A. Rüfenacht, A. E. Fox, S. B. Waltman, J. Brevik, and S. P. Benz: “Three Volt Pulse-Driven Josephson Arbitrary Waveform Synthesizer”, Conference on Precision Electromagnetic Measurements, Paris, France, July 2018.
[15] M. Šíra, O. Kieler, R. Behr: “A Novel Method for Calibration of ADC Using JAWS”, IEEE Trans. Instrum. Meas., vol. 68, issue 6, June 2019.
[16] P. Crisp, “Getting the best out of long scale DMMs in metrology application,” in NCSL Workshop & Symposium, pp. 151–160, 1997.
[17] G. Ramm, H. Moser, and A. Braun, “A new scheme for generating and measuring active, reactive and apparent power at power frequencies with uncertainties of 2.5×10^{-6},” IEEE Trans. Instrum. Meas., vol. 48, no. 2, pp. 422-426, Apr. 1999.
[18] https://www.ptb.de/empir/quadc-project.html
[19] M. Starkloff et al., "The AC Quantum Voltmeter Used for AC Current Calibrations," CPEM 2018, 2018, pp. 1-2.
[20] A. Pokatilov *et al*., “Application of simultaneous sampling of two voltages for direct digital determination of a voltage ratio,” DIG-AC Project, Internal Report, January 2022.
[21] Y.A. Sanmamed, J. Díaz de Aguilar, R. Caballero Santos, J. R. Salinas: "Temperature influence on the establishment of a digital voltage reference", Conference on Precision Electromagnetic Measurements (CPEM 2020) Digest, Denver, Colorado, 24-28 August 2020.
[22] G. Rietveld, et. al., “Characterization of a Wideband Digitizer for Power Measurements up to 1 MHz” IEEE Trans. Instr. Meas Vol. 60, n. 7, 2011.
[23] M. K. Mayes, “No Latency Delta-Sigma ADC Techniques for Optimized Performance”, Linear Technology Magazine, May 2002
[24] National Instruments, “NI 9239 Data sheet”, April 2016.
[25] P. S. Filipski and M. Boecker, "AC-DC Current Shunts and System for Extended Current and Frequency Ranges", IEEE Instrum. and Meas. Tech. Conf. Proc., 2005, pp. 991-995, doi: 10.1109/ IMTC.2005.1604287.
[26] T. Bergsten, V. Tarasso, K. E. Rydler, „Determining voltage dependence of the phase response in voltage dividers,” *CPEM Digest (Conference on Precision Electromagnetic Measurements), 2012.* IEEE. DOI: 10.1109/CPEM.2012.6250912.

[27] A. Huang, T Lipe, J. Kinard, and C. Childers, "AC-DC difference characteristics of high-voltage thermal converters," IEEE Trans. Instrum. Meas., vol. 44, no. 2, pp. 387-390, Apr. 1995.

[28] S. Svensson, K.-E. Rydler, V. Tarasso, "Improved model and phase-angle verification of current shunts for AC and power measurements", *Conf. Dig. CPEM,* pp. 82-83, 2004.

[29] J.D. de Aguilar, J.R. Salinas, O. Kieler, R. Caballero, R. Behr, Y.A. Sanmamed, A. Méndez, "Characterization of an analog-to-digital converter frequency response by a Josephson arbitrary waveform synthesizer", Meas. Science and Technology, 2019, vol. 30, No. 3, 035006, https://doi.org/10.1088/1361-6501/aafb27.

[30] D. Peral, Y. A. Sanmamed, J. Díaz de Aguilar, "Feasibility of a digital counterpart of thermal converter-based current step up", submitted to 25th IMEKO TC4 Symposium on Measurement of Electrical Quantities, September 2021.

[31] Y. A. Sanmamed, J. R. Salinas, J. Díaz de Aguilar, F. García-Lagos and R. Caballero, "Temperature influence on the frequency response of the Keysight 3458A digital multimeter", Proc. of the 24th IMEKO TC4 International Symposium, September 2019, Xi'an, China.

[32] J.R. Salinas et al., "Study of Keysight 3458A Temperature Coefficient for Different Aperture Times in DCV Sampling Mode", Conference on Precision Electromagnetic Measurements (CPEM), 2018, pp. 1-2, doi: 10.1109/CPEM.2018.8500883.

4. COMMON DATA FORMAT AND REQUIRED SOFTWARE STRUCTURE

4.1. Introduction

Following text describe motivations and selection of Common Data Format (CDF) properties. The CDF is intended to be used for easy exchange of sampled data between laboratories. The document and format are based on the data format developed in 15RPT04 TracePQM project, document A2.3.1.

Abbreviations:

LV – LabVIEW,
CVI – LabWindows CVI,
EOS – End of string,
DWORD – unsigned 32bit variable,
INT16 – signed 16bit integer,
INT32 – signed 32bit integer,
Float32 – 32-bit real number,
BYTE – unsigned 8bit variable,
HDD – Hard drive,
TWM – The LV program developed in scope of TracePQM project,
GUI – Graphical User Interface,
HW – HardWare,
QWTB – Q-Wave toolbox,
INFO – Brain-dead structured, human readable text file,
Matlab – Mathworks Matlab,
GNU Octave – Open-source computational software, Matlab compatible,
m-script – Matlab/Octave's function file.

4.2. General perspective

4.2.1. Requirements

Main requirements for storage of the captured records are following:

1. Must be easy to handle in LV, CVI, Octave and Matlab or plain C/C++.
2. Must be human readable and editable.
3. Must be memory-saving because of streaming modes from fast digitizers.
4. Must allow writing of small and large matrices.

The requirements are contradicting. A human readable format is hardly memory saving. There is not a data format that fulfil all requirements. The most promising are XML, Yaml, INI, JSON, TOML, GNU Octave native format, INFO, Mat-vX:

- XML: very structured, supported, matrices are hard to read and write by human, memory inefficient,
- Yaml: human readable, easy to read and write, matrices are hard to read and write, memory inefficient,
- TOML: human readable, easy to read and write, matrices are hard to read and write, memory inefficient,

- INI: human readable, easy to read and write, matrices are not supported, memory inefficient,
- GNU Octave native format: human readable, easy to read, hard to write, matrices are easy to read and write, memory inefficient,
- Mat-vX: not human readable, binary format, very supported, hard to read write, memory efficient,
- INFO: human readable, not supported anywhere, easy to read write, memory inefficient.

4.2.2. Solution

After analysing possibilities, it was decided to use combination of two files. First, the raw data are stored in binary format. Second, the header is stored as a human readable text file. To keep the files together, the sampled data are stored in a single folder.

Organization of the files in the measurement folder is following:

Measurement folder named by user

↳ **session.info** - *text file with measurement header*

↳ RAW - *folder with raw waveform records*

↳ ***.mat** - *binary file with raw waveform records*

4.3. Binary files with raw waveform records

4.3.1. Requirements

Requirements for the binary format are following:

1. easy to handle,
2. support in LabVIEW, Matlab and GNU Octave (based on questioning the participants).

There are many binary formats for data storage. Yet the support for the formats is various.

4.3.2. Solution

After analysing possibilities, it was decided to use Matlab MAT version 4 format. **MAT-v4** file format is very primitive and easy to handle format. It has already support in many data analysing software.

Format description

The **MAT-v4** format has following file structure:

Offset	Item type	Description
0	DWORD	ID if the variable data type.
4	DWORD	Rows count M.
8	DWORD	Columns count N.
12	DWORD	Is complex flag.
16	DWORD	Length Q of the name.
20	[BYTE*Q]	Name of the variable including '\0' EOS.
20+Q	[M*N*item_size]	Array of the items organized per columns [column_1, column_2, …, column_M].
…	… next variable …	

The limitation of the format is the data cannot have more than 4 GSa as the matrix dimensions are store in 32-bit variables (Matlab actually states only 100 M items are allowed). However, the format may be in future replaced by plain binary if the limitation became important. Only difference will be saved routine in LV/CVI and a few lines of a loader function in Matlab/GNU Octave. The concept of the measurement data is prepared on possibility of multiple formats.

Variables

The sample data from all channels are merged and stored into the 2D matrix variable called '**y**', one row per channel. Traditional order one column per channel is not possible due to internal structure of MAT format – during streaming of data to the file it is easy to add columns, however whole file has to be reordered to add rows. In order to minimize HDD usage and maximize the data throughput, the sample data are stored directly in the integer format generated by the digitizers. So far, only two formats are considered (i) INT32 and when possible, in terms of resolution (ii) INT16. If the selected HW supports logging of the temperature, the MAT file will also contain two variables with temperatures. Two variables are related to the temperature:

temp_sample – 1D array of the sample indices when the temperature was measured (float32)

temp_data – 2D array of measured temperatures in float32 (rows: channels, columns: readings)

Note the '**temp_sample**' values are indices of the sample where the temperature was measured, i.e., value 100 means hundredth sample, 1000 means thousandth sample, etc. The sampling rate for the temperature is set to 10 seconds so there is not unnecessarily lot of values.

The file naming rules for the record data are show in the following table:

RAW records data (./RAW/):

G0001-A0001.mat - *record for 1. average of 1. group*

G0001-A0002.mat - *record for 2. average of 1. group*

G0002-A0001.mat - *record for 1. average of 2. group*

G0002-A0002.mat - *record for 2. average of 2. group*

4.4. Data header format

4.4.1. Requirements

File related to the raw records should be a human readable header. The file structure must support following:

1. sections/subsections/...,
2. numeric matrices,
3. string matrices.

Up to it, the format must be:

1. easy to write and read programmatically,
2. easy to write and read manually.
3. using standards if available.

While it is not expected to make whole header files manually, it is common practice by users to fix some values "later" or read properties by various software.

The minimum required information written to the header are:

- digitizer designation,
- digitizer serial number,
- count of used channels,
- range,
- sampling mode (if available),

- sampling rate,
- aperture,
- trigger mode,
- timestamps (if available).

4.4.2. Solution

After analysing possibilities, it was decided the header will be stored as text file in INFO format developed at CMI [1]. This is very simple 'braindead' text format which can be generated by any program or can be written manually, and it is also very easy to read. Libraries are available for LV, Octave and Matlab and can be implemented even for C/C++.

Each header of the measurement (= one measurement session) is structured into following levels: (i) Session, (ii) Repetition group, (iii) Record. The groups are intended for statistical processing. E.g.: the N records made within the group will be averaged and type A uncertainty will be calculated. Each group has different sampling setup which is intended for the future sequenced measurements, such as frequency dependence, level dependence, etc.

Each session (i) contains one or more repetition groups (ii) defined by item '**groups count**'. The session (i) always contains setup of the HW, which is common for all groups (ii), such as HW identifiers, capabilities of HW, etc. Next, it contains '**measurement group G**' sections (ii), where **G** is index of the group. Each group (ii) contains setup that is unique for each group, such as number of samples, sampling rate, etc. Finally, each group also contains information about particular records (iii) within the group.

The example of the header of the record that contains one measurement group is shown in the following text:

// ====== COMMON SETUP ======
// Unique identifiers of each channel:
#**startmatrix**:: channel descriptors
HP3458A, sn. MY45053095
HP3458A, sn. MY45053104
#**endmatrix**:: channel descriptors
// unique identifiers of auxiliary HW (AWG, Counter, …):
#**startmatrix**:: auxiliary HW descriptors

#**endmatrix**:: auxiliary HW descriptors
// number of virtual channel of the digitizer:
channels count:: 2
// file format of the sample data:
sample data format:: mat-v4
// name of the variable with the sample data:
sample data variable name:: y
// number of measurement groups:
groups count:: 1
// digitizer has temperature measurement capability?:
temperature available:: 0
// digitizer has temperature logging during sampling?:
temperature log available:: 0
// DMM sampling mode (HW specific attribute):
sampling mode:: DCV
// DMM synchronization mode (HW specific attribute):
synchronization mode:: MASTER-SLAVE, MASTER clocked by TIMER

#startsection:: measurement group 1
// ====== GROUP #1 ======

// number of repetition cycles (repeated records):
repetitions count:: 3
// number of desired samples per record:
samples count:: 10000
// set sampling rate:
sampling rate [Sa/s]:: 48000.0000000000
// voltage ranges for each channel:
#startmatrix:: voltage ranges [V]
1.00; 1.00
#endmatrix:: voltage ranges [V]
// DMM aperture time (HW specific attribute):
aperture [s]:: 1e-6
// trigger setup:
trigger mode:: Immediate

// ====== RECORDS ======
// relative file paths to the files with sample data:
#startmatrix:: record sample data files
RAW\G0001-A0001.mat
RAW\G0001-A0002.mat
RAW\G0001-A0003.mat
#endmatrix:: record sample data files
// actual samples counts for each record file:
#startmatrix:: record samples counts
10000
10000
10000
#endmatrix:: record samples counts
// time increment (sampling period) for each record:
#startmatrix:: record time increments [s]
2.08333333333333E-5
2.08333333333333E-5
2.08333333333333E-5
#endmatrix:: record time increments [s]
// gain factors for scaling of the sample data for each channel and record:
#startmatrix:: record sample data gains [V]
9.9999997E-10; 9.9999997E-10
9.9999997E-10; 9.9999997E-10
9.9999997E-10; 9.9999997E-10
#endmatrix:: record sample data gains [V]
// offset for scaling of the sample data for each channel and record:
#startmatrix:: record sample data offsets [V]
0.0000000; 0.0000000
0.0000000; 0.0000000
0.0000000; 0.0000000
#endmatrix:: record sample data offsets [V]
// relative timestamp for each channel and record (initial time of first sample):
#startmatrix:: record relative timestamps [s]

0.0312291666666667; 0.0312291666666667
0.406229166666667; 0.406229166666667
0.687479166666667; 0.687479166666667
#endmatrix:: record relative timestamps [s]
// absolute timestamps of each record start (using low. res system time):
#startmatrix:: record absolute timestamps
2014-03-03T22:18:53.77343750000000000001
2014-03-03T22:18:54.16308593749999999997
2014-03-03T22:18:54.47265625000000000002
#endmatrix:: record absolute timestamps

#endsection:: measurement group 1

Meaning of the particular items of the header file should be obvious from the attached comments. Note the comments introduced by '***//***' are not required. It is just for documentation. Note the INFO format can handle any text aside of the keys and keywords. However, the keys and key words starting with '#' must be the first non-white symbol in the line.

4.5. References

[1] INFO-STRINGS, url: https://github.com/KaeroDot/info-strings
[2] QWTB toolbox, url: https://qwtb.github.io/qwtb/

5. STUDY OF SUITABLE ALGORITHMS

5.1. Software for calculation and propagation of uncertainties

5.1.1. Q-Wave Toolbox

A common situation in the data processing of sampled signal is the estimation of multiple quantities using the same record. The user is interested in the amplitude and the phase of the main signal component, in a spectrum and stability of these quantities during multiple records. For the case of evaluating the properties of a digitizer, spurious free dynamic ratio (SFDR), total harmonic distortion (THD) and effective number of bits (ENOB) are important quantities. Algorithms exists for all of these quantities, but it is a complex task to learn how to use every single algorithm.

Q-Wave toolbox (QWTB) can help with this situation [1]. It is a software toolbox written in M-code and is running in *Matlab* [2] or *GNU Octave* [3]. It aims for the aggregation of high-quality algorithms required for data processing of sampled measurements. QWTB consist of data processing algorithms from different sources, unifying application interface and graphical user interface.

The toolbox gives the possibility to use different data processing algorithms with one set of data and removes the need to reformat data for every particular algorithm. Toolbox is extensible.

5.1.2. TracePQM wattmeter

The QWTB was designed to help using general quantity estimating algorithm. However, it was not tailored for actual metrological measurements. Therefore, during development of TWM (TracePQM Wattmeter) an extension of the QWTB interface was formulated.

TWM is a transparent, metrology grade measurement system for traceable measurement of Power and Power Quality (PQ) parameters. It is designed to allow recording of voltage and current waveforms using various digitizers and processing the measured waveforms using any algorithm.

TWM defined name space for quantities needed for transducers, errors of connecting transducers to digitizers. During the TracePQM project [4], new versions of algorithms were developed capable of using the defined quantities. The core of TWM relies on QWTB.

5.1.3. QWTB variator

The estimation of algorithm errors was not solved successfully in QWTB nor in the TWM extension. Therefore, a Q-Wave toolbox variator *QWTBvar* was developed. It is a system that can:

- variate input quantities or its uncertainties,
- calculate errors of output quantities to the nominal values,
- plot dependence of output quantities on the varied input quantities or its uncertainties,
- create lookup table of uncertainties of output quantities,
- interpolate the lookup table for quick estimation of uncertainties.

5.2. Algorithms

Two algorithms have been selected:

- TWM-THDWFFT
- TWM-MFSF

The TWM-THDWFFT algorithm is designed for calculation of the harmonics and THD of the non-coherently sampled signal. It uses windowed FFT to detect the harmonic amplitudes, which limits the achievable accuracy of the harmonics detection due to the window scalloping effect.

TWM-MFSF is an algorithm for estimating the frequency, amplitude, and phase of the fundamental and harmonic components in a waveform. Amplitudes and phases of harmonic components are adjusted to find minimal sum of squared differences between the sampled signal and the multi-harmonic model.

A detailed description of both algorithms can be found in TWM project documentation [5].

5.3. Method overview

First a simulated signal is constructed. Next both algorithms are used to calculate THD value using GUF (GUM uncertainty framework) [6], and Monte Carlo [7] methods. Both results are plotted into figures.

The framework used to run the simulations is QWTB. Script `alg_compare.m` is used to set values and plot figures. For every dependence (e.g., THD on noise or THD on signal frequency) script calls function `qwtbvar` that is responsible for variation of inputs. `qwtbvar` calls the script `thdtest.m` that constructs a signal and calls `qwtb` to calculate results.

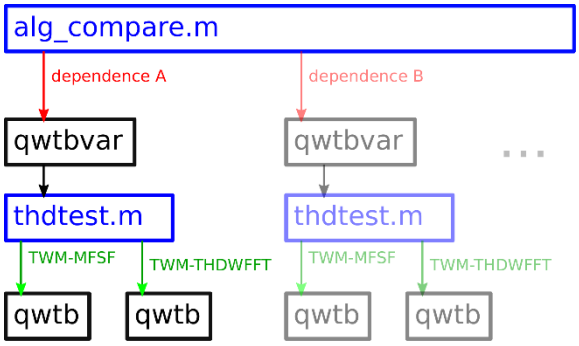

Fig. 5.1. *Overview of the method: alg_compare.m sets values and plot figures, qwtbvar variates inputs, thdtest.m construct a signal, qwtb to calculate results.*

5.4. The testing signal

The following properties of the testing signal were used during comparison. Acquisition quantities:

- sampling frequency: 50 kHz,
- record length 100 kSa,
- resolution of the digitizer: 24 bit.

Signal quantities:

- frequency: 50.01 kHz,
- main signal component amplitude: 1 V,
- number of signal components: 5,
- amplitudes of harmonics 2 to 4: 0.01 V,
- signal components phases: 0 rad,
- offset: 0 V,
- standard deviation of noise: 10 μV.

5.5. Comparison results

5.5.1. Influence of noise

Following figures show out the dependence of the THD value on the sigma of the noise simulated in the signal. Fig. 5.2 was generated for uncertainties calculated using GUF, Fig. 5.3 with uncertainties calculated using MCM.

The value of THD calculated using THDFFT algorithm shows out a small offset, compared to the results of the MFSF algorithm. The uncertainties are mostly covering the error of the THD for both methods. However, the WFFT algorithm does not implement MCM uncertainties correctly and only uncertainties calculated by GUF are relevant.

The uncertainties are affected by the noise and increased linearly with increasing noise, as can be expected.

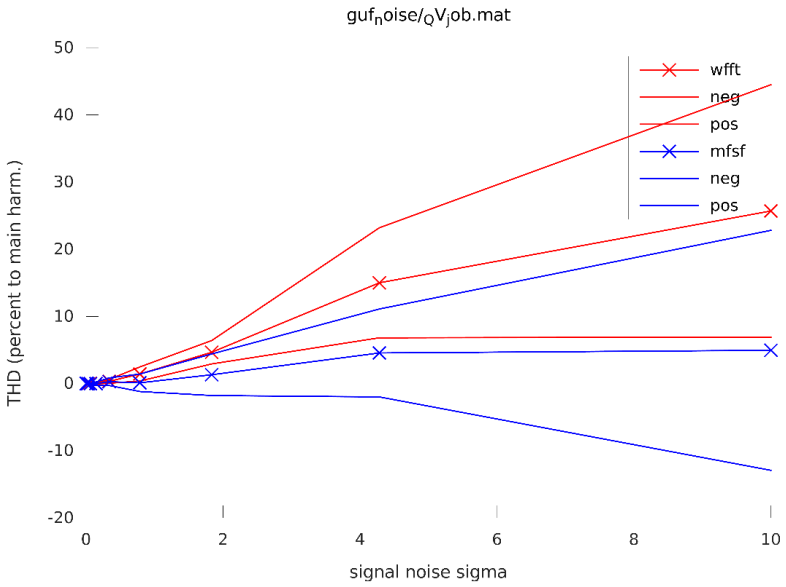

Fig. 5.2. *THD vs sigma of the noise. Uncertainty bounds are calculated using GUF.*

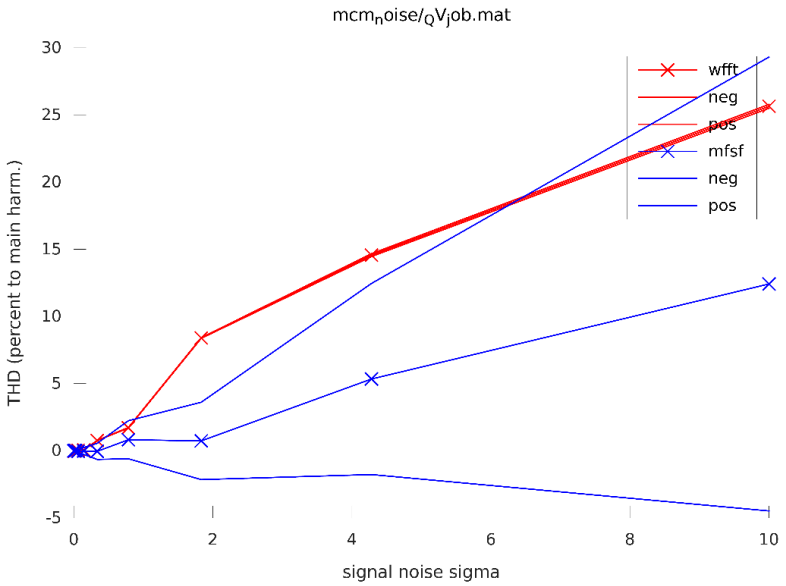

Fig. 5.3. *THD vs sigma of the noise. Uncertainty bounds are calculated using MCM.*

5.5.2. Influence of signal frequency

Fig. 5.4 shows out the dependence of THD value on the frequency of the main signal component with uncertainties calculated using GUF.

The value of THD calculated using THDFFT shows a variation on the signal frequency, which is to be expected due to principles of the implemented Discrete Fourier Transformation. The MFSF is not affected by signal frequency because of the implemented fitting method.

The uncertainties cover the THD errors for both methods.

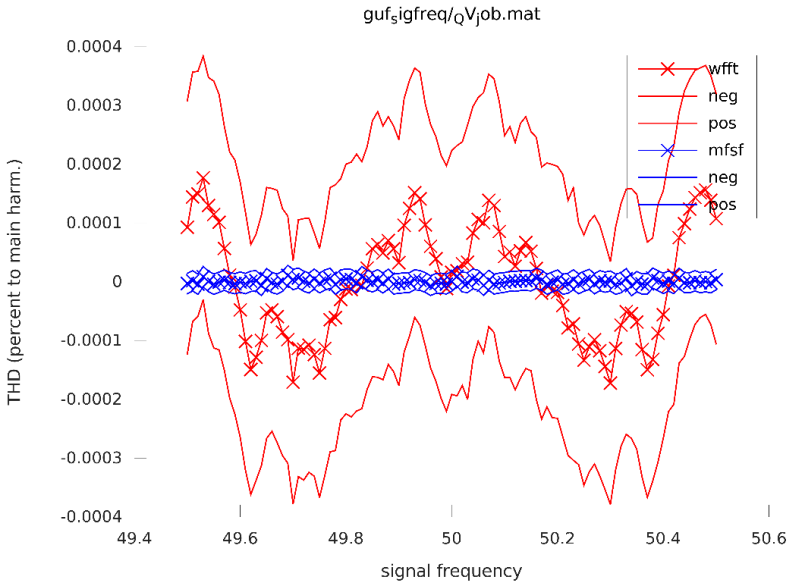

Fig. 5.4. *THD vs signal frequency. Uncertainty bounds are calculated using GUF.*

5.5.3. Influence of signal length

Fig. 5.5 shows out the dependence of THD value on the length of the record component with uncertainties calculated using GUF.

Again, the value of THD error is smaller for MFSF method. The uncertainties cover the THD errors for both methods.

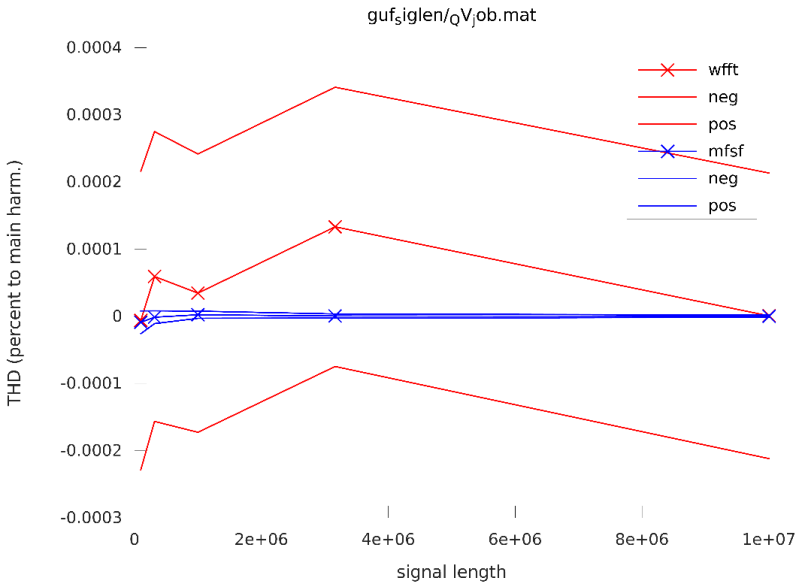

Fig. 5.5. *THD vs length of record. Uncertainty bounds are calculated using GUF.*

5.5.4. Influence of THD

Fig. 5.6 shows out the dependence of calculated THD value on the simulated THD value of the signal with uncertainties calculated using GUF. The errors are very small for both methods. The most interesting fact is zero or small dependence of MFSF uncertainty on the THD value.

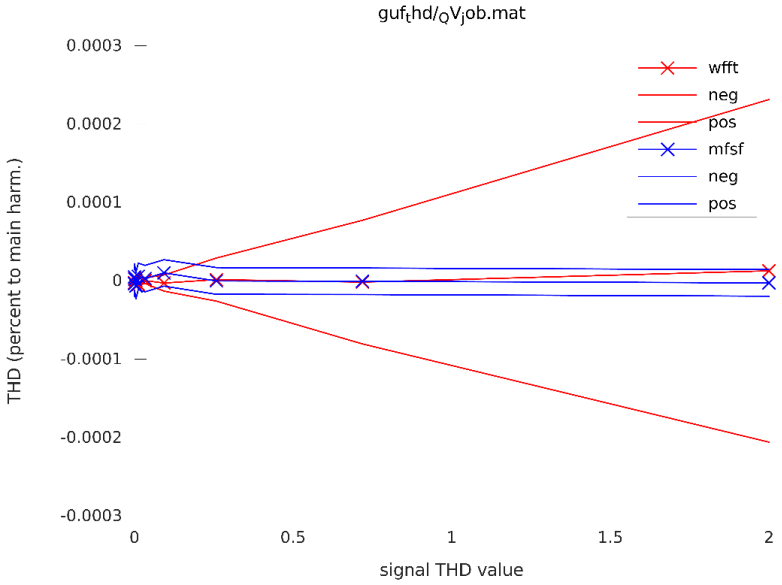

Fig. 5.6. *THD vs THD value. Uncertainty bounds are calculated using GUF.*

5.6. Comparison conclusion

The comparison showed out several things.

1. Both algorithms calculate GUF uncertainties correctly, i.e., the uncertainty is greater than the error of the algorithm, for at least 95 % of results.
2. The MFSF algorithm errors are much smaller than the WFFT algorithm ones.
3. For several cases the uncertainties of the MFSF algorithm are much smaller than the uncertainties of the WFFT algorithm.

Results validated the use of both algorithms, as described in item 1. As uncertainties are greater than the errors originated in the algorithm, the calculation can be considered as validated.

It seems that performance of MFSF algorithm is greater than WFFT one. However, the algorithms differ in one important point. The WFFT algorithm only requires a maximal harmonic to be evaluated. On the contrary, the MFSF algorithm requires the knowledge of all harmonics present in the signal. In the case of incorrect input information, the results will also be incorrect. This feature has yet to be properly evaluated.

5.7. References

[1] M. Šíra, *QWTB - Software Toolbox for Sampling Measurements*, Czech Metrology Institute, 2017. [Online]. Available: https://qwtb.github.io/qwtb/ (visited on 05/24/2019).
[2] *Matlab*, 2012. [Online]. Available: http://www.mathworks.com.
[3] *GNU Octave*, 2012. [Online]. Available: https://www.gnu.org/software/octave/.
[4] TracePQM consortium. (2019), [Online]. Available: http://tracepqm.cmi.cz.
[5] S. Mašláň, “Report A2.4.4: TWM algorithms description,” Czech Metrology Institute, A2.4.4, p. 38. [Online]. Available: https://github.com/smaslan/TWM/blob/master/doc/A244%20Algorithms%20description.pdf visited on 31/05/2021).

[6] JCGM, *Evaluation of Measurement Data - Guide to the Expression of Uncertainty in Measurement*. Bureau International des Poids et Measures, 1995, ISBN: 92-67-10188-9. [Online]. Available: https://www.bipm.org/en/publications/guides/.

[7] JCGM, *Evaluation of Measurement Data - Supplement 1 to the "Guide to the Expression of Uncertainty in Measurement" - Propagation of Distributions Using a Monte Carlo Method*. Bureau International des Poids et Measures, 2008. [Online]. Available: https://www.bipm.org/en/publications/guides/.

6. UNCERTAINTY ESTIMATION

6.1. Introduction

The aim of this task is to evaluate the sources of uncertainties in digital measurement of waveforms and to calculate uncertainty propagation for the whole traceability chain. The output of this task is to provide models and approaches for fast on-site calculations of uncertainties.

The uncertainties of voltages higher than 10 V are calculated according to best calibration capabilities based on established voltage metrology. This report is prepared in this stage to share experience and knowledge on digital traceability.

Uncertainty estimation is based on the measurement procedures and the algorithms used to obtain measurement parameters as well as uncertainty sources. Current measurements are also based on voltage measurements. For these reasons the report is planned as follows:

- Firstly, detailed instructions on measurement procedure for voltage are presented, including equipment/systems which are available in the market, possible measurement setups and explanation of the calibration process which defines with which setup/configuration to use which algorithm and presents ideas for choosing references to be used to reach the uncertainty goals.
- Briefly steps of calibration for both voltage sampler and voltage source calibration are defined.
- Model functions of the measurements are given in detail including the uncertainty sources and their estimated values.
- Finally, information about uncertainty calculations and the scope is presented.

6.2. Calibration procedure

6.2.1. Brief description of the calibration

AC voltage measurement with sampling techniques is used in the amplitude calibration of low frequency voltage sources, frequency response calibration of ADCs and measurement of the effective (RMS) value of multi-tone stable voltage waves [8].

In this report, measurement setups used for voltage measurement with sampling techniques are introduced, the principles to be followed in sample gathering and how to calculate the effective value of AC voltage depending on these are defined.

If the calibration object is the sampler (ADC) or voltage-meter, the reference device is the voltage source. If the calibration object is the DAC or voltage source, the reference device is the sampler.

6.2.2. Quantity/calibrated instrument

Voltage (Effective Value of Voltage Wave), Voltage Gain, Non-Linearity Parameters (INL, ENOB, SINAD), Voltage Source, Signal Source, Calibrator, Sampler, ADC

6.2.3. Range

Voltage ranges: 5 mV to 700 V, 10 mHz to 100 kHz.

6.2.4. Calibration setup

Depending on the synchronization capabilities (CLK IN, CLK OUT, Phase Lock...) of the calibration object and the reference device, three different measuring setups can be defined for sample collection. These arrangements are given in Fig. 6.1 to Fig. 6.3.

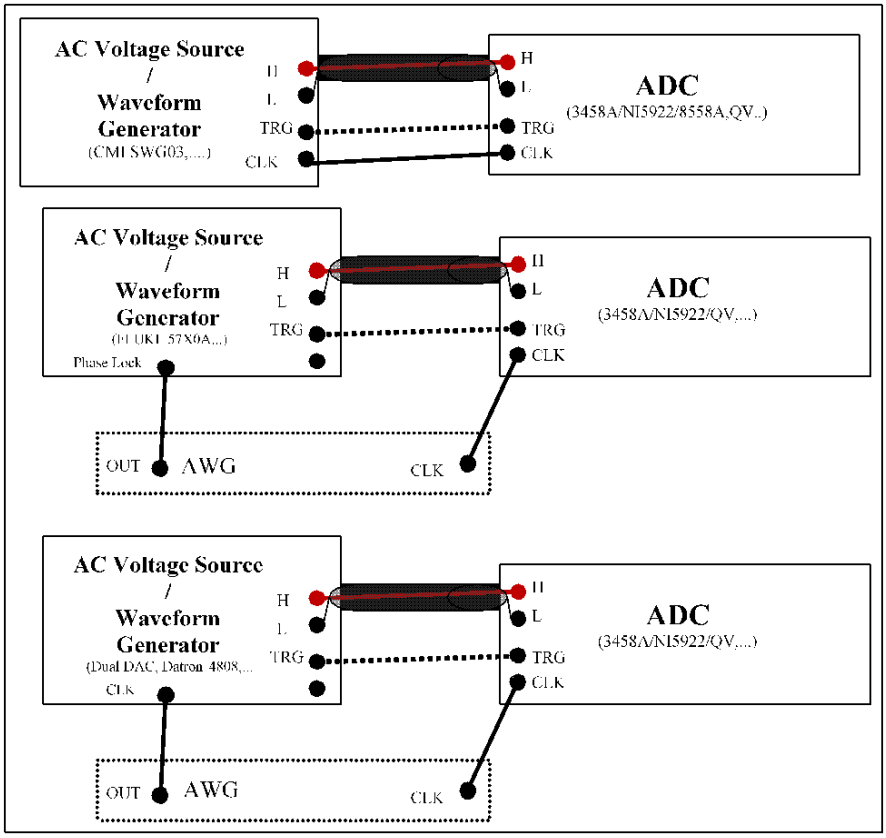

Fig. 6.1. *Synchronous Sampling*

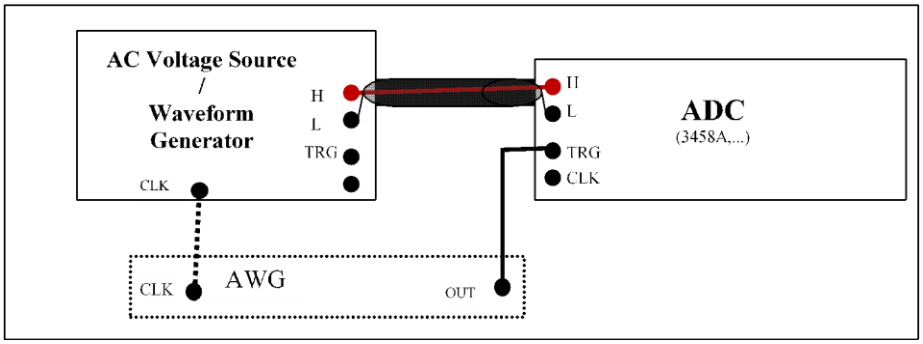

Fig. 6.2. *Semi - Synchronous Sampling*

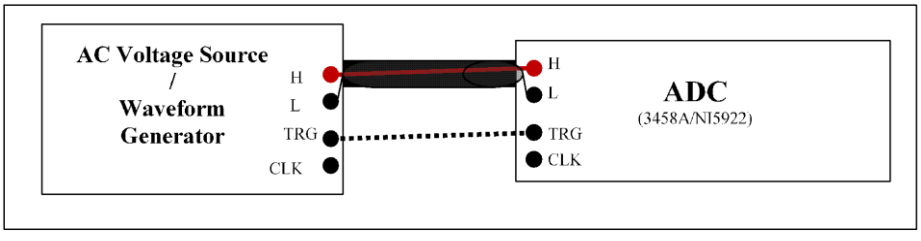

Fig. 6.2. *Asynchronous Sampling*

6.2.5. Equipment required

Table 6.1. *Overview of the needed equipment.*

Equipment	Manufacturer	Model
Sampler	Fluke	8558A
	HP/Agilent/Keysight	3458A
	NI	5922
	Quantum Voltmeter (QV)	
	ADC	
AC Voltage Source	FLUKE	57X0A
	FLUKE	55X0A
	Datron	4808
	LeCroy	ArbStudio 1104
	Tektronix	AFG 3022C
	DAC	
	JAWS	
	PJVS	
	Aivon	DualDAC
	CMI	SWG03
Arbitrary Waveform Generator	LeCroy	ArbStudio 1104
	Tektronix	AFG 3022C

6.2.6. Explanation of the calibration process

The first step in sampling measurements is to obtain voltage samples. Voltage measurement with sampling techniques is basically performed in three different setups. According to the periods (frequencies) of measuring and generating signals; it can be defined as synchronous sampling, semi-synchronous sampling and asynchronous sampling. These setups require the use of different methods/algorithms and/or the evaluation of different sources of uncertainty in calculating and evaluating the uncertainty of AC voltage parameters from the collected samples.

The measurement setup for synchronous sampling is given in Fig. 6.1. In these setups, the timing signals of the voltage source and the sampler (ADC) are matched and the condition $f_s = f_m \times N$ ($N \epsilon Z^+$, Z^+: set of positive integers) is satisfied. If the timing (CLK) inputs and outputs of both the signal source and the sampler are compatible, the setup shown in Figure 1 at the top is set up. When the frequencies of the timing output (CLK) of the sampler and the timing (CLK) input of the AC voltage source are different (as in the FLUKE 57X0A calibrators), to synchronize the source and sampler the timing signal of an arbitrary waveform generator (CLK of AWG) and the timing signal of the sampler are synchronized as shown in Fig. 6.1 at the middle. In Fig. 6.1, at the bottom setup, the measurement setup used is given when the frequencies of the timing signals of the voltage source and the sampler are compatible, but the amplitude and waveforms are not.

When the CLK of the ADC is not accessible by the user, as with the 3458A sampler, the CLK of the AC signal source is matched with the CLK of the AWG, making the AWG generate a signal at the sampling frequency. This signal is applied to the trigger input of the sampler as shown in Fig. 6.2. The methods of calculating the effective value from the samples obtained using this setup are the same as with the synchronized measurements, and the jitter of the sampling period should be taken as half of the CLK of the sampler when evaluating the measurement uncertainty.

In the case that the AC voltage source and the sampler's CLKs cannot be matched, the sampler and the AC voltage source are directly connected. This measurement setup is called Asynchronous Sampling and is given in Fig. 6.3.

The phase of the measured signal has no effect on the effective value measurement. Therefore, it is not necessary to use the trigger signal to start the measurement and the trigger signal is shown with a dashed line in the measurement setups in Fig. 6.1 to Fig. 6.3.

In order to use this instruction, in all measurements the ratio of the sampling frequency (f_s) of the sampler (ADC) to the frequency of the source (f_m), in other words, the sampling rate ($R= f_s/f_m$) must be at least two. If the sampling rate is below 2, the guidelines in [1] should be taken into account.

In sampling measurements, samples are obtained with ADC, IADC or ΣΔ-ADC or QV. Examples are a two-dimensional array with one dimension containing time and the other amplitude data. Table 6.2 describes how the effective value of the sinusoidal (single tone) signal can be calculated from these samples. Table 6.3 summarizes how the effective value of each tone of multi-tone signals can be calculated.

Table 6.2. *Methods/algorithms for calculating effective value of single tone voltage waves.*

Measuring Setup	Sampler	RMS formula	Discrete Fourier Transform	3-Parameter Sine Fitting	4 Parameter Sine Fitting
Synchronous	IADC	✓	✓	✓ [5]	✓ [6]
	ΣΔ-ADC	✓	✓	✓ [5]	✓ [6]
	QV	✓	× [4]	✓ [5]	✓ [6]
Semi-synchronous	IADC	✓ [1]	✓ [1]	✓ [1,5]	✓ [1,6]
Asynchronous	IADC	× [2]	× [3]	✓ [7]	✓ [8]
	ΣΔA-DC	× [2]	× [3]	✓ [7]	✓ [8]

[1] - Half of the CLK period of the ADC should be considered as the jitter parameter.

[2] - Samples may not represent a whole period, as it may not be an integer when the sampling (f_s) frequency of the sampler (ADC) is divided to the frequency of the source (f_m). Therefore, instability between measurements may be high.

[3] - The window effect should be evaluated, as the ratio obtained when the sampling (f_s) frequency of the sampler (ADC) is divided to the frequency of the source (f_m).

[4] - Samples will not be evenly spaced in time domain when the QV's sampler is the NI5922.

[5] - Fitting frequency should be taken $f_m=f_s/N$

[6] - Starting frequency should be taken $f_m=f_s/N$

[7] - When f_m and f_s are determined according to the same frequency standard and time data of the sampler is corrected according to the frequency measurement result, the algorithm gives results with high accuracy. The amount of data must be greater than one period.

[8] - This algorithm can be used when f_m is too small to be measured with a frequency counter. There must be at least five periods of data. When f_m is estimated correctly, the signal-to-noise ratio of the fitted curve (SNR=10*log($\frac{V_{RMS\_D}^2}{P_{error}}$) is calculated within expected values. If the SNR is worse, by trying different starting frequencies for f_m, iteration should be continued for the lowest SNR.

Table 6.3. *Methods/algorithms for calculating effective value of each tone of multi-tone voltage waves[1].*

Measuring Setup	Sampler	Discrete Fourier Transform	3-Parameter Sine Fitting	4 Parameter Sine Fitting
Synchronous	IADC	✓ [2]	✓ [3]	✓ [3]
Synchronous	ΣΔ-ADC	✓ [2]	✓ [3]	✓ [3]
Synchronous	QV	×	✓ [3]	✓ [3]
Semi-synchronous	IADC	✓ [2]	✓ [3]	✓ [3]
Asynchronous	IADC	×	✓ [4]	✓ [5]
Asynchronous	ΣΔ-ADC	×	✓ [4]	✓ [5]

[1] - The footnotes given in Table 6.2 are taken into account.

[2] - Tones must be harmonics of f_m ($k \times f_m$; k=0,1,2,3... , where $k \times f_m < f_s/2$).

[3] - Tones $f_k = k \times f_s/(M \times N)$; k=0,1,2,3... where $f_k < f_s/2$.

[4] - f_k frequencies must be estimated/measured correctly.

[5] - Footnote ([8]) in Table 6.2 should also be taken into account for f_k frequencies.

6.2.7. Calibration process

Voltage Source

If the calibration object is the voltage source/DAC, select the appropriate reference sampler given in Table 6.4 according to the frequency, amplitude and uncertainty target of the voltage quantity to be calibrated.

Table 6.4. *Amplitude frequency ranges and least possible uncertainties of reference device/systems.*

Calibration Object	Reference System/Device	Amplitude Range	Frequency Range	Possible Uncertainties
Voltage Source/DAC	IADC	5 mV to 750 V	1 mHz to 2 kHz	1,5 µV/V to 55 µV/V
	ΣΔ-ADC	<3 V	≤100 kHz	>100 µV/V
	QV	<8 V	1 Hz to 2 kHz	0.5 µV/V to 3 µV/V
Voltage Sampler	Calibrator (FLUKE 57X0A, Datron 4808)	0.8 V to 700 V	10 Hz-100 kHz	>20 µV/V
	PJVS	<1 V	< 500 Hz	0.5 µV/V
	Aivon DualDAC	< 10V	6 Hz to 10 kHz	>50 µV/V
	CMI SWG03	<10 V	< 100 kHz	>50 µV/V

Select the appropriate sampling type, taking into account the timing signals of the reference sampler and the source.

Set up the measurement setup suitable for the sampling type and device as given in Fig. 6.1 to Fig. 6.3.

Select the Sampling Rate ($R = f_s/f_m = N > 8$) where f_s is the sampling frequency and f_m is the frequency of the sampled voltage wave. Determine the number of periods to be collected as $M = f_s/f_{network}$ integer and $f_m \neq f_{network}$.

Collect voltage samples by adjusting the voltage generator, voltage sampler and AWG according to the use in Fig. 6.1 to Fig. 6.3. using the device manufacturers' manuals. If software is used to collect voltage samples, validate the software as in [2, 3].

Using the samples collected, if the calibrated voltage is single tone, choose the appropriate method from Table 6.2 and calculate the effective value of the signal using the model functions given in Section 6.2.8.

If the calibrated voltage wave is multi-tone, choose the appropriate method from Table 6.3 and calculate the effective value of each tone of the signal by using the model functions given in Section 6.2.8.

Apply the correction according to the bandwidth of the sampler used, using the model functions given in Section 6.2.8.

Apply the corrections from the stray circuit parameters of the sampler, voltage source and cables used, using the model functions given in Section 6.2.8.

Find the calibration result using the equations given in Section 6.2.8.

Voltage Sampler

If the calibration object is voltage-sampler/ADC, select the appropriate reference voltage source given in Table 6.4 according to the frequency and amplitude of the voltage quantity to be calibrated and the uncertainty target.

Select the appropriate sampling type, taking into account the timing signals (CLK) of the reference source and sampler.

Set up the measurement setup suitable for the sampling type and device as given in Fig. 6.1 to Fig. 6.3.

Select the Sampling Rate ($R = f_s/f_m = N>8$) where f_s is the sampling frequency and f_m is the frequency of the sampled voltage wave. Determine the number of periods to be collected as $M = f_s/f_{network}$ integer and $f_m \neq f_{network}$.

Collect voltage samples by adjusting the voltage generator, voltage sampler and AWG according to the use in Fig. 6.1 to Fig. 6.3 using the device manufacturers' manuals. If software is used to collect voltage samples, validate the software as in [2, 3].

Using the samples collected, if the calibrated voltage is single tone, choose the appropriate method from Table 6.2 and calculate the effective value of the signal using the model functions given in Section 6.2.8.

If the calibrated voltage wave is multi-tone, choose the appropriate method from Table 6.3 and calculate the effective value of each tone of the signal by using the model functions given in Section 6.2.8.

Apply the correction according to the bandwidth of the sampler used, using the model functions given in Section 6.2.8.

Apply the corrections from the stray circuit parameters of the sampler, voltage source and cables used, using the model functions given in Section 6.2.8.

Using the equations given in Section 6.2.8, find the calibration result by calculating the gain of the voltage sampler for the f_m frequency if the sampled wave is single tone. Find the calibration result by calculating the gain of the voltage sampler for the f_k frequencies if the sampled wave is multi-tone (dynamic gain).

6.2.8. Model functions

The model function of an $x[n]$ sample is given in (6.1). M is the number of periods sampled, $n = 1, 2, \ldots, M \times N$, where $N=R$ is the number of samples per period.

$$x[n] = V_J + \frac{1}{T_i+\delta_{JTi}}\left(1 + \delta_{REF} + \delta_G + \frac{\delta_{LIN}+\delta_{RES}}{|V_{ADC}|}V_{FS}\right)\int_{vT_a+\delta_{JTa}}^{vT_a+\delta_{JTa}+T_i+\delta_{JTi}}\{v_i(t) + v_s(t)\}dt + v_{sn}(t) \quad (6.1)$$

Calculation of Effective Value by the RMS Formula

$$V_{RMS\_D} = \sqrt{\frac{1}{M\times N}\sum_{n=1}^{M\times N} x[n]^2} \tag{6.2}$$

If the sampled signal is a sinusoidal voltage wave with frequency f_m, the corrections in (6.3) are applied to the calculated value of V_{RMS_D}.

$$V_{RMS\_D} = \frac{V_{rms\_D}}{\mathrm{sinc}(\pi\times f_m\times T_i)} \tag{6.3}$$

Calculation of Effective Value by Discrete Fourier Transform (DFT)

By treating the real part of DFT as a separate magnitude defined by (6.5), and the imaginary part as a separate quantity defined by (6.6) [4], the effective value of the sampled voltage is determined by (6.7) [4] for tones at $k \times f_m$ frequencies by taking k = 0,1,2,…

$$X[k] = \frac{2}{K}\sum_{n=0}^{K-1}\frac{x[n+1]}{\left|sinc\left(\frac{\pi T_i k}{KT_a}\right)\right|}.e^{-\mathrm{j}2\pi f_k nT_a}.e^{-\mathrm{j}\frac{\pi T_i k}{KT_a}} \text{ , } K=M\times N \tag{6.4}$$

$$F_1(k,n) = \cos\left(\frac{2\pi kn}{K}\right), \quad F_2(k,n) = -\sin\left(\frac{2\pi kn}{K}\right)$$

$$F_3(k,n) = \frac{-2\pi kT_i\times\cos\left(\frac{2k\pi T_i}{KT_a}\right)\times\sin\left(\frac{2k\pi T_i}{KT_a}\right)}{KT_a\left(\frac{2k\pi T_i}{KT_a}-1\right)} \text{ , } F_4(k,n) = \frac{2\pi kT_i\times\sin\left(\frac{2k\pi T_i}{KT_a}\right)\times\sin\left(\frac{2k\pi T_i}{KT_a}\right)}{KT_a\left(\frac{2k\pi T_i}{KT_a}-1\right)}$$

The Real Part of the Discrete Fourier Transform

$$Re(X[k]) = \frac{2}{K}\sum_{n=0}^{K-1} x[n+1]\{F_1(k,n)F_3(k,n) - F_2(k,n)\times F_4(k,n)\} \tag{6.5}$$

The Imaginary Part of the Discrete Fourier Transform

$$Im(X[k]) = \frac{2}{K}\sum_{n=0}^{K-1} x[n+1]\{F_1(k,n)\times F_4(k,n) + F_2(k,n)\times F_3(k,n)\} \tag{6.6}$$

$$V_{RMS\_D}(k) = \frac{\sqrt{Re(X[k])^2+Im(X[k])^2}}{\sqrt{2}} \tag{6.7}$$

Calculation of Effective Value by Three Parameter Sine Fitting

The ***S*** matrix, minimizing the P_{error} term defined below, is found by (6.8) [1]. The ***S*** matrix is the signal parameters of the fitted $x[n]'$ curve. After finding the ***S*** matrix, calculate the effective (RMS) value of each tone using (6.9).

$$P_{error} = \frac{\sum_{n=1}^{M\times N}\left(x[n]-x[n]'\right)^2}{M\times N}$$

$$x[n]' = A_1\cos\left(2\pi f_1 t[n]\right) + B_1\sin\left(2\pi f_1 t[n]\right) + C_0 + \cdots + A_k\cos\left(2\pi f_k t[n]\right) + B_k\sin\left(2\pi k f_k t[n]\right)$$

$$D_0 = \begin{vmatrix} \cos(2\pi f_1 t[1]) & \sin(2\pi f_1 t[1]) & 1 & \cdots & \cos(2\pi f_k t[1]) & \sin(2\pi f_k t[1]) \\ \vdots & \vdots & \vdots & \ldots & \vdots & \vdots \\ \cos(2\pi f_1 t[n]) & \sin(2\pi f_1 t[n]) & 1 & \ldots & \cos(2\pi f_k t[n]) & \sin(2\pi f_k t[n]) \end{vmatrix}$$

$$\mathrm{x}=\begin{vmatrix} x[1] \\ x[2] \\ \vdots \\ \vdots \\ \vdots \\ x[M\times N] \end{vmatrix}; \qquad \mathrm{S}=\begin{vmatrix} A_1 \\ B_1 \\ C_0 \\ \vdots \\ A_k \\ B_k \end{vmatrix}$$

$$S = (D_0^T D_0)^{-1}(D_0^T x) \tag{6.8}$$

$$V_{RMS\_D}(f_1) = \frac{\sqrt{\frac{{A_1}^2+{B_1}^2}{2}}}{\mathrm{sinc}(\pi \times f_1 \times T_i)}, \ldots, V_{RMS\_D}(f_k) = \frac{\sqrt{\frac{{A_k}^2+{B_k}^2}{2}}}{\mathrm{sinc}(\pi \times f_k \times T_i)},\ V_{RMS\_D}(0) = C_0 \tag{6.9}$$

Calculation of Effective Value by Four Parameter Sine Fitting

In four parameter sine fitting, the frequency *f* is estimated as well as the coefficients A_k, B_k, C_0 minimizing the P_{error} term defined below. However, since the *f* estimation is not linear, the ***S*** matrix that minimizes the P_{error} term is found by running (6.10) iteratively [1]. The coefficients in the initial iteration (A_0, B_0, C_0) are decided by the 3-parameter sine-fit algorithm for the default initial frequency (f_0). The values of the previous iteration are assigned to the A_0, B_0, C_0 and f_0 parameters of the second and subsequent iterations. The ***S*** matrix in the iteration that minimizes the P_{error} value is used as the measurement result.

When P_{error} is minimum, the SNR of the measurement will be within the expected values (footnote 8 in Table 6.2). In that case, calculate the effective (RMS) value of each tone using (6.11).

$$P_{error} = \frac{\sum_{n=1}^{M\times N}(x[n]-x[n]')^2}{M\times N}$$

$$x[n]' = A_1\cos(2\pi f_1 t[n]) + B_1\sin(2\pi f_1 t[n]) + C_1 + \cdots + A_k\cos(2\pi f_k t[n]) + B_k\sin(2\pi f_k t[n])$$

$$\mathrm{D}_0 = \begin{vmatrix} \cos(2\pi f_0 t[1]) & \sin(2\pi f_0 t[1]) & 1 & \{-A_0 2\pi t[1]\sin(2\pi f_0 t[1]) + B_0 2\pi t[1]\cos(2\pi f_0 t[1])\}\cdots \\ \vdots & \vdots & \vdots & \vdots \\ \cos(2\pi f_0 t[n]) & \sin(2\pi f_0 t[n]) & 1 & \{-A_0 2\pi t[n]\sin(2\pi f_0 t[n]) + B_0 2\pi t[n]\cos(2\pi f_0 t[n])\}\cdots \end{vmatrix}$$

$$\mathrm{x} = \begin{vmatrix} x[1] \\ x[2] \\ \vdots \\ \vdots \\ x[M\times N] \end{vmatrix}; \qquad \mathrm{S} = \begin{vmatrix} A_1 \\ B_1 \\ C_1 \\ \Delta f \\ \vdots \end{vmatrix}$$

$$S = (D_0^T D_0)^{-1}(D_0^T x)\ ;\ f_1 = f_0 + \Delta f, \ldots \tag{6.10}$$

$$V_{RMS\_D}(f_1) = \frac{\sqrt{\frac{{A_1}^2+{B_1}^2}{2}}}{\mathrm{sinc}(\pi \times f_1 \times T_i)}, \ldots, V_{RMS\_D}(f_k) = \frac{\sqrt{\frac{{A_k}^2+{B_k}^2}{2}}}{\mathrm{sinc}(\pi \times f_k \times T_i)}, V_{RMS\_D}(0) = C_0 \tag{6.11}$$

Correction for Sampler's Band-Pass Filters (G_{filt})

Correction G_{filt} is applied to correct errors caused by the band-pass filters of the ADC. Apply correction when the effective value is calculated with the RMS formula by (6.12), when the effective value is calculated with the Discrete Fourier Transform by (6.13) for each tone, and when the effective value is calculated with sine fitting algorithms by (6.14) for each tone. Select the G_{filt} coefficient for each tone according to the sampler as follows:

$$V_{RMS} = V_{RMS\_D} G_{filt};\ f = f_m \tag{6.12}$$

$$V_{RMS}(k) = V_{RMS_D}(k) G_{filt};\ f = k \times f_m \text{ where } k = 0, 1, 2, \ldots, N/2,\ k \in Z^+ \tag{6.13}$$

$$V_{RMS}(f) = V_{RMS\_D}(f_k) G_{filt};\ f = f_k \text{ where } f_k = 0, f_1, f_2, \ldots, f_k < f_s/2 \tag{6.14}$$

If the sampler is 3458A and measurement range is 100 V or 1000 V [5]:

$$G_{filt} = \sqrt{1 + \left(\frac{f}{36\ \mathrm{kHz}}\right)^2}$$

If the sampler is 3458A and measurement range is 1 V or 10 V [5]:

$$G_{filt} = \sqrt{1 + \left(\frac{f}{120\ \text{kHz}}\right)^2}$$

If the sampler is 3458A and measurement range is 100 mV [5]:

$$G_{filt} = \sqrt{\left(1 + \left(\frac{f}{120\ \text{kHz}}\right)\right)^2 \left(1 + \left(\frac{f}{82\ \text{kHz}}\right)\right)^2}$$

If dynamic frequency response calibration is available for the sampler 3458A at f_m frequency, use the correction obtained from the frequency response calibration (G coefficient as G_{filt})

If the sampler is ΣΔ-ADC, use the frequency response calibration correction (G coefficient as G_{filt}) if available. Otherwise, use the frequency response statement in the manufacturer's specifications.

If the sampler is QV, take G_{filt}=1 to ignore the effect of the band-pass filter.

If the calibration object is the voltage sampler, take G_{filt}=1 and ignore the effect of the band-pass filter.

Correcting the Effect of Stray Electrical Circuit Components in the Measurement Setup

Stray circuit parameters are shown in Fig. 6.4. Due to the influence of stray circuit elements of voltage source, voltage sampler, and connection cables the voltage source and the sampled voltage cannot be equal and are transferred with a ratio that we denote with T_{tran}.

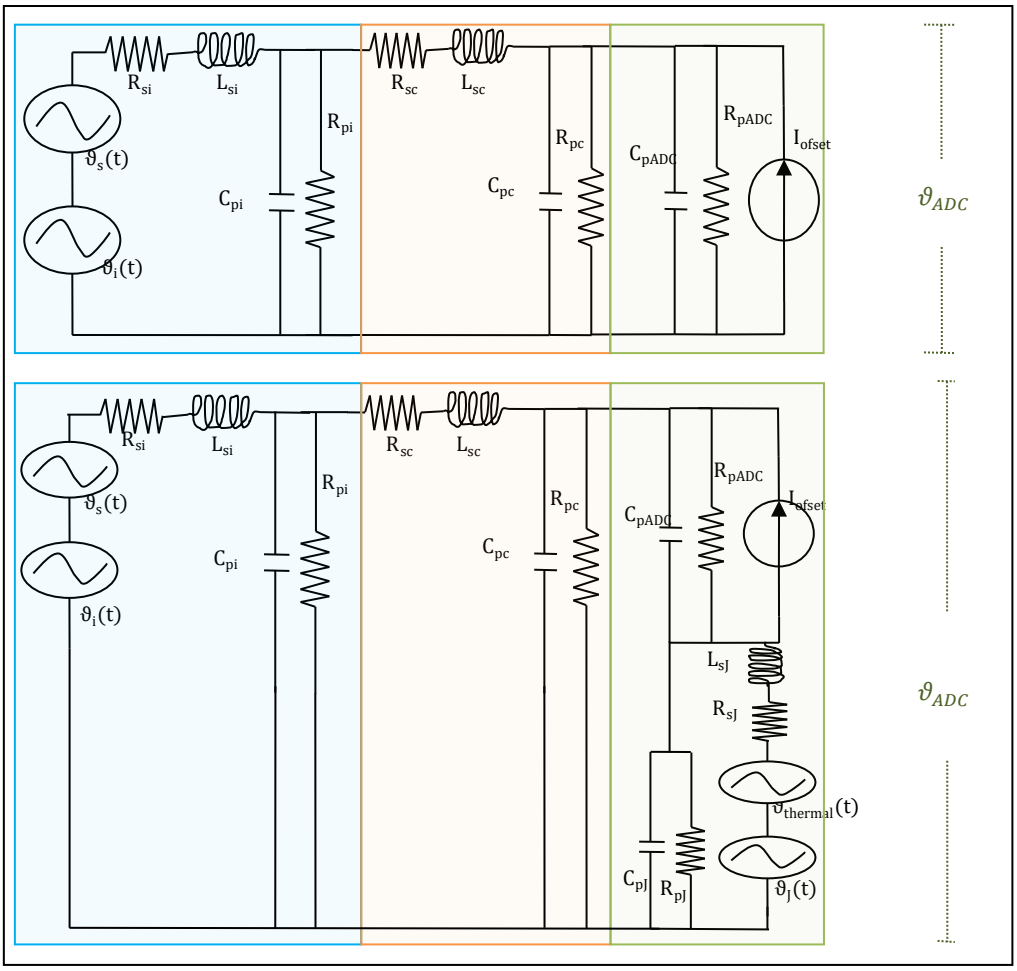

Fig. 6.4. *Electrical circuits showing the distribution of stray circuit components of the measurement setup (The stray circuit components of the quantum voltmeter are depicted with the electrical circuit given in the bottom; The stray circuit components of the voltage source are represented in the blue rectangle, the cables in the orange rectangle, and the sampler in the green rectangle.).*

Ideally, the correction is desired to be $|T_{tran}|e^{j\theta}$=1. Correct it by calculating the actual value or treat the difference from the ideal as uncertainty. Apply correction for the values calculated with the RMS formula by (6.15), for the values calculated with FFT by (6.16) and for the values calculated with sine-fitting by (6.17). Apply correction for each tone of multi-tone voltages.

T_{tran} is calculated for each f using the equations given in [3, 6]. T_{tran}=1 is obtained when the sampler is QV. The stray circuit components given in Fig. 6.4 are determined by measuring and using the literature as described in [3, 6]. The graphs in Fig. 6.5 give frequency dependent T_{tran} for IADC and ΣΔ-ADC using half-meter twisted FLUKE cables.

$$\vartheta_{ADC} = \vartheta_i(t) \times T_{tran}$$

$$V_{RMS} = V_{RMS}/T_{tran};\ f=f_{\text{m}} \tag{6.15}$$

$$V_{RMS}(k) = V_{RMS}(k)/T_{tran};\ f=k\times f_{\text{m}} \text{ where } k=0, 1, 2, \ldots, N/2,\ k\in Z^{+} \tag{6.16}$$

$$V_{RMS}(f) = V_{RMS}(f)/T_{tran};\ f=f_{\text{k}} \text{ where } f_{\text{k}}=0, f_1, f_2, \ldots, f_{\text{k}}<f_{\text{s}}/2 \tag{6.17}$$

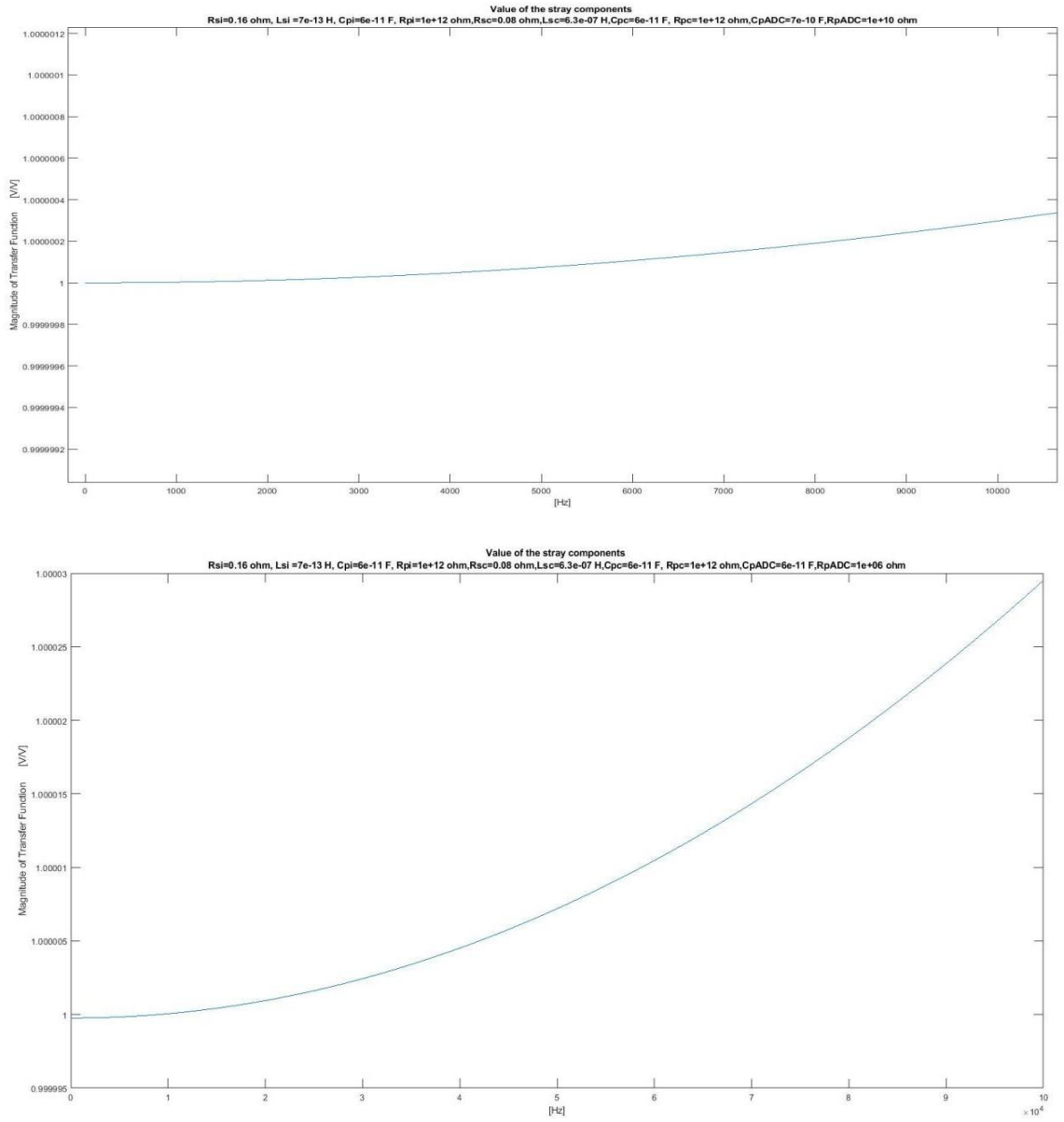

Fig. 6.5. *Frequency dependent T_{tran} (3458A top, NI5922 bottom for 1 V to 10 V measuring ranges).*

Calculating Effective Value of Multi-tone Signals

Apply frequency-dependent corrections for each tone separately, as described above. Find the effective value of multi-tone voltage waves by (6.18).

$$V_{RMS} = \sqrt{\sum_{f=0}^{<f_s/2} V_{RMS}^2(f)} \quad V_{RMS} = \sqrt{\sum_{k=0}^{<N/2} V_{RMS}^2(f)} \tag{6.18}$$

6.3. Calibration result

Calibration object is the voltage source

If the calibration object is a voltage source, find the calibration result by (6.19).

$$V_x = V_i = V_{RMS} = \frac{V_{RMS\_D} \times G_{filt}}{T_{tran}} \tag{6.19}$$

Calibration object is the voltage sampler

If the calibration object is the voltage sampler and the frequency response of the sampler is being determined, find the calibration result using (6.20) for static gain and (6.21) for dynamic gain.

$$G(f) = \frac{V_{RMS}}{V_i + \delta V_{i-cal} + \delta V_{i-D}} = \frac{\frac{V_{RMS\_D} \times G_{filt}}{T_{tran}}}{V_i + \delta V_{i-cal} + \delta V_{i-D}} \tag{6.20}$$

$$G(f) = \frac{V_{RMS}(k)}{V_i(kf_m) + \delta V_{i-cal}(kf_m) + \delta V_{i-D}(kf_m)} = \frac{V_{RMS}(f)}{V_i(f) + \delta V_{i-cal}(f) + \delta V_{i-D}(f)} \tag{6.21}$$

Linearity error

The linearity error of the sampler or voltage source is important when the device is used as a reference. The measure of linearity error under dynamic condition is the THD. THD can be estimated using measured $V_{\mathrm{RMS}}(f)$ values.

The noise and distortion parameter (NAD) includes both the noise and linearity error under dynamic conditions. NAD can be determined from the collected samples as follows and can be used as the linearity uncertainty in Table 6.5:

$$NAD\_r = \frac{NAD}{V_{FS}} = \frac{\sqrt{\frac{\sum_{n=1}^{M \times N} (x(n) - x'(n))^2}{M \times N}}}{V_{FS}} = u(\delta_{LIN})$$

Likewise, for dynamic measurements, the number of bits (ENOB - Effective Number of Bits) of the sampler can be determined by the following equation:

$$\mathrm{ENOB} = \log_2(NAD\_r \times \sqrt{12})^{-1} \tag{6.22}$$

The signal to noise and distortion ratio parameter (SINAD) is also the measure of the linearity and noise that is determined by the following equation:

$$\mathrm{SINAD} = 20 \times \log_{10}\left(\frac{V_{RMS}}{NAD\_r \times V_{FS}}\right) = 20 \times \log_{10}\left(\frac{V_{RMS}}{NAD}\right) \tag{6.23}$$

Table 6.5. *Uncertainty Components.*

Component		Definition and Its Value	Probability Distribution Function	Uncertainty	Correlation Between Samples
1	V_J	● Quantum voltage of the n^{th} sample when the sampler is QV ● Its value is zero when sampler is 3458A, ΣΔ-ADC, ADC			
2	V_{FS}	Full Scale of the sampler			
3	V_{ADC}	Nominal Value of the samples obtained by the sampler			
4	$v_i(t)$	Mathematical function of the signal applied to the sampler's input: $\sin\left(2\times\pi\times\frac{1}{T_o}\right)+\sin(2\times\pi\times k\times\frac{1}{T_o})$+....			
5	T_i	Integration/Sample-hold time ● Value determined by APER command when sampler is 3458A and T_i=T_a-25 µs, T_i ≥ 10 µs; T_i=100 ns×z; $z\in Z^+$ ● 17 ns when sampler ΣΔ-ADC ● The value suitable for the sampler in the QV system when the sampler is QV			
6	δ_{JTi}	Jitter in integration time ● 3458A ● ΣΔ-ADC	Rectangular	● <500 ps ● <3 ps	No
7	T_a	Sampling period ● Value determined by TIMER command when sampler is 3458A and T_i=T_a-25 µs, T_i ≥ 10 µs; T_i=100 ns×z; $z \in Z^+$ ● If the sampler is NI5922, the period of the equivalent sampling frequency			
8	δ_{jTa}	Jitter in sampling period ● 3458A internal CLK ● ΣΔ-ADC ● 3458A Semi-Synchronous	Rectangular	● <500 ps ● 3 ps ● 50 ns	No
9	T_o	Period of the input signal ($v_i(t)$)			
10	δ_{JTo}	Jitter in the period of input signal ($v_i(t)$)			No
11	δ_{REF}	The correction of the reference voltage of the sampler. It is relative to the V_{ADC}, its value is 0 when calibrating the sampler. ● 3458A ● ΣΔ-ADC	Normal	● 0.5 µV/V ● <20 µV/V	Yes
12	δ_G	The correction of the gain of the sampler. It is relative to the V_{ADC}, its value is 0 when calibrating the sampler. ● 3458A < 100 Hz ● 3458A > 100 Hz ● ΣΔ-ADC	● Normal ● Rect. ● Rect.	● 0.5 µV/V ● int(0.002/T_i) to <30 µV/V ● 30 µV/V	Yes

Component		Definition and Its Value	Probability Distribution Function	Uncertainty	Correlation Between Samples
13	δ_{LIN}	The correction of the linearity of the sampler. It is relative to the V_{FS}, its value is 0 when calibrating the sampler.	Normal / Rectangular	It is the ADC's INL fault. It can be obtained from the SINAD parameter for dynamic measurements. δ_{RES}=0 can be obtained when obtained from SINAD	No
14	δ_{RES}	The resolution correction of the sampler is relative to the measuring range, the value is 0 in the sampler calibration ● Dynamic ● 3458A	Normal / Rectangular	● It is the resolution of the ADC. It can be obtained from the ENOB parameter of the ADC for dynamic measurements. δ_{LIN}=0 can be obtained when obtained from ENOB ● Calculated by (6.28)	No
15	$v_{sn}(t)$	The quantization noise of the sampler. In sampler calibration, the value is assumed as 0. ● 3458A ● ADC	Rectangular	● Calculated by (6.24) ● Calculated assuming one-bit error by (6.25)	No
16	$v_s(t)$	The noise of the signal at the sampler input ● 57X0, Datron 4808, .. ● Aivon Dual DAC, CMI SWG03...	Rectangular	● Calculated by (6.26) ● Calculated by (6.27)	No
17	G_{filt}	Coefficient of correcting the effect of the sampler's filters that suppress input noise (anti-aliasing filter)	Rectangular / Normal	Manufacturer's declaration / Calibration Result	
18	T_{tran}	The rate at which the applied voltage from the voltage source is transferred to the sampler due to stray circuit elements of the setup	Rectangular	The values of stray circuit elements given in Fig. 6.4 are assigned and using their values the value of T_{tran} and its uncertainty is calculated according to electrical circuit theories.	No
19	δV_{i-cal}	Correction due to calibration of the reference voltage source	Normal	Obtained from the certificate	No
20	δV_{i-D}	Correction due to the drift of the reference voltage source over time since its last calibration	Rectangular	History or manufacturer's tolerance statement	No

$$u_{v_{sn}}{}^2 = \left(0.9\sqrt{\frac{0.001}{T_i}}V_{FS}\right)^2 \tag{6.24}$$

$$u_{v_{sn}}{}^2 = \int_{1/(M\times N\times T_a)}^{1/(2T_a)} \left\{\left(\frac{V_{FS}}{2^{L-1}}\right)^2 \frac{2}{12 f_s}\right\} df \tag{6.25}$$

$$u_{v_s}{}^2 = \int_{1/(M\times N\times T_a)}^{1/(2T_a)} \left\{(v_s)^2 \frac{1}{B}\right\} df \ ; \tag{6.26}$$

where v_s: manufacturer's noise declaration; B: manufacturer's noise band width statement.

$$u_{v_s}{}^2 = \int_{1/(M\times N\times T_a)}^{1/(2T_a)} \left\{\frac{KF}{f} + S_n + \left(\frac{V_{FS\_DAC}}{2^{L_{DAC}-1}}\right)^2 \frac{2}{f_{s\_DAC}}\right\} df \tag{6.27}$$

where V_{FS_DAC}: Full Scale of the DAC; L_{DAC}: bit number of the DAC; f_{s_DAC}: Sampling frequency of the DAC.

T_i	$u(\delta_{RES})$
$T_i \geq 600$ µs	$5\times10^{5}\times10^{-(0.2229\times\ln(Ti)+7.7449)}$
100 µs ≤ T_i <600 µs	$5\times10^{5}\times10^{-(0.473\times\ln(Ti)+9.5932)}$
10 µs ≤ T_i <100 µs	$5\times10^{5}\times10^{-(0.5502\times\ln(Ti)+10.85)}$

(6.28)

6.4. Measurement uncertainty

If the calibration object is a voltage source, the measurement uncertainty is the uncertainty of the measured V_{RMS} value. If the calibration object is a sampler, when evaluating the uncertainty of the measurement, calibration of the voltage source (V_i) used as a reference and its drift uncertainties since last calibration should also be taken into account.

Within the scope of this report the uncertainty budget for the Discrete Fourier Transform and the RMS formula has been prepared in templates (using Excel sheets). In these templates, firstly the uncertainty of each x[n] sample is determined. The uncertainty from these two methods is evaluated by taking into account the model functions of the Discrete Fourier Transform and the RMS formula and the propagation of the uncertainty, using the analogies given in [4]. While evaluating the uncertainty for the AC voltage parameters obtained from the curve fitting algorithms, random numbers are generated for each uncertainty of x[n] and t[n] which are already calculated in uncertainty budget templates (Excel sheets mentioned above). The amount of random numbers is at least 200000. Numerical calculations according to [7] are performed using numeric calculation platform (like MATLAB). Uncertainties for the parameters are estimated from the histograms of the calculated AC voltage parameters.

6.5. Scope

Quantity and Calibrated Instruments	**Measurement Range**	**Measurement Conditions**	**Calibration and Measurement Capabilities (Expanded Uncertainty (k=2)**	**Remarks**
Voltage / Voltage Source, calibrator	5 mV to 80 mV	≤ 100 Hz	180 µV/V to 20 µV/V	Calibration with modified IADC
		≤ 400 Hz	180 µV/V to 20 µV/V	
		≤ 1 kHz	180 µV/V to 20 µV/V	
	100 mV to 800 mV	≤ 100 Hz	10 µV/V to 1.5 µV/V	
		≤ 400 Hz	15 µV/V to 4 µV/V	
		≤ 1 kHz	55 µV/V	
	1 V to 8 V	≤ 100 Hz	1.5 µV/V	
		≤ 400 Hz	4 µV/V	
		≤ 1 kHz	55 µV/V	
	10 V to 80 V	≤ 100 Hz	6 µV/V to 4 µV/V	
		≤ 400 Hz	15 µV/V	
		≤ 1 kHz	55 µV/V	
	100 V to 700 V	≤ 100 Hz	6 µV/V to 4 µV/V	
		≤ 400 Hz	15 µV/V	
		≤ 1 kHz	55 µV/V	
	1 V to 3 V	≤ 100 kHz	110 µV/V	Calibration with ΣΔ-ADC
	0.8 V to 8 V	≤ 1 kHz	0.8 µV/V to 0.5 µV/V [6]	QV
	0.8 V to 8 V	≤ 100 kHz	[10]	QV

Voltage, Voltage Gain / Voltage Sampler, ADC	0.8 V to 8 V	≤ 100 Hz	0.5 µV/V	PJGS
	0.8 V to 8 V	≤ 400 Hz	2 µV/V	
	20 mV to 100 mV	≤ 400 Hz	< 20 µV/V [9]	JAWS
	0.8 V to 3 V	10 Hz to 100 kHz	50 µV/V to 30 µV/V	Reference Calibrator
	3 V to 700 V	≤ 1 kHz ≤ 100 kHz	50 µV/V to 30 µV/V No equipment in the market	Reference Calibrator

6.6. Conclusion & future work

Detailed report on uncertainty estimation of AC voltage parameters obtained by sampling techniques is presented.

In the scope given in section 6.5 is aimed to cover the calibrations of the commercial equipment. It is clear that below 400 Hz and below 8 V_{rms} the established AC voltage can be improved by sampling techniques.

Enabling voltage dividers in digital traceability also will improve the uncertainty above 8 V_{rms}. Using sub sampling techniques with QV will improve the uncertainties up to 100 kHz.

6.7. References

[1] IEEE Instrumentation and Measurement Society, "IEEE Standard for Digitizing Waveform Recorders", IEEE Std. 1057-2007, 2007

[2] "Comparison of Sampling Voltage Measurements of Multi-tone Signals", CPEM 2018

[3] "Improving Digital Metrology Using Josephson Voltage Standards", T.C.Öztürk

[4] https://tez.yok.gov.tr/UlusalTezMerkezi/tezSorguSonucYeni.jsp (04.02.2021)

[5] "Maintenance and traceability of AC voltages by synchronous digital synthesis and sampling", PTB Report E-75, 2001

[6] "A 10 ppm Accurate Digital AC Measurement Algorithm"

[7] "Using Programmable Josephson Voltage Standard for Static and Dynamic Gain Characterization of Integrating ADC", IEEE TIM

[8] “Guide to the Expression of Uncertainty in Measurement”, GUM,1995

[9] "Measurement of Arbitrary Waveforms at Low Frequencies", CPEM 2020

[10] "Testing the Sampling System Using Josephson Arbitrary Waveform Synthesizer Established in TÜBITAK UME”, CPEM 2020

[11] "An AC quantum voltmeter for frequencies up to 100 kHz using subsampling"

7. INTEGRATED SOFTWARE FOR DATA PROCESSING AND UNCERTAINTY ESTMATION

7.1. Sampling and data analysis software

While older analog methods were usable without any computer processing, modern digital methods require vast usage of software, automatization and data processing algorithms. Several applications have been developed by ADC chips manufacturers, measurement devices manufacturers, users or National Metrology Institutes. Generally, these applications do not deal with uncertainties.

A common situation in the data processing of sampled signals is the estimation of multiple quantities using the same record. The user is interested in amplitude and phase of the main signal component, in a spectrum, and stability of these quantities during multiple records. For the case of evaluating the properties of a digitizer, spurious free dynamic ratio (SFDR), total harmonic distortion (THD) and effective number of bits (ENOB) are important quantities. Algorithms exist for all of these quantities, but it is complex task to learn how to use every single algorithm.

Q-Wave toolbox (QWTB) [1, 2] deals with this situation. It is an open-source software toolbox written in M-code and is running in Matlab [3] or GNU Octave [4]. It aims for aggregation of high-quality algorithms required for data processing of sampled measurements. QWTB consists of data processing algorithms from different sources, unifying application interface and graphical user interface. The toolbox gives the possibility to use different data processing algorithms with one set of data and removes the need to reformat data for every particular algorithm. The Toolbox is also extensible. The QWTB was designed to help with using general quantity estimating algorithms.

However, it was not tailored for actual metrological measurements. Therefore, a TWM (TracePQM Wattmeter) [5, 6] was developed. TWM is an open source, transparent, metrology grade measurement system for traceable measurement of the voltage, current, power and power quality (PQ) parameters. It is designed to allow recording of the voltage and current waveforms using various digitizers and processing the measured waveforms using any algorithm. TWM defined QWTB name space needed for quantities needed for transducers, errors of connecting transducers to digitizers. The core of TWM relies on the QWTB capabilities. An image of the user interface of the software is shown in Fig. 7.1.

The estimation of algorithm errors was not fully covered in QWTB nor in the TWM extension. Therefore, a Q-Wave toolbox variator QWTBvar was developed. It is a system that can easily variate input quantities or its uncertainties, calculate errors of output quantities to the nominal values, plot dependence of output quantities on the varied input quantities or its uncertainties, create a lookup table of uncertainties of output quantities and interpolate the lookup table for quick estimation of uncertainties.

Details on the usage of QWTB, TWM and QWTBvar are described in respective documentation. Deliverable 4 [57] describes general theory on errors and uncertainties of any quantity estimation algorithm. An application to an actual algorithm is presented. Deliverable contains full documentation of software QWTBvar with its interface and usage. Two examples are provided to provide usage reference of the software. Final chapters of Deliverable 4 describe results from uncertainty estimation and validation of algorithm for estimation of Total Harmonic Distortion, Spurious Free Dynamic Range, Integral and Differential non-linearity.

The QWT, TWM and QWTBvar can be found on following public repositories together with its documentation:

https://qwtb.github.io/qwtb/

https://github.com/smaslan/TWM

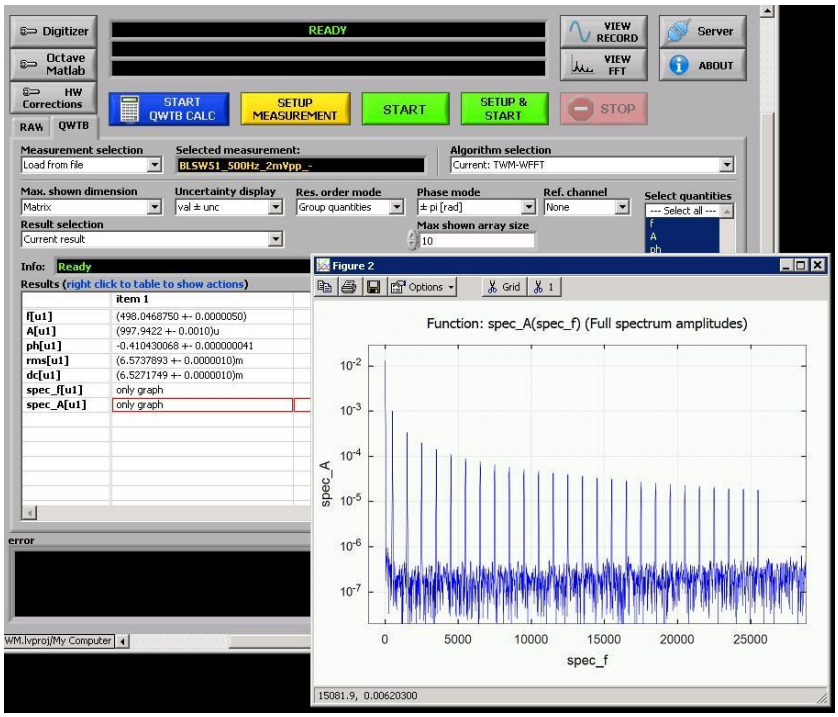

Fig. 7.1. *Example screenshot of the sampling software TWM with spectrum calculated by a QWTB algorithm. The source signal was a bandwidth limited square wave generated by JAWS.*

7.2. References

[1] Šira M 2017 QWTB - Software Toolbox for Sampling Measurements URL https://qwtb.github.io/qwtb/

[2] Šira M, Mašlan S and Novakova Zachovalova V 2016 QWTB – Software Tool Box for Sampling Measurements *Conference on Precision Electromagnetic Measurements Digest* (IEEE) p 2 ISBN 978-1-4673-9133-7 URL http://ieeexplore.ieee.org/document/7540599/?reload=true

[3] 2012 Matlab URL http://www.mathworks.com

[4] 2012 GNU Octave URL https://www.gnu.org/software/octave/

[5] Mašlan S TWM tool https://github.com/smaslan/TWM

[6] Mašlan S and Power O 2019 *Cal Lab: The International Journal of Metrology* 27–35 ISSN 1095-4791 URL https://www.callabmag.com

[7] EMPIR Project 17RPT03 DIG-AC, Deliverable D4: Report on the integrated software for data processing and uncertainty estimation of dynamic measurements, including related methods and algorithms; available on the project web site http://digac.gum.gov.pl/

8. VALIDATION AGAINST JOSEPHSON VOLTAGE STANDARDS

8.1. Introduction

With the redefinition of the SI unit the Ampere in 2019 [1], all electrical units are now defined by fixed numerical values of the defining constants *e* (elementary charge) and *h* (Planck's constant) and are realized and disseminated [2] via the Quantum Hall Resistance (QHR) standard and the Josephson Voltage Standard (JVS). In practice, the Josephson effect has been used to realise the DC Volt at National Measurement Institutes (NMIs) for many decades, prior to the redefinition. Typically, an uncertainty of the order of 0.2 µV/V (k = 2) can be achieved on a 10 V DC measurement [3].

However, the same is not true of AC voltage where NMIs typically rely on thermal based methods for dissemination of the scale (Fig. 8.1a). A thermal voltage converter (TVC) is used as an AC-DC transfer standard [4, 5] and a typical uncertainty on the amplitude of a 1 V sinusoidal AC voltage waveform of frequency 1 kHz is of the order of 10 µV/V (k = 2) [3]. The TVC is used to obtain the DC voltage that results in the same heating as an applied AC voltage. Traceability to the SI is obtained using a DC voltage transfer standard (for example a Zener reference standard) which has been calibrated against a DC Josephson voltage standard to provide the reference rms voltage value. This thermal method is time consuming as it requires averaging each set of measurements over a time period of the order of 1 h. It also requires historic knowledge of the TVC performance. The thermal method provides only the rms value of the voltage waveform and therefore cannot provide any spectral information. An alternative to the use of thermal devices in the AC voltage and current traceability chain is to transfer the scale directly to a high-performance digitizer from a JVS [6]. High-performance digitizers, AC Josephson systems and their combined use with TVCs has been subject to a large body of research, briefly described below.

Josephson voltage standards are in widespread use globally both at NMIs and at top tier research and calibration laboratories (for a general review see [7] or [8]). AC Josephson systems have been developed using either Programmable Josephson Voltage Standards (PJVS) or Josephson Arbitrary Waveform Synthesizers (JAWS).

High-performance digitizers in common use in electrical metrology include the National Instruments NI5922 and the Keysight 3458A (for a thorough review see [9]). These digitizers are used in this work and have previously been the subject of several investigations using TVCs. For example, the use of a TVC to characterize the NI5922 digitizer is described in [10, 11, 12]. Josephson systems have also been used to calibrate TVCs. For example, references [13] and [6] use PJVS and [14] uses JAWS to calibrate a TVC. TVCs have also been used to characterise digitizers [10].

There has been significant interest in the use of Josephson voltage standards to characterize the performance of digitizers, particularly for use in power measurements. Examples include the use of a PJVS to characterise the NI5922 digitizer [15], the 3458A [16, 17, 18, 19, 20] and the Fluke 8558A [21]. A Primary AC Power Standard based on a PJVS has been developed [22] and an AC power standard comparison with PJVS and JAWS has been undertaken [23]. There is ongoing research into the quantum-based power standard [24]. JAWS systems have been used to characterize both the NI5922 [25, 26] and the 3458A at higher frequencies [27, 28].

The new method for traceability proposed in this work is shown in Fig. 8.1b. This method builds on the work described above and uses Josephson voltage standards to directly calibrate the digitizer, operating under certain conditions, using a set of precisely known voltage waveforms. This provides direct traceability to the SI. For AC current measurements a current shunt is inserted into the circuit to convert AC current to AC voltage which is measured by the digitizer. For inputs outside the calibrated range of the digitizer the current shunt (for current measurements) or resistive divider (for voltage measurements) is used as a scaling device to access a wide range of possible input currents and voltages. We here describe this proposed new traceability route for current and voltage based directly on Josephson

standards and present measurements on the components of the system including digitizers and scaling devices. We also describe the measurement software and algorithms used to obtain results as well as calculate uncertainties. The motivation is to provide faster measurement times and reduced uncertainties in some parameter ranges. The method is more flexible allowing future spectral characterisation of instruments using Josephson based systems. There is also the ambition to construct an agreed European system for digital traceability using this method [29]. This system is based on a shared hardware, software and data analysis process across several NMIs.

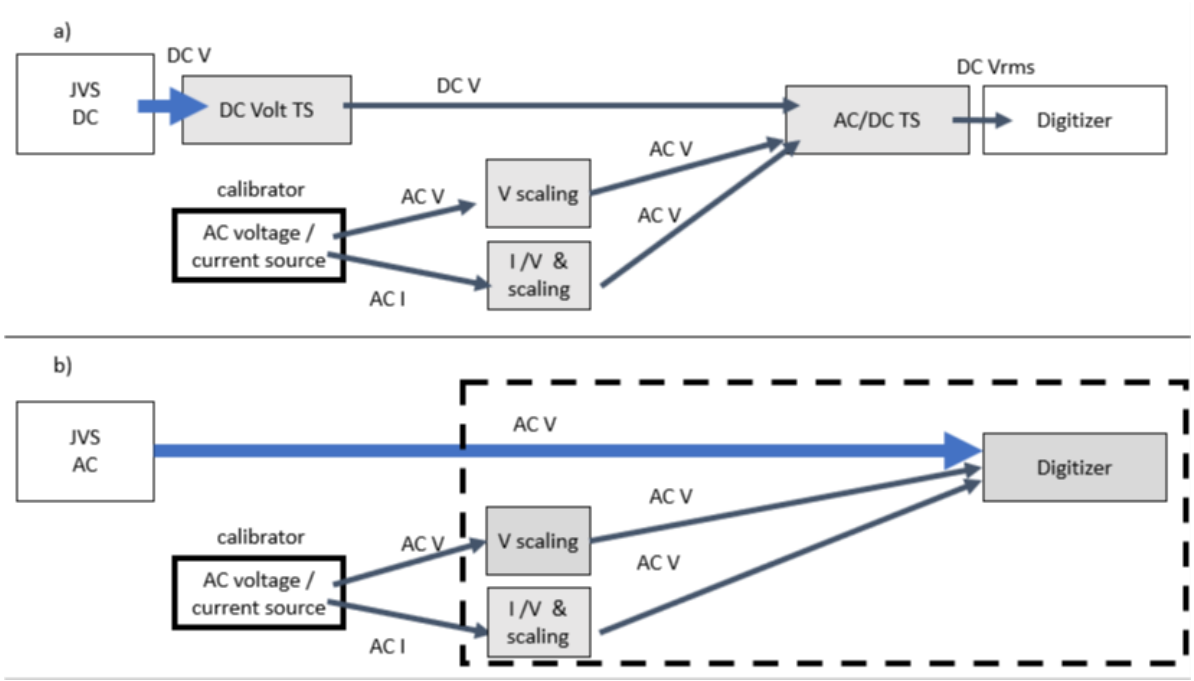

Fig. 8.1. *Traceability route for AC current and voltage at an NMI for a) existing route and b) route proposed in this work. In a) the Josephson Voltage Standard (JVS) provides calibration of a DC voltage transfer standard (DC Volt TS) which is applied to the thermal voltage converter transfer standard (AC-DC TS) and measured by a digitizer. This is compared with the output of the AC current/voltage source under test which is applied to the AC-DC TS via voltage or current scaling devices (if required) and a current to voltage converting device (current shunt) in the case of current. In this way the output of the AC voltage/current source is traceable to the SI via thermal methods. In b) the output of the AC voltage/current source combined with the scaling and converting device is applied directly to the digitizer. A JVS is used to characterise the dynamic performance of the digitizer providing direct traceability to the SI. Grey shading denotes items that require characterization. Blue arrows show traceability to the SI via the Josephson effect. DC V, AC V and AC I denote DC voltage and AC voltage and current waveforms respectively. Items characterized in this work are shown in the dashed box.*

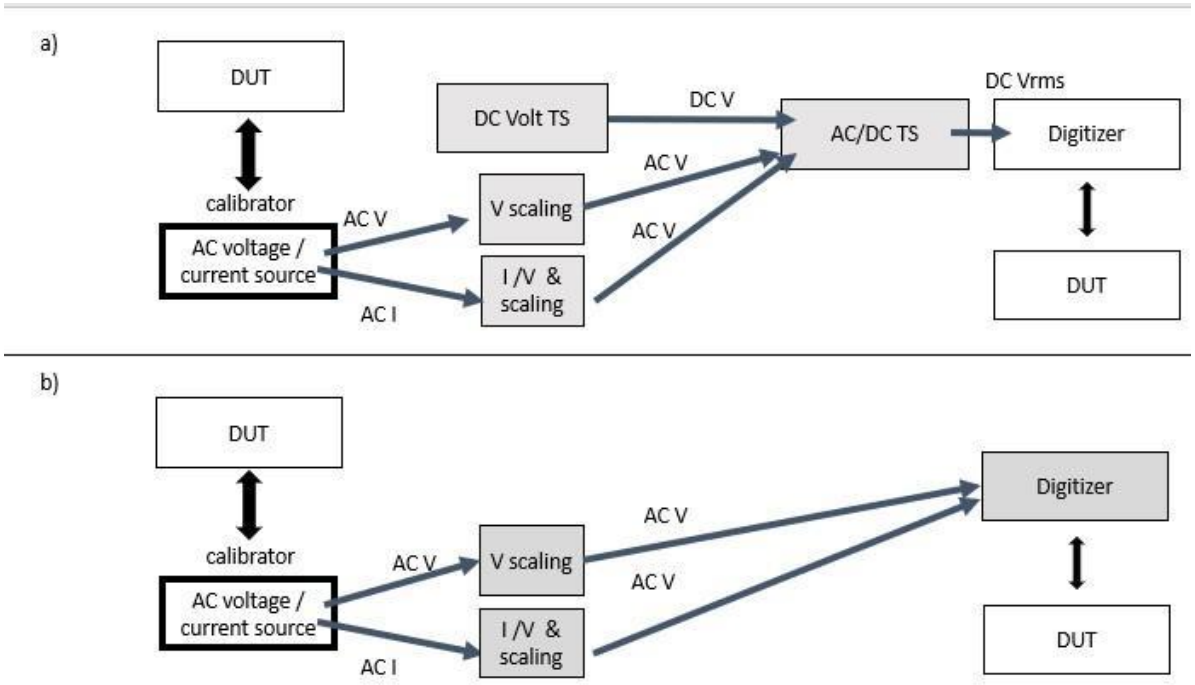

Fig. 8.2. *Schematic diagrams showing the traceability route at an industrial user laboratory to calibrate a device under test (DUT) for example a digitizer or AC source.*
a) denotes the existing and b) the proposed route. The grey items are items that have been characterized by an NMI against Josephson standards as described in this work.

8.2. Measurement setup

We describe the measurement configuration required by an NMI to deliver the traceability route shown in Fig. 8.1b. In this proposed new route, an industrial user requiring traceability will benefit from the reduced steps in their traceability chain as shown in Fig. 8.2b compared to the existing route shown in Fig. 8.2a. The industrial user requires the NMI to provide direct traceability using a Josephson voltage standard to calibrate the user's digitizer, voltage divider and current shunt. Computer software to sample data using the digitizer and analyse the results is also required. These items are described below.

8.2.1. Josephson Voltage Standards

The typical operating parameters of the two types of Josephson system used in this work are shown in Table 8.1. The PJVS can be utilized at frequencies up to 1 kHz whilst the JAWS can be used up into the megahertz range.

8.2.1.1. Programmable Josephson voltage standard

The PJVS systems used in this work are described in more detail in [30], [31] and [32]. A particular feature of the system described in [30] is the ability to use either the direct output of the PJVS (a stepwise waveform) or to use a quantum-reference continuous waveform produced by a digital to analog converter (DAC) locked to the output of the PJVS. This continuous waveform can be matched to the signal under test (a sine wave) to within the limit of the smallest voltage output of the array. This has the advantage of removing the harmonic content of the stepwise waveform which can produce unwanted effects in the digitizer measurement. For example, in a delta sigma-based digitizer, large changes in voltage result in the need for a time delay to allow the output to settle to a stable value.

Table 8.1. *Operation parameters of the Josephson voltage systems used in this work; PJVS (programmable Josephson voltage standard) and JAWS (Josephson arbitrary waveform synthesizer which is based on a pulse-driven Josephson array).*

	PJVS	JAWS
Frequency (Hz)	DC to 1 kHz	DC to 1 MHz
Voltage (V)	± 10 V	± 1 V_{rms}

8.2.1.2. JAWS

The basic principle of JAWS can be described as follows: a current pulse, with a time dependent pulse-repetition frequency $f_p(t)$ transfers N flux quanta Φ_0 through M Josephson junctions [33]. The signal voltage V(t) in pulse-mode operation can be calculated with the Josephson equation: $V(t) = N \cdot M \cdot \Phi_0 \cdot f_p(t)$. According to this equation a quantized, time-dependent voltage is generated at the junction series array output leads, because only flux quanta $\Phi_0 = h/2e$ are transferred and N and M are integer numbers. Typically, the modulator frequency corresponds to the characteristic frequency of the Josephson junctions, about 15GHz, and provides large oversampling ratios up to frequencies of 1 MHz. On-chip filters exploit superconducting inductances to filter quantization noise at the output used for metrological purposes [34] which are typically analysed by a commercial fast digitizer. A higher-order sigma-delta modulation [35] is used to digitize analog waveforms into a bit pattern containing +1, 0 and 1. Commercial Pulse Pattern Generators (PPGs) are used to store these patterns of positive and negative current pulses that generate the desired waveform across the M Josephson junctions in the series array. As a flux-quanta delivers only a very small voltage $\Phi_0 \approx 2$ µV/GHz many Josephson junctions implemented in a series array are necessary to achieve practicable large output voltages. Recently a maximum voltage of 4 V rms was achieved [36]. Within this project we either operate a single or eight JAWS arrays in series to achieve higher voltages, namely 100 mV with 9000 or 1 V with about 60000 Josephson junctions [37]. The so-called AC coupling technique [38] is used to enable the JAWS arrays to produce floating AC voltages with operating margins always larger than 0.5 mA.

8.2.2. Digitizers

Key to the success of this new traceability method is the availability of high-performance digitizers that exhibit long term stable measurement capability. The digitizers considered in this project are shown in Table 8.2. A principle of this work is that the digitizer is characterised under a particular set of conditions and then used with the same operating parameters for all measurements while the scaling is performed by a voltage divider or current shunt as appropriate.

Table 8.2. *Types of digitizers characterized in this work including their operation parameters.*

Digitizer	Type	Settings used
National Instruments NI5922	Delta Sigma	2 V range, 1 MΩ input impedance, 48 tap FIR filter.
Keysight 3458A	Integrating	1 V range, 10 GΩ input impedance DCV mode
Fluke 8588A	Integrating	0.1 V and 10 V range, 10 MΩ input impedance, sampling mode

8.2.3. AC voltage and current source

An arbitrary reference source of AC voltage and current is required at the industrial user lab as shown in Fig. 8.2b. This source must be highly stable and typically a multifunctional calibrator is used. The user will set the source to a fixed output and transfer the scale from the calibrated digitizer to the digitizer under test by applying this signal to both instruments. Conversely, if the device requiring calibration by the user is a current or voltage source then this can be applied directly to the digitizer, via voltage divider or current shunt if required, to obtain traceability.

8.2.4. Voltage dividers

To extend the operating range of the quantum standard over the much wider interval of values required for calibration services, suitable methods for scaling are needed (Fig. 8.1b). A simple approach would be to use the well-known analogue techniques, yet digital solutions are interesting for improving performances closer to quantum accuracy. Very successful results were obtained in DC measurements with integrating digitizers found in the core of DMMs. They show extremely linear behaviour, with intrinsic accuracy better than 0.1 μV/V and even better stability over time [39]. It is then possible to characterize the residual nonlinearity of such converters using a JVS, to verify the specifications and apply further correction. A DMM characterized against a JVS can be effectively used in place of resistive dividers in DC, but this technique cannot be transferred “as is” to AC. Performances of ADCs degrade as frequency increases, according to the rule: “more speed means less resolution” that holds true for all conversion technologies, including those used in metrological labs (integrating and sigma-delta). Voltage ratio calibrations to extend the operating range of an AC quantum standard therefore cannot be suitably done by applying two quantum accurate AC voltages to calibrate the “AC linearity” of an ADC. Alternatively, the very high performances of internal DC references currently available in top-level instruments allow sampling AC signals with a DMM and measuring AC voltages over a wide range of values and frequencies, with the only proviso of 1 % maximum distortion level of the measured signal [40]. This solution suffers from the aforementioned limitations of measurements limited to rms voltage and will not be considered. The extreme accuracy of well-known analog techniques must also be taken into account in discussing AC voltage ratio techniques. Inductive dividers were proven long ago [41] to provide accuracy at the level of few nV/V. The high performances of inductive dividers are appealing for integration with quantum standards [42, 43], but are limited to pure sinusoidal signals over a limited frequency range, spanning from tens of hertz to a few kilohertz. The interest in arbitrary waveform metrology based on sampling methods with quantum traceability suggests the adoption of wide bandwidth, resistive dividers.

In any case, suitable integration of analog and digital techniques can be considered the best way to cover all the calibration ranges. The approach given here integrates quantum standards, sampling techniques and analog methods to take advantages of all these techniques. In such a method, the role of quantum-calibrated ADC is to sample and quantize the signal within its most accurate operating range, as shown in Fig. 8.1b, with ordinary dividers allowing suitable up/down scaling over the whole required range. A similar approach was adopted, for instance, with DC voltage signals in [44]. Research in this field is ongoing and several solutions were proposed, that may be chosen according to specific needs or operating conditions. Two sampling voltmeters and a set of traditional dividers are integrated in a method developed within the project [29], where they are considered and calibrated together, with the divider connected directly to the voltmeters inputs to improve repeatability. For the even number of steps in the scaling procedure the ratio correction due to the linearity of the voltmeters can be estimated by applying the same voltage to the inputs of the voltmeters. Both step-up and step-down scaling is feasible with this method and AC voltage calibrations attaining 50 μV/V accuracy up to 5 kHz frequencies were demonstrated in the step-up scaling from 12 V to 220 V. In Fig. 8.3, the results for the voltage level of 220 V obtained from the voltage of 12 V by four ratio measurements in the scaling up procedure were compared to the 220 V level calibrated directly against the AC-DC transfer standard. In designing the divider in this setup care must be taken to keep low temperature, voltage and power coefficients. An interesting solution to support voltage divider operation by minimizing loading effects can be useful. It is based on a new prototype divider that uses the split guard technique along with a buffer amplifier [45]. The technique enabled the construction of a buffer with input capacitance below 1 pF, output impedance

below 11 mΩ for frequencies below 100 kHz and overall amplitude and phase transfer error below 2 µV/V and 2 µrad.

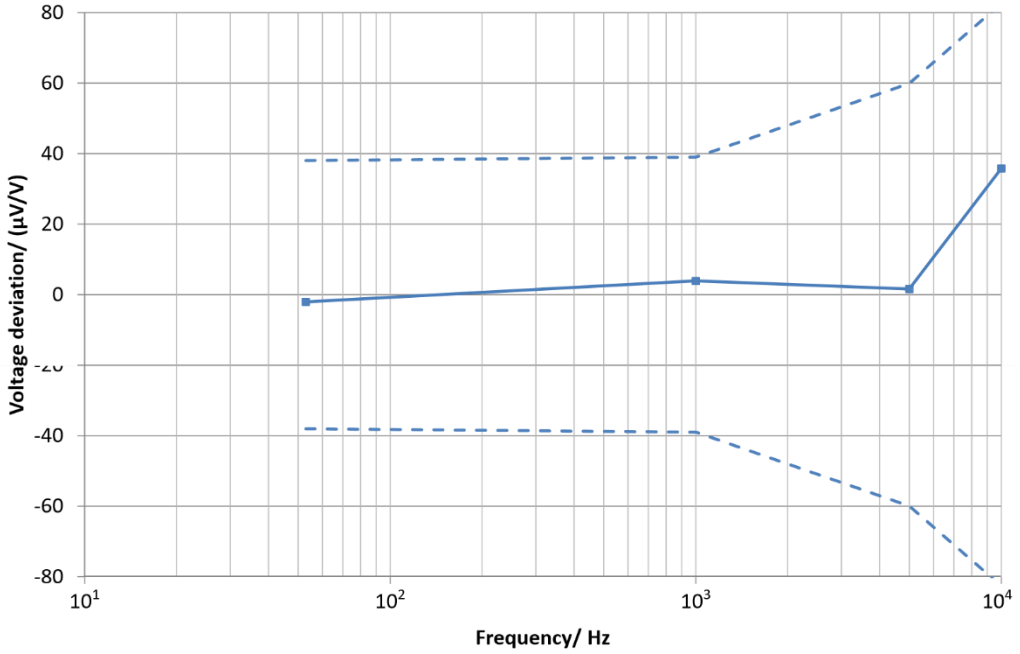

Fig. 8.3. *Deviation in the voltage level obtained by the scaling up procedure against the same voltage level of 220 V calibrated directly by the AC-DC transfer standard. Dashed curves denote the measurement uncertainty (k = 2).*

Inductive voltage dividers (IVDs) are an alternative reliable tool for realizing metrology class AC voltage ratios. In this way voltages of up to 120 V can be traced to quantum voltage standards such as JAWS [46]. However, ratios of conventional dividers must be accurately determined. Pulse-driven Josephson voltage standards can be employed for this work as they can generate any voltage signal with excellent accuracy. It is possible to form highly accurate AC voltage ratios in a broad frequency range with two synchronized JAWS systems [47]. At a 1:1 ratio such calibration is very similar to a direct JAWS versus JAWS comparison [48]. We performed measurements at frequencies 120 Hz, 225 Hz, and 497 Hz. The agreement with a conventional bootstrapping method especially the in-phase calibrations was very well within 1.1 parts in 10^8 for all divider ratios.

8.2.5. Current Shunts

Since analog-to-digital conversion operates with voltage signals, for AC current measurements it is necessary to convert current to voltage, and for that purpose traditional resistive shunts are used. The shunt is also a scaling element, since its value can be selected to produce voltages suited to the ADC over a wide range of current values. For instance, use of four different shunts with the nominal rms currents of 1 mA, 20 mA, 200 mA and 2 A (and with nominal rms output voltages of 0.8 V, respectively) can cover the output of commercial calibrators that generate currents up to a typical value of 2.2 A. Of course, shunts up to 100 A are also available, making even higher scaling possible. With the approach tackled in [49] and [50] it is possible to calibrate AC currents with direct traceability to a quantum voltage standard by means of a shunt resistor. The calibration procedure includes the calibration of an AC shunt by DC reference resistors, traceable to Quantum Hall Resistance, at DC current. In that measurement setup the AC-QVM (AC Quantum Voltmeter) is used as a DC quantum voltage standard for the resistance comparisons using a 3458A as a null-detector. It was shown, for example, that the ratio of two resistances can be measured with a relative uncertainty of 0.2 µΩ/Ω for a current of 0.9 mA. Self-heating of the shunt is one problem which needs to be addressed, and it depends on the type of the

shunt, on the current level applied, and on the measurement procedure. It is of great importance if such current measurement is made in a step-up or step-down procedure using the same shunt at different current levels. After the above calibration at DC current, the resistance of the shunt is known, and it can be used for AC current measurements by using the AC-QVM, with stable results up to 1 kHz. For instance, the stability of an AC current measurement at 62.5 Hz using a Fluke A40B-10mA AC shunt at 3.3 mA can be done within the time interval of two to five minutes with a relative uncertainty of 0.2 µA/A to 0.3 µA/A (providing that the measured source is very stable and synchronized to AC-QVM). Thus, it was demonstrated that by optimizing AC current measurements procedures and using ACQVM, it is possible to obtain accurate results within short measurement durations with direct traceability to quantum voltage standards.

8.2.6. Sampling and data analysis software

Sampling and data analysis software is described in detail in the Section 7 of this document.

8.3. Results

Various parts of the proposed system for digital traceability were characterized and a selection of the results are presented below. In these measurements, Josephson voltage systems were used to provide precisely known stable inputs in order to characterize performance. To investigate the suitability of various digitizers for use as transfer standards, measurements were made of both the static (section 8.3.1) and dynamic AC voltage and current traceability based on Josephson voltage standards (section 8.3.2) gain stability as a function of time. The target is to achieve better than 1 µV/V stability in gain over the time between the calibration of the digitizer against a quantum standard and its use as a transfer standard. The effect of the temperature of a digitizer on its static gain stability was also measured (section 8.3.1.2) to investigate the performance under different operating conditions. The combination of digitizers with current shunts to provide traceability for current measurements was investigated in section 8.3.3. A comparison of the proposed method against the existing thermal method was performed. Finally, a novel method using a multi-tone waveform of combined sine waves for a faster calibration method was investigated (section 8.3.3.2).

8.3.1. Characterization of static performance of digitizers

8.3.1.1. Static stability of integrating digitizer 3458A

Static gain stability and nonlinearity of a 1 V range of a 28 bit integrating ADC was investigated using a 1 V PJVS system described in [19, 20]. The static gain is observed a few times each day during a Helium fill. This observation was repeated at different times over more than two years. Custom developed software evaluates the quantum state (if the PJVS is within its operating margins) of the measurements as described in [19, 20]. Quick and automatic switching ability of the PJVS between quantum voltages helps the gain measurements to be free from thermal noise and offset errors as proved in [20]. This also helps obtain sufficient measurements in a short time to observe statistics of the gain and nonlinearity as shown in the data presented in [19]. The daily and long-time gain stability of the ADC was investigated for metrological purposes is shown in Fig. 8.4. The y axis of Fig. 8.4 represents the difference of static gain of the ADC which is depicted with m_{400ms} (the static gain when the aperture time is equal to 400 ms) from the ideal gain 1 V/V. Daily drift of the gain of this ADC is much less than 0.5 µV/V and the drift during an hour is less than 0.05 µV/V. The INL is also measured as described in [19, 20]. The INL was measured to be less than 0.12 µV/V even for the 1 V range of the ADC.

8.3.1.2. Static gain stability of integrating digitizer 8588A

To estimate gain stability over time, the Allan deviation is a good measurement method. The digitizer is set to sample a large amount of data and the Allan deviation is calculated for different observation periods. The results show the typical deviation of the gain after a selected time. This is especially

important for measurement setups where digitizer gain is calibrated, and the same digitizer is used to calibrate DUT at some later time. Allan deviation provides information on how much the gain can deviate in the time between the gain calibration and the DUT calibration. This value should be included in the uncertainty budget of the measurement.

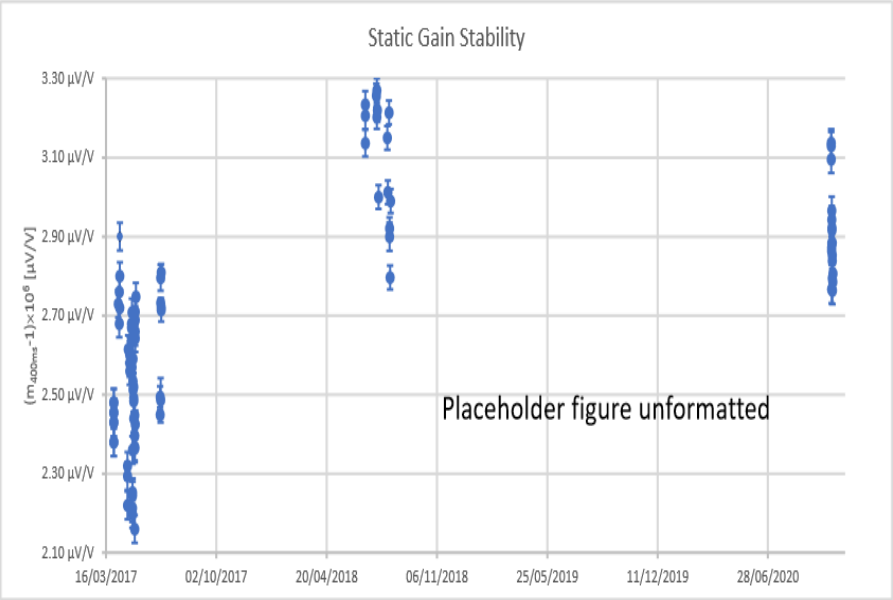

Fig. 8.4. *Static Gain Stability of an Integrating ADC as a function of time.*

An example of a gain stability estimation is shown in [57]. The digitizer was connected to a stable signal of approx. 10V generated by PJVS. A very long record was sampled and analysed by the Overlapped Allan Deviation (OADEV) function. Such a measurement can be done not only for the gain, but also for the case of shorted inputs to identify internal noise properties. An example of such a measurement is shown in Fig. 8.5. The figure reveals that averaging up to 0.03 s helps to decrease type A uncertainty. However, for apertures 0.2 µs and longer the drift starts to be important.

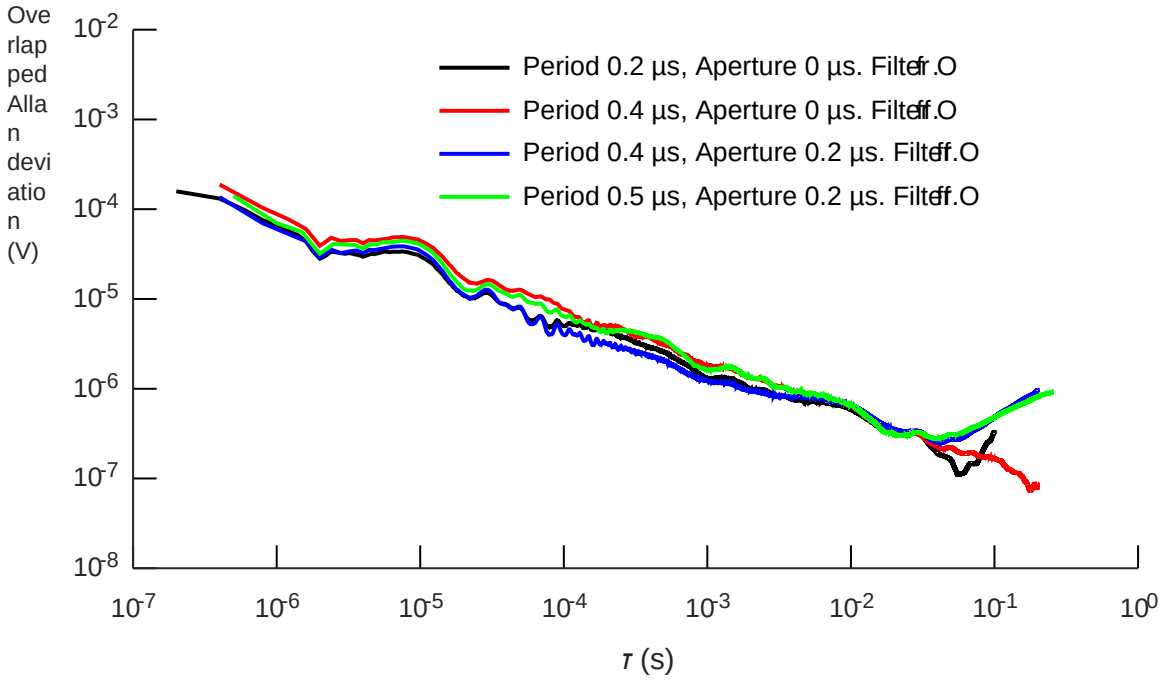

Fig. 8.5. *Dependence of Overlapped Allan deviation on observation time τ for digitizer Fluke 8508A set to range 0.1V with shorted input. Results for four settings of the multimeter aperture and sampling periods are shown.*

8.3.1.3. Static Gain thermal drift (3458A)

The temperature influence on the frequency response of Keysight 3458A digitisers on DCV sampling mode has been studied in [58] for DC voltage references and in [59] for AC input signals up to 1 kHz. Results show a similar behaviour for both DC and AC signals, with two very well differentiated behaviours of the temperature coefficients when aperture time is higher and lower than 100 µs. This behaviour is a consequence of the ADC switching between 10 kΩ and 50 kΩ inputs at 100 µs. For high integration times (T_a > 100 µs) the temperature influence is negligible, whereas in low integration times (T_a < 100 µs) the temperature influence is important, and it should be characterized for each digitiser when measurement temperature is different from digitiser calibration temperature.

8.3.2. Characterisation of dynamic performance of digitizers

8.3.2.1. Dynamic gain and dynamic gain stability

The NI PXI 5922 sampler was investigated using a JAWS with 80 mV amplitude (7500 Josephson junctions operated at 14.1 GHz) as described in 8.2.1.2. Well-quantized sine waves within the frequency range from 1 kHz to 100 kHz were directly applied to the sampler. The sampler was synchronized and triggered by the JAWS, and set to the 2 V range, 1 MΩ input impedance, standard 48-tap FIR filter. 40000 sine wave periods were measured using a sampling rate of 4 MSa/s. All data were averaged to one period as shown in Fig. 8.6. The measured deviation to the JAWS input sine (red curve in Fig. 8.6) shows a specific 'pattern' which remains independent from frequency and deviations from the nominal value vary within ±7 µV/V, but can be as large as 13 µV/V. We note that the spikes around maximum amplitudes are present after averaging 40000 periods i.e., they are not caused by spurious jumps but are in fact a nonlinearity existing in the sampler.

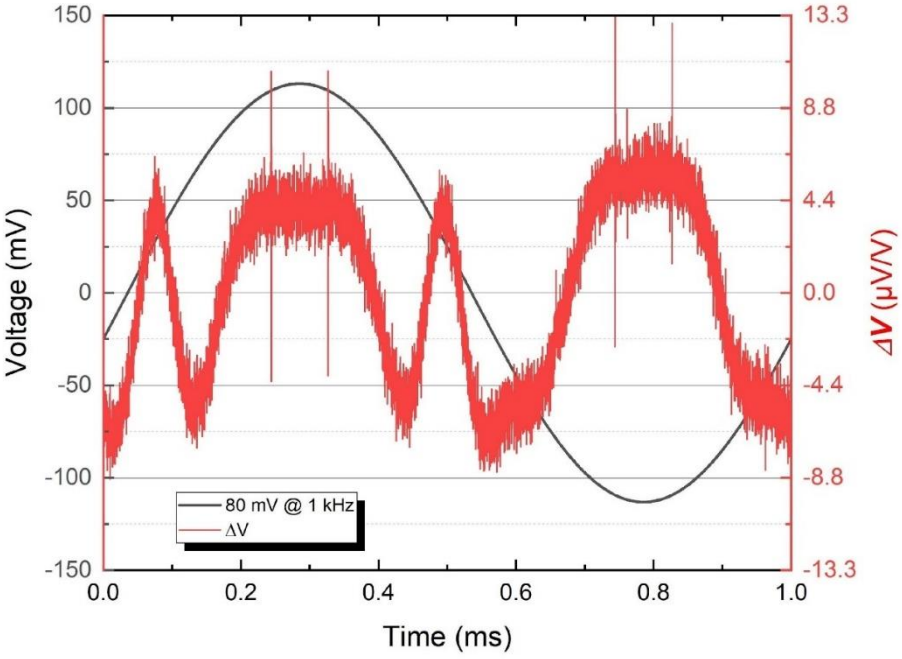

Fig. 8.6. *Linearity measurement of an 80mV sine wave at 1kHz (black line, left axis). The red curve shows deviations from this sine wave, right axis.*

We also investigated the gain stability of the sampler by running an overnight measurement. The setting of the sampler was the same as for the previous experiment. The JAWS sine wave frequency was set to 100 kHz and measured with the sampler for 15 h. It is expected that the JAWS output does change

with time. Fig. 8.7 shows the result for such a measurement. The gain variation stays within ±15 µV/V over the time of the exercise, however, a gain change of 25 µV/V within less than 1 h is also possible. All deviations are well within the specifications of the instrument [60]. Furthermore, the sampler is very well suited for differential measurements in an AC quantum voltmeter [61]. However, both investigations show that sampler has a limited linearity and stability which make it challenging to use it for scaling applications aiming at the µV/V level.

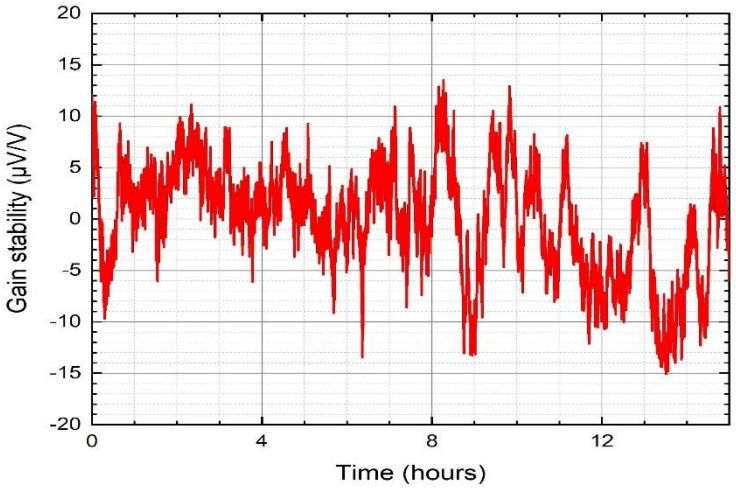

Fig. 8.7. *Long-term gain stability measurement of the sampler for an 80mV JAWS sine wave at 100 kHz.*

8.3.2.2. Dynamic Gain stability

The dynamic gain stability can be estimated in similar way as the static gain stability. Such a method was shown in [26]. An AC signal was generated by JAWS and applied to a National Instruments 5922 digitizer. The signal was divided into a number of sections and processed by amplitude estimating algorithms. The calculated amplitude was further process by the OADEV algorithm. Due to highly stable properties of JAWS, all measured stability can be accredited to digitizer and the amplitude estimating algorithm. Multiple of these algorithms have been used to demonstrate that the measured stability was inherent to the digitizer. The results show the stability of the digitizer for various time periods, this time for an AC signal of selected frequency or amplitude. Fig. 8.8 shows such a measurement for signals of frequency 150 Hz and amplitudes from ≈0.092 V to ≈0.646 V. One can see that for time periods longer than ≈10 s the drift is dominant over the random noise of the digitizer gain.

8.3.3. Characterisation of complete system

In the new digital method for current and voltage traceability (as shown in Fig. 8.1b), TVCs are replaced by digitizers. In this way, a current source provides the same current to two combinations of shunt-digitizer: the shunt-digitizer under test and the standard shunt-digitizer, as shown in Fig. 8.9. By comparison of the digitizers output and knowing the correction of the combination standard shunt-digitizer (by characterization against Josephson voltage standard), the correction of the shunt-digitizer under test can be calculated. By repeating this process for higher currents, a complete digital traceability chain can be established.

This new method described above, and a primary validation is described in [62]. Two digitizers (Keysight 3458A) were used to step up from 20 mA to 1 A in five steps. Nine frequencies, from 10 Hz to 10 kHz were considered. The validation consisted of the comparison of the shunt AC-DC difference obtained by thermal and digital methods. In this comparison DC measurements were performed because the traditional TVC approach provides just the AC-DC difference. Nevertheless, in a digital-based current step up, DC measurements are not necessary. The comparison of both methods can only be based on

the AC-DC difference of the shunts alone. Therefore, the influence of the TVC and digitizers had to be eliminated from the measurements. In the thermal converter method, it is assumed that the AC-DC difference of the shunt and TVC combination adds arithmetically. The AC-DC difference of the TVC is known. To eliminate the digitizer influence in the digital method, two sets of measurement were performed, one with the setup shown in Fig. 8.10 and another swapping digitizer. The combination of these two measurements allowed the elimination of the digitizers influence and the comparison of the two methods. A detailed description and results are also described in [3]. Results show that up to 1 kHz the difference between both techniques is very small (<2 μA/A at 1 kHz).

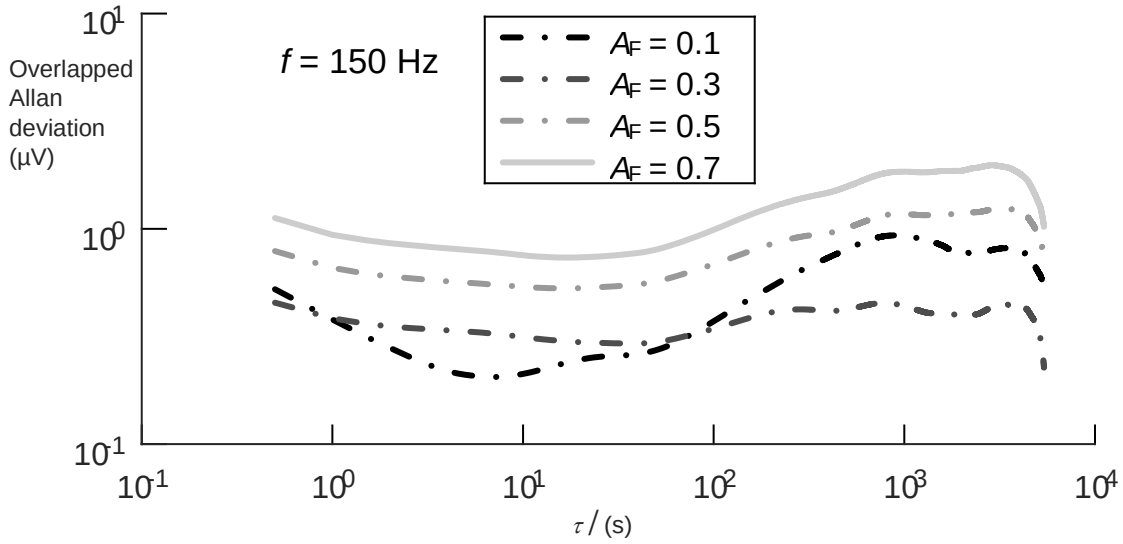

Fig. 8.8. *Dependence of Overlapped Allan deviation on observation time τ for digitizer National Instruments 5922 set to 1 V range. Results for four signals of amplitudes: ≈0.092 V (A_F = 0.1), ≈0.277 V (A_F = 0.3), ≈0.461 V (A_F = 0.5), and ≈0.646 V (A_F = 0.7).*

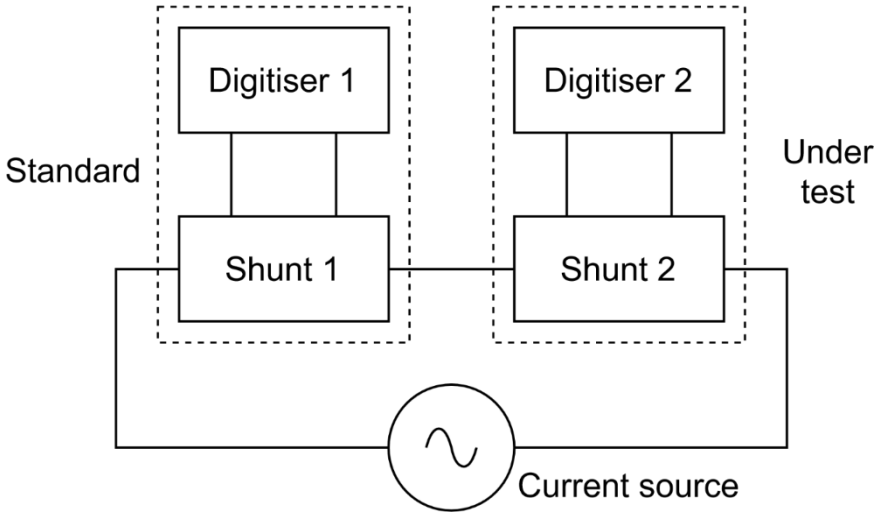

Fig. 8.9. *Setup of the new digital current step up. The standard shunt-digitizer is calibrated against Josephson voltage standard. Then the digitizers output is compared, and the correction required for the shunt-digitizer under test is calculated. The complete digital traceability chain is established by repeating the process for higher currents.*

Following this initial work, a quantum validation of the digital step-up technique was performed. Two digitizers (Keysight 3458A) were used together with two shunts of 20 mA and 50 mA. Three signals with three different frequencies (100 Hz, 400 Hz and 1 kHz) were input singly and combined allowing the analysis of dynamic signals. The combinations included the same amplitude / same phase, different amplitude / same phase, and same amplitude / different phase. The quantum validation was divided into three phases as indicated in Fig. 8.10. In phase A, the quantum calibration of the shunts was performed as explained in 2.5, resulting in the determination of shunts resistance with an uncertainty in the sub ppm range. In phase B, digitizers were characterized against JAWS, calculating the correction necessary for each singled or combined signal, frequency and digitizer. Finally, in phase C, the validation is performed comparing the shunts ratio after digitizer output correction, using the setup shown in Fig. 8.9, and the ratio from quantum calibration.

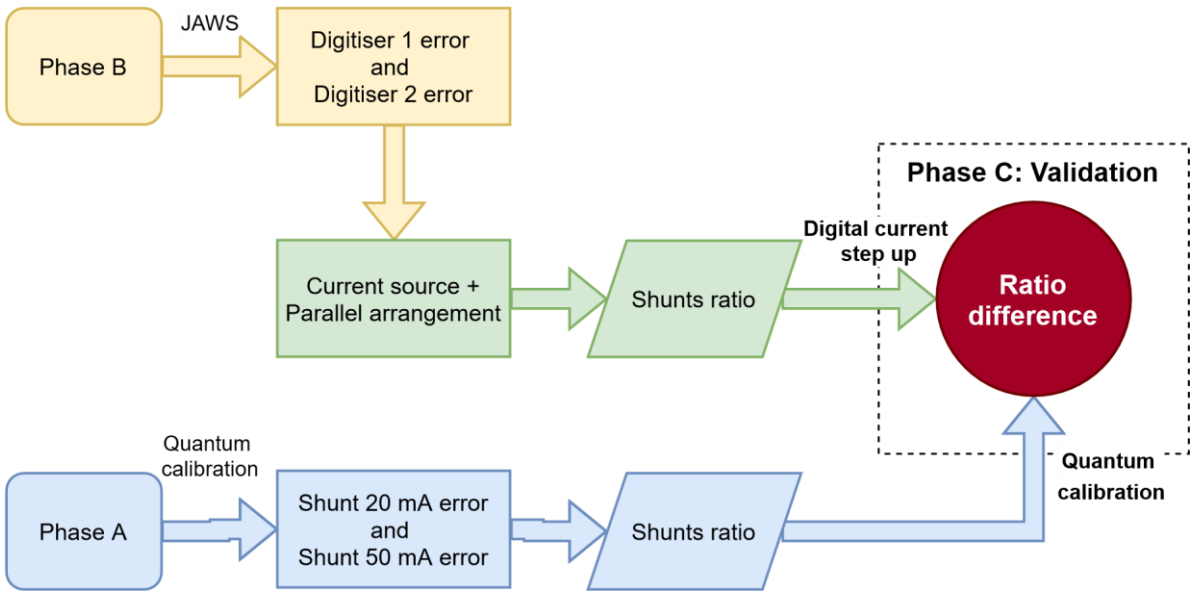

Fig. 8.10. *Quantum validation of digital current step-up. In phase A the quantum calibration of shunts is performed. In phase B digitisers are calibrated against JAWS. In phase C the corrected shunts ratio is compared to shunts ratio from quantum calibration.*

Results showed that the ratio difference obtained by quantum calibration and the step-up method after digitizer correction is in the order of few µV/V, validating the new digital method for traceability of current. This allows high accuracy dissemination for complex waveforms that vary with time or have a significant amount of harmonic content, at the same time that calibration procedures are simpler and shorter. Further details and results will be included in an article in preparation [63].

8.4. Uncertainties

Uncertainties of quantities estimated from sampled data are based on the following uncertainties of input quantities:

i) type A uncertainty,
ii) type B uncertainties estimated from hardware,
iii) type B uncertainties caused by a data processing.

The first type of uncertainty, type A, is caused by external or internal sources that cannot be repeated and quantified in other ways than by statistical means. Type A uncertainty is estimated by repeating the measurements which can usually be performed by any available sampling software. The second and third type of uncertainty, type B, is the *prior knowledge*. Any hardware used in the measurement setup

increases the uncertainty of measurement, such as transducers, transmission cables, digitizers, signal sources. Calibration data, correction coefficients and the related uncertainties of measurement elements have to be known to successfully estimate output quantities and its uncertainty. Both types of uncertainties are extensively described in the existing literature.

The third type of uncertainty, caused by imperfections of quantity estimating algorithms, are very hard to estimate and not yet sufficiently described in the literature. A basic description can be found in [64]. Example of algorithms errors can be found e.g., in [65]. Various algorithms return different results for the same input data due to different underlying calculation methods. It is very hard to discover the errors of the algorithm for the actual measurement. One has to know all errors and sources of uncertainties to find out value of the algorithm error. However, there are at least two unknown sources of errors during a calibration of a DUT: the DUT itself and the algorithm. Therefore, simulations are used to estimate algorithm errors, e.g. [66]. Simulation provides the possibility to control errors and input uncertainties to find out the error of the algorithm. Based on the simulation, an uncertainty can be assigned to the algorithm and used in the real measurements. Unfortunately, simulation cannot cover all the details of a real measurement.

The propagation of type B uncertainties is carried out using GUM Uncertainty Framework (GUF) [67] or Monte Carlo Method (MCM) [68, 69]. Yet using both methods is very complex as the sampling measurement methods use a large amount of data and implements numerous sources of uncertainties.

QWTB was developed with the aim of easy uncertainty propagation, and TWM was developed to use these qualities for actual sampling measurements. Calibration data of the measurement setup can be loaded into the TWM system, and the algorithm can use it for evaluation of the output uncertainty. TWM can cover many corrections and uncertainties for the whole measurement chain from transducer, connecting cable to digitizer. Fig. 8.11 shows the basic correction design for a single ended direct connection measurement. However, other correction configurations including buffer, differential connection or combinations are available, as detailed comprehensively in [70]. Several algorithms have been extended to utilize the corrections and uncertainties.

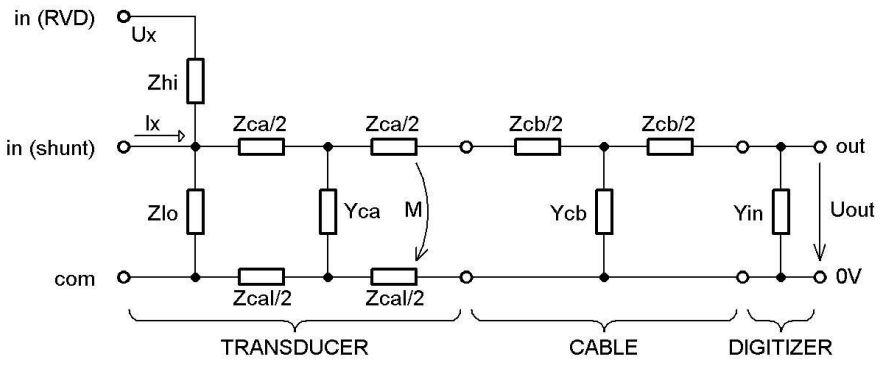

Fig. 8.11. *TWM correction design for single ended direct connection measurement. Impedance values (Z, Y) and its uncertainties for transducer, cable and digitizer can be used to calculate correct value and uncertainty of estimated quantities. More complex designs are available.*

8.4.1. Example of algorithm validation

Quantum systems are suitable for finding algorithm errors due to the ability to generate signals with known values. Yet the DUT can still cause unknown errors and it is difficult to establish if the source of the error is part of the DUT or the data estimation algorithm. The following method can be used to characterize the performance of the algorithm. One can artificially limit the measured data and examine the performance of the algorithm. An example of this method is shown in the following example testing the validity of uncertainties estimated by the algorithm calculating Total Harmonic Distortion (THD).

Algorithm TWM-THD with uncertainty estimation was validated in [71]. The algorithm is capable of estimating the uncertainty and using multiple records to estimate the influence of the noise. Multiple

records are used to perform averaging of complex values of DFT (discrete Fourier transform) outputs, and the averaged spectra are used to estimate noise level and value of THD. Thus, it is not a simple average of THD values, but an averaging of noise in the complex plane of the Fourier transformation. The algorithm partly uses MCM, therefore it is not possible to build an uncertainty budget. Based on simulations, the performance of the algorithm increases with increasing averaging and length of the records.

To test validity of the uncertainty estimation, a sine wave signal of frequency 4.8 kHz and amplitude 25 mV has been generated by the JAWS system and was applied to a digitizer (National Instruments 5922) of unknown harmonic distortion. The sampling frequency was set to 48 kHz. The digitizer sampling was coherent to the signal source. The records have been split into multiple sections of the same length. The THD was calculated for various number of sections (increased complex averaging) and various number of samples in the sections. Based on the simulation, the value calculated from the highest number of longest sections is the most probable value. However even for smaller number of sections of shorter length the THD uncertainty should be correctly estimated by the algorithm.

The resulting THD and its uncertainty is shown in Fig. 8.12. The plots cover the span of averaging from 1 (no averaging) to average from 40 records, and the record length span is from section of 40 signal periods (4000 samples) to section of 1600 signal periods (160×10^3 samples). The record length is expressed as multiples of 40 signal periods. The THD value tends towards a value of 0.46×10^{-6} with increasing number of averaging and increasing length of record. The uncertainty behaves similarly and tends towards to a value of 0.61×10^{-6}. For clarity, Fig. 8.13 shows only the value from the diagonal of the previous figure. One can see all but first two values of calculated THD uncertainties encompass the most probable value for highest number of sections and longest records showing that the uncertainty estimation of the algorithm was correct for the majority of the results.

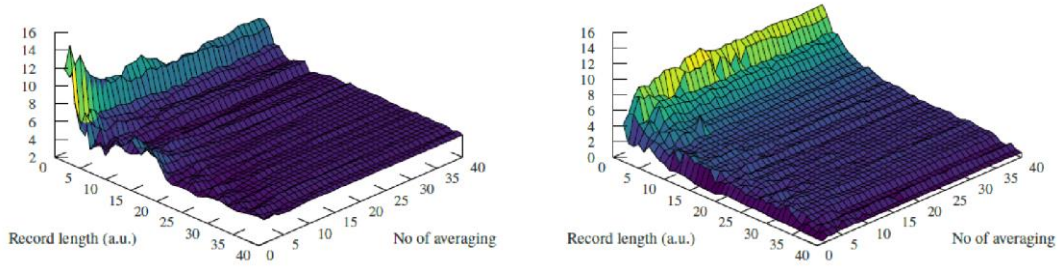

Fig. 8.12. *THD value (left) and uncertainty (right) as calculated from record of various lengths and number of averaging. The record length is expressed as multiple of 40 signal periods. Values of THD and uncertainty are multiplied by 1×10^6.*

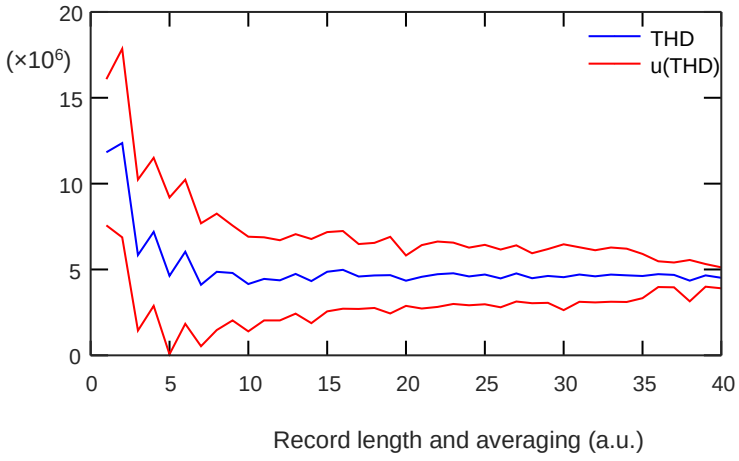

Fig. 8.13. *THD value and its uncertainty for increasing record length and number of averaging. Line graph represents diagonal cross section of graphs shown in Fig. 8.12.*

8.5. Conclusion

We propose a new method for providing traceability to the SI for AC voltage and current. This method is based on the utilization of PJVS and JAWS to characterize high performance digitizers. When used with voltage dividers and current shunts, these digitizers can provide a more direct traceability chain having the advantages of reduced measurement time as well as reduced complexity. The components of this proposed method should be selected on an individual basis depending on the facilities and availability of individual components. We have presented details on the commonly available systems and instruments typically found at NMIs and present various results of the characterization of these components.

An approach combining traditional scaling methods with the use of a digitizer operating within its optimum range was adopted. In this way, Josephson systems can be used to fully characterize the digitizer under the conditions under which it will be used. The use of resistive and inductive voltage dividers for voltage scaling were investigated as well as the use of current shunts.

Measurements of the static gain stability of the Keysight 3458A have shown long term stability. The temperature effect on this instrument has been found to be significant only above 100 µs aperture time where correction must be made if using the instrument at a different temperature. The Fluke 8588A has shown gain stability reaches an optimum at around 0.03 s sample time. The dynamic performance of the NI 5922 has revealed larger variation in gain with time up to 25 µV/V indicating it is not suitable for use as a transfer standard. For this digitizer drift dominates over a 10 s measurement time so the uncertainty cannot be reduced by sampling for longer time periods.

Traceability for current measurements using a digitizer and current shunt characterized as a single unit has shown good agreement with thermal methods.

Initial study of the use of multi tone waveforms shows promising potential for reducing measurement time via the application of several frequencies at once with no loss of accuracy.

Uncertainty analysis methods have been developed to accommodate the non-ideal performance of system components. An example of the use of this method to measure THD has shown that this analysis method is a useful tool for determining the measurement time required to achieve lowest uncertainty, reducing the use of unnecessary lengthy measurements which are not required to reduce the uncertainty past the limiting value.

In summary, the initial measurements and investigation of a new digital traceability chain for AC voltage and current have shown promising results and it is expected that future work will involve the integration of these digital methods into NMI traceability chains and will replace thermal based methods in the longer term.

8.6. References

[1] BIPM 2019 The International System of Units (SI brochure (EN)): 9th edition, 2019
[2] 2018 Mise en pratique for the definition of the ampere and other electric units in the SI
[3] BIPM KCDB database URL https://www.bipm.org/kcdb/
[4] Williams E S 1971 Journal of Research of the National Bureau of Standards - C. Engineering and Instrumentation **75C** 145–154
[5] Inglis B D 1992 METROLOGIA **29** 191–199
[6] Budovsky I, Georgakopoulos D, Hagen T, Sasaki H and Yamamori H 2011 IEEE Transactions on Instrumentation and Measurement **60** 2439–2444
[7] Rüfenacht A, Flowers-Jacobs N E and Benz S P 2018 Metrologia **55** S152–S173 URL https: //doi.org/10.1088/1681-7575/aad41a
[8] Kohlmann J, Behr R and Funck T 2003 Measurement Science and Technology **14** 1216–1228 URL https://doi.org/10.1088/0957-0233/14/8/305
[9] Lapuh R 2018 Sampling with 3458A (Ljubljana: Left Right)

[10] Konjevod J, Malarić R, Mostarac P and Jurčević M 2021 The ac amplitude measurement characteristics of high-resolution digitizers based on calibration with thermal voltage converter and swerlein algorithm 2021 IEEE International Instrumentation and Measurement Technology Conference (I2MTC) pp 1–5
[11] Konjevod J, Malarić R, Jurčević M, Mostarac P and Dadić M 2020 IEEE Transactions on Instrumentation and Measurement **69** 3719–3728
[12] Wijayasundara G, Kim M S, Park S N and Lee H K 2018 Calibration of ac voltage for a high-speed sampling adc board using thermal voltage converters 2018 Conference on Precision Electromagnetic Measurements (CPEM 2018) pp 1–2
[13] Amagai Y, Maruyama M and Fujiki H 2013 IEEE Transactions on Instrumentation and Measurement **62** 1621–1626
[14] van den Brom H E, Kieler O F O, Bauer S and Houtzager E 2017 IEEE Transactions on Instrumentation and Measurement **66** 1391–1396
[15] Overney F, Rüfenacht A, Braun J P, Jeanneret B and Wright P S 2011 IEEE Transactions on Instrumentation and Measurement **60** 2172–2177
[16] Kim M S, Cho H, Chayramy R and Solve S 2020 Metrologia **57** 065020
[17] Kurten W, Mohns E, Behr R, Williams J, Patel P, Ramm G and Bachmair H 2005 IEEE Transactions on Instrumentation and Measurement **54** 649–652
[18] Henderson D, Williams J M and Yamada T 2012 Measurement Science and Technology **23** 124006 URL https://doi.org/10.1088/0957-0233/23/12/124006
[19] Oztürk T C, Ertürk S, Tangel A and Arifovic¸ M 2020¨ IEEE Transactions on Instrumentation and Measurement **69** 4425–4435
[20] Oztürk T C, Ertürk S, Tangel A, Arifoviç M and Turhan S 2017 Metrological measurements using¨ programmable josephson voltage standard 2017 10th International Conference on Electrical and Electronics Engineering (ELECO) pp 1117–1121
[21] Kim M S, Cho H and Solve S 2022 Metrologia **59** 015006 URL https://doi.org/10.1088/ 1681-7575/ac438f
[22] Palafox L, Ramm G, Behr R, Kurten Ihlenfeld W G and Moser H 2007 IEEE Transactions on Instrumentation and Measurement **56** 534–537
[23] Waltrip B C, Nelson T L, Berilla M, Flowers-Jacobs N E and Dresselhaus P D 2021 IEEE Transactions on Instrumentation and Measurement **70** 1–6
[24] EMPIR Joint Research Project 2020 - 23 Quantumpower - quantum traceability for ac power standards URL quantumpower.cmi.cz
[25] Rietveld G, Zhao D, Kramer C, Houtzager E, Kristensen O, de Leffe C and Lippert T 2011 IEEE Transactions on Instrumentation and Measurement **60** 2195–2201
[26] Šira M, Kieler O and Behr R 2019 IEEE Transactions on Instrumentation and Measurement **68** 2091–2099 ISSN 0018-9456
[27] Lapuh R, Voljč B, Lindič M and Kieler O F O 2017 IEEE Transactions on Instrumentation and Measurement **66** 1089–1094
[28] de Aguilar J D, Salinas J R, Kieler O, Caballero R, Behr R, Sanmamed Y A and Mendez A 2019´ Measurement Science and Technology **30** 035006 URL https://doi.org/10.1088/1361-6501/ aafb27
[29] EMPIR Joint Research Project 17RPT03 DIG-AC 2018 - 22 A digital traceability chain for ac voltage and current URL https://digac.gum.gov.pl/
[30] Williams J 2011 IET Science, Measurement & Technology **5**(5) 163–174(11) ISSN 1751-8822 URL https://digital-library.theiet.org/content/journals/10.1049/iet-smt.2010.0168
[31] Ozturk T C, Erturk S, Tangel A and Arifoviç M 2020 IEEE TRANSACTIONS ON INSTRUMENTATION AND MEASUREMENT **69** 4425–4435 ISSN 0018-9456
[32] Lee J, Behr R, Palafox L, Katkov A, Schubert M, Starkloff M and Boeck A C 2013 METROLOGIA **50** 612–622 ISSN 0026-1394
[33] Benz S P and Hamilton C A 1996 Applied Physics Letters **68** 3171–3173 URL https://doi.org/10.1063/1.115814
[34] Watanabe M, Dresselhaus P and Benz S 2006 IEEE Transactions on Applied Superconductivity **16** 49–53

[35] Kieler O F, Iuzzolino R and Kohlmann J 2009 IEEE Transactions on Applied Superconductivity **19** 230–233
[36] Flowers-Jacobs N E, Rüfenacht A, Fox A E, Dresselhaus P D and Benz S P 2020 Calibration of an ac voltage source using a josephson arbitrary waveform synthesizer at 4 v 2020 Conference on Precision Electromagnetic Measurements (CPEM) pp 1–2
[37] Kieler O F, Behr R, Wendisch R, Bauer S, Palafox L and Kohlmann J 2015 IEEE Transactions on Applied Superconductivity **25** 1–5
[38] Benz S, Burroughs C and Dresselhaus P 2001 IEEE Transactions on Applied Superconductivity **11** 612–616
[39] Sosso A and Roberto C 2000 Calibration of multimeters as voltage ratio standards 2000 Conference on Precision Electromagnetic Measurements (CPEM 2000) pp 375–376
[40] Swerlein R L 1991 A 10 ppm accurate digital ac measurement algorithm Proceedings NCSL pp 17–36
[41] Hill J and Deacon T 1968 Proc. IEE 727–735
[42] Hsu J C, Chen S F, Kuo C J and Hsiao M 2016 Calibration of inductive voltage dividers at power frequencies using an ac-pjvs 2016 Conference on Precision Electromagnetic Measurements (CPEM 2016) pp 1–2
[43] Ramm G, Moser H and Braun A 1999 IEEE Transactions on Instrumentation and Measurement **48** 422–426
[44] Cassiago C, Cerri R, Paglia G L and Sosso A 2004 Application of dmm linearity to dc volt traceability 2004 Conference on Precision Electromagnetic Measurements pp 176–177
[45] Mašláň S, Šira M and Skalická T 2018 Precision Buffer with Low Input Capacitance˘ 2018 Conference on Precision Electromagnetic Measurements (CPEM 2018) (IEEE) pp 1–2 ISBN 978-1-5386-0973-6
[46] Georgakopoulos D, Budovsky I and Benz S P 2019 IEEE Transactions on Instrumentation and Measurement **68** 1935–1940
[47] Herick J, Bauer S, Behr R, Beug M F, Kieler O F O and Palafox L 2018 Calibration of an Inductive Voltage Divider using Pulse-Driven Josephson Arrays 2018 Conference on Precision Electromagnetic Measurements (CPEM 2018), Paris, FRANCE, JUL 08-13, 2018
[48] Kieler O F, Behr R, Schleussner D, Palafox L and Kohlmann J 2013 IEEE Transactions on Applied Superconductivity **23** 1301404–1301404
[49] Starkloff M, Bauer M, Schubert M, Lee J, Behr R, Palafox L, Schaidhammer L, Böck A and Fleischmann P 2018 The ac quantum voltmeter used for ac current calibrations 2018 Conference on Precision Electromagnetic Measurements (CPEM 2018) (IEEE) pp 1–2
[50] Ilić D, Behr R and Lee J 2020 24th IMEKO TC4 International Symposium 369–373
[51] Šira M 2017 QWTB - Software Toolbox for Sampling Measurements URL˘https://qwtb.github.io/qwtb/
[52] Šira M, Mašláň S and Nováková Zachovalová V 2016 QWTB – Software Tool Box for Sampling˘ Measurements Conference on Precision Electromagnetic Measurements Digest (IEEE) p 2 ISBN 978-1-4673-9133-7 URL http://ieeexplore.ieee.org/document/7540599/?reload=true
[53] 2012 Matlab URL http://www.mathworks.com
[54] 2012 GNU Octave URL https://www.gnu.org/software/octave/
[55] Mašláň S TWM tool https://github.com/smaslan/TWM
[56] Mašláň S and Power O 2019 Cal Lab: The International Journal of Metrology 27–35 ISSN 1095-4791 URL https://www.callabmag.com
[57] Šira M 2020 Noise and stability of Fluke 8588A in digitizing mode 2020 Conference on Precision Electromagnetic Measurements (CPEM) pp 1–2 ISBN 978-1-72815-899-0 ISSN 2160-0171 URL https://ieeexplore.ieee.org/document/9191833
[58] Salinas J, de Aguilar J D, Garcıa-Lagos F, Joya G, Sanmamed Y, Caballero R, Neira M and Sandoval F 2018 Study of Keysight 3458a temperature coefficient for different aperture times in dcv sampling mode 2018 Conference on Precision Electromagnetic Measurements (CPEM 2018) (IEEE) pp 1–2
[59] Sanmamed Y, Salinas J, de Aguilar J D, Garcıa-Lagos F and Caballero R 2019
[60] Ni 2018 pxi/pci-5922 specification
[61] Behr R and Palafox L 2021 Metrologia **58** 025010

[62] Peral D, Sanmamed Y A and Diaz de Aguilar J 2022 Submitted to IMEKO 2022 - Brescia, Italy
[63] Peral D, Diaz de Aguilar J, Behr R, Ilić D, Kieler O, Herick J and Sanmamed Y A 2022 In preparation for CPEM 2022 - Wellington, New Zealand
[64] Lapuh R, Šira M, Lindič M and Voljč B 2016 Uncertainty of the Signal Parameter Estimationˇ from Sampled Data Conference on Precision Electromagnetic Measurements Digest p 2 ISBN 978-1-4673-9133-7 URL http://ieeexplore.ieee.org/document/7540770/
[65] Slepicka D, Agrez D, Lapuh R, Nunzi E, Petri D, Radil T, Schoukens J and Sedlacek M 2010 Comparison of nonparametric frequency estimators Instrumentation and Measurement Technology Conference (I2MTC), 2010 IEEE (IEEE) pp 73–77 URL http://ieeexplore.ieee.org/xpls/abs_all.jsp?arnumber=5488181
[66] Šira M, Mašláň S and Skalická T 2018 Uncertainty of Phasor Measurement Unit Calculated byˇ Means of Monte Carlo Method 2018 Conference on Precision Electromagnetic Measurements (CPEM 2018) (IEEE) pp 1–2 ISBN 978-1-5386-0973-6
[67] JCGM 1995 Evaluation of Measurement Data - Guide to the Expression of Uncertainty in Measurement (Bureau International des Poids et Measures) ISBN 92-67-10188-9 URL https://www.bipm.org/en/publications/guides/
[68] JCGM 2008 Evaluation of Measurement Data - Supplement 1 to the “Guide to the Expression of Uncertainty in Measurement” - Propagation of Distributions Using a Monte Carlo Method (Bureau International des Poids et Measures) URL https://www.bipm.org/en/publications/ guides/
[69] JCGM 2011 Evaluation of Measurement Data – Supplement 2 to the “Guide to the Expression of Uncertainty in Measurement” – Extension to Any Number of Output Quantities (Bureau International des Poids et Measures) URL https://www.bipm.org/en/publications/guides/
[70] TracePQM consortium 2018 TWM correction datasets reference manual URL https://github.com/smaslan/TWM
[71] Horska J, Maslan S, Streit J and Sira M 2014 A validation of a THD measurement equipment with a 24-bit digitizer 2014 Conference on Precision Electromagnetic Measurements (CPEM 2014) pp 502–503
[72] J Ireland, P G Reuvekamp, J M Williams, D Peral, J Díaz de Aguilar, Y A Sanmamed, M Šíra, S Mašlán, W Rzodkiewicz, P Bruszewski, G Sadkowski, A Sosso, V Cabral, H Malmbekk, A Pokatilov, J Herick, R Behr, T Coşkun Öztürk, M Arifoviç and D Ilić, “A method for using Josephson voltage standards for direct characterization of high performance digitizers to establish AC voltage and current traceability to SI”, paper submitted for publishing with open access, 2022.

9. THERMAL CONVERTER-BASED AC VOLTAGE STANDARD

9.1. Principles of AC-DC converters

AC-DC converters allows the traceability between AC and DC voltage standards. To precisely provide such transfer the thermal method is used. This concept is the comparison of two voltages: AC RMS and DC. The Input voltage is converted to the nonelectrical quantity such as temperature. It causes the induction of the output electrical quantity such as thermoelectric force or the current of emitter in transistor. The following diagram (see Fig. 9.1) illustrates the principle of such measurement.

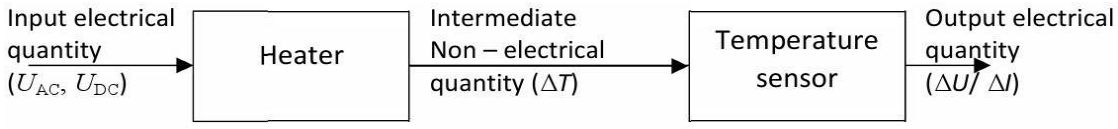

Fig. 9.1. *Principles of TVC operation.*

From the measurement point of view the most important parameter of the thermal voltage converters is AC-DC transfer difference which is given by equation:

$$\sigma_{AC\text{-}DC}(f) = (U_{AC} - U_{DC})/\, U_{DC}, \text{ for } E_{AC} = E_{DC} \tag{9.1}$$

where $\sigma_{AC\text{-}DC}(f)$ – the transfer difference, U_{AC} – the RMS value of the converter AC input voltage, U_{DC} – the value of the converter's DC input voltage, E_{AC} – the converter output voltage at the AC input signal, E_{DC} – the converter output voltage at the DC input signal.

9.1.1. Single Junction Thermal Voltage Converters (SJTVC)

This is the oldest one and still used AC-DC converter. In the single junction TVC resistance wire under input voltage heats up insulated thermocouple. Heater wire, thermocouple and leads are placed in vacuum glass bulb (see Fig. 9.2 and Fig. 9.3).

Fig. 9.2. *Single-junction TVC; left: schematics, right: photograph.*

Fig. 9.3. *Holt model 11 SJTVCs*

Under the nominal current heater temperature raises up to about 150 °C. It can cause approx. 7 mV thermal EMF thermocouple junction. Such low voltage is difficult to measure precisely. This kind of the thermal converter is characterized by the quasi-quadratic function of the output voltage given by:

$$E = cV_I^n \tag{9.2}$$

where c – proportional coefficient, V_I – input voltage, n – transfer function exponent ($n \approx 1.7 \div 2$).

Therefore, it practically limits the use of SJTVC with a voltage of less than 50 % of its nominal input value. This type of the voltage converter is sensitive to input overvoltage. Using higher values of the input voltage than its nominal value the converter can be damaged as a result of overheating.

9.1.2. Multi Junction Thermal Voltage Converters (MJTVC)

Unlike single-junction TVCs, MJTVC converters contain multiple thermocouples in series. The main advantage of such devices is higher output signal which can be measured more easily and precisely. The output thermoelectrical voltage typically is about 90 mV. It can be manufactured in traditional glass bulb. Currently multi-junction converters are also produced in planar form, using semiconductor fabrication processes and micromachining techniques. Such TVCs have planar or thin-film form on substrate material like silicon or quartz crystal.

9.1.3. Semiconductor TVC

It can be manufactured in the form of two monolithic integrated circuit boards. They are placed in a vacuum casing for thermal insulation. With the bipolar transistor integrated circuit consists of diffusion resistor as a heater. Both converter boards are connected to the differential amplifier. The advantage of such setup is elimination of the temperature influence. Another benefits of semiconductor TVC are higher sensitivity and time stability. For example, Fluke 792A or Fluke 5790A (Fig. 9.4). Using Semiconductor TVC is easier to operate because the higher output voltage (about 2 V) at the nominal input voltage. Another difference in this type of converters is linear output voltage characteristics. Unlike junction thermal converters it has overload protection. Semiconductor converters typically operates using battery power.

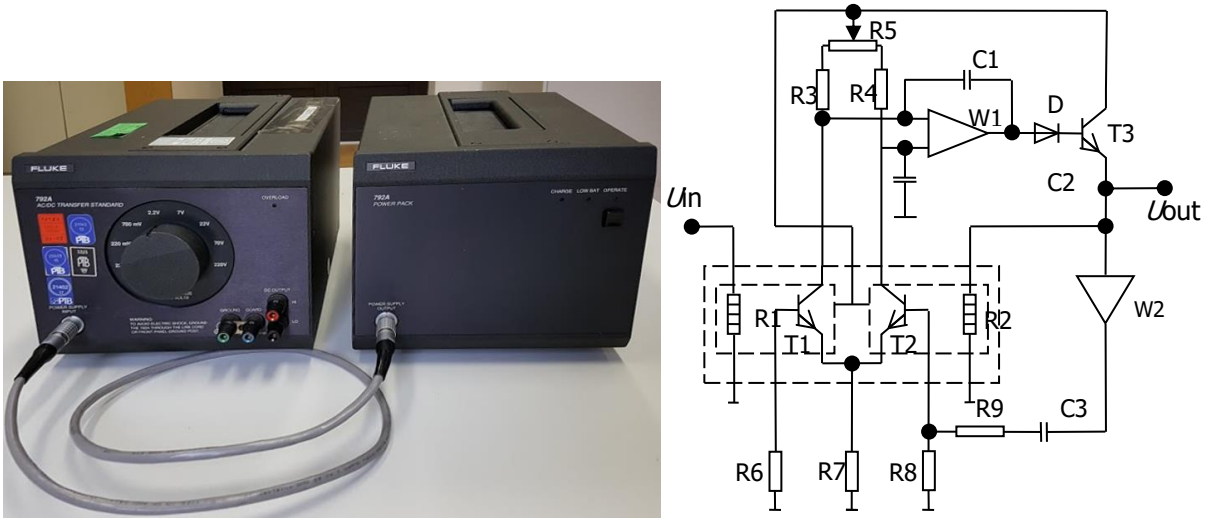

Fig. 9.4. *Semiconductor TVC; left: Fluke 792A photo, right: schematics.*

9.2. Measurement system of the thermal converter-based AC voltage standard

In Fig. 9.5 is given the schematic diagram of an AC-DC difference comparator system, which incorporates DC voltage source, AC voltage sources, two nanovoltmeters, and reference AC-DC converter. Unit under test is marked as UUT.

To ensure needed stability and accuracy, as voltage sources (DC and AC) the best possible calibrators are usually used, or at least ones with very good short-term and long-term amplitude stability, and specifically for AC part, a low harmonic content. In Fig. 9.6 is given the outlook of one real system implemented in GUM.

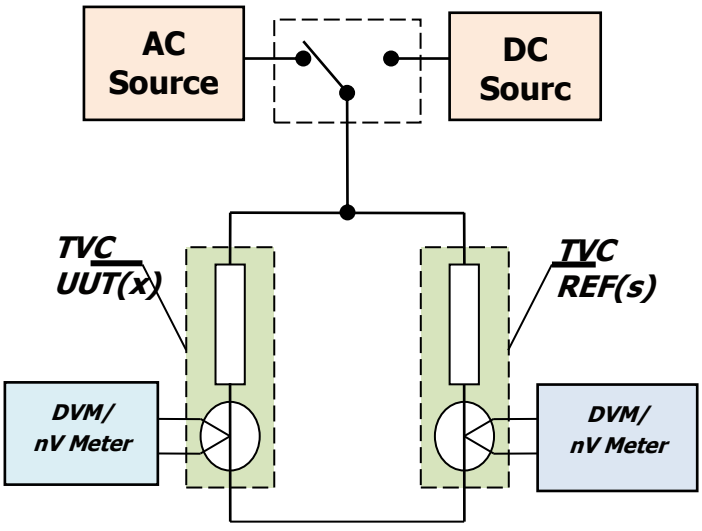

Fig. 9.5. *Schematic diagram of an AC-DC difference comparator system.*

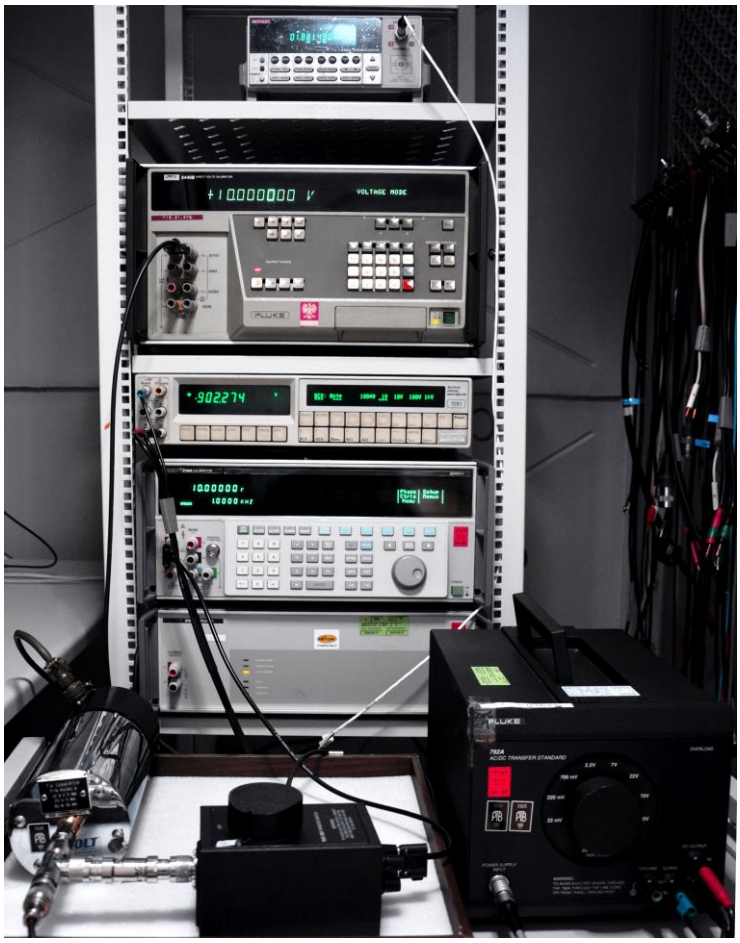

Fig. 9.6. *AC-DC difference comparator system placed in GUM. The measuring station consists of: DC voltage source FLUKE 5440B calibrator, AC voltage sources FLUKE 5720A/5700A calibrator, Keithley 2182A nanovoltmeter, AC-DC Voltage Tee, reference converter HOLT model 11, UUT Fluke 792A.*

9.2.1. AC-DC converters

Practically AC-DC converters are enclosed in electrostatically screened chassis. Additional resistor is connected to thermal converter for current adjustment.

Typical to connect converters type N or General Radio GR874 connectors are used with coaxial cables. Wrapping wires around ferrite ring favours better performance (Fig. 9.7 to Fig. 9.9).

Fig. 9.7. *Male (upper) and female (lower) N connector and GR874 hermaphroditic connector (right).*

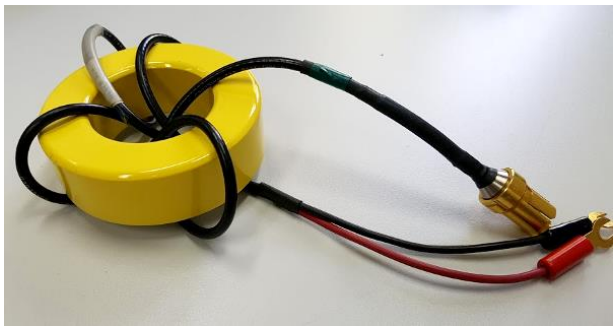

Fig. 9.8. *Connection wires wounded around ferrite choke toroidal core.*

Fig. 9.9. *AC-DC Voltage Tee used in difference comparator system.*

9.2.2. Voltmeters

The best performance of the measurement could be obtained by using nanovoltmeters. Currently, industry standard is the choice between Keithley 2182 and Keysight (formerly Agilent) 34420A. Instead nanovoltmeters reference 8 ½ digits voltmeters like Fluke 8508A of Keysight 3458A can be used.

9.2.3. Voltage sources

The High accuracy multifunction calibrators such Fluke 5720 can be used as the AC and DC source. As DC source can be used semiconductor voltage reference Fluke 732B.

9.2.4. AC-DC switching and timing

AC-DC switching have significant role in measurement process. Best performance can be obtained using reliable switches that allows to switch as quickly as possible and have negligible influence on frequency response of thermal converter. It is necessary to maintain an appropriate sequence of measurements (for example: AC, DC+, AC, DC-, AC). It is important DC voltage should be applied to converter in both polarities. It minimizes reversion error.

After applying DC voltage in both polarities input is switched to AC. Typically after switching settle time between 30 s and 90 s is needed. It is necessary because resistance wire needs time to heat up and to be stabilized. From the practical point of view twelve measurements in series gives the best trade-off between time of measurement and accuracy. Typical one series of measurements time is about 40 min.

9.3. Comparison of thermal voltage converters

Possession of voltage thermal converters with known AC-DC transfer difference can be used to calibration of another thermal voltage converters involving measurement system described in 9.2.

9.3.1. Comparison principle

To compare thermal voltage converters to channel method can be used. Input of reference TVC with known AC-DC transfer difference (REF) is connected to power selection switch parallel to calibrated converter (UUT). As described in 9.2.4 in the first step DC voltage is applied in positive and negative polarization and output voltage is measured for both TVCs. Its mean value is given by:

$$E_{\mathrm{DC}} = \frac{E_{\mathrm{DC+}} + E_{\mathrm{DC-}}}{2}$$

Next input voltage is switched to AC and E_{AC} output voltage is measured for REF and UUT thermal converters.

Measurement difference is given by:

$$\Delta_{\mathrm{B}} = \frac{E_{\mathrm{SAC}} - E_{\mathrm{SDC}}}{n_{\mathrm{S}}\, E_{\mathrm{SDC}}} - \frac{E_{\mathrm{XAC}} - E_{\mathrm{XDC}}}{n_{\mathrm{X}}\, E_{\mathrm{XDC}}}$$

where:
E_{XAC}, E_{XDC} - value of the output voltage of the UUT converter at AC and DC input signals,
E_{SAC}, E_{SDC} - value of the output voltage of the reference converter at AC and DC input signals,
n_{x} - exponent of the processing function of the UUT converter,
n_{s} - exponent of the processing function of the reference converter.

Transfer difference measurement equation is given by:

$$\Delta_{\mathrm{X}} = \Delta_{\mathrm{B}} + \Delta_{\mathrm{A}} + \Delta_{\mathrm{S}}$$

where:
Δs - correction of the reference converter (parameter from the certificate calibration of the reference converter).

9.3.2. Sources of uncertainties

Uncertainty of such transfer can be expressed as:

$$u(\Delta_{\mathrm{X}}) = \sqrt{u^2(\Delta_{\mathrm{B}}) + u^2(\Delta_{\mathrm{A}}) + u^2(\Delta_{\mathrm{S}})}$$

where:
$u(\Delta_{\mathrm{A}})$ - uncertainty of the correction due to lack of repeatability of results, calculated using A method,
$u(\Delta_{\mathrm{S}})$ - uncertainty of the transfer difference of the standard converter (from the calibration certificate of the template), calculated using a B method,
$u(\Delta_{\mathrm{B}})$ - uncertainty arising from the measurement system, calculated using B method.

Measurement difference uncertainty is type B uncertainty and is expressed as:

$$u(\Delta_{\mathrm{B}}) = \sqrt{c_1^2 u^2(E_{\mathrm{SAC}}) + c_2^2 u^2(E_{\mathrm{SDC}}) + c_3^2 u^2(n_{\mathrm{S}}) + c_4^2 u^2(E_{\mathrm{XAC}}) + c_5^2 u^2(E_{\mathrm{XDC}}) + c_6^2 u^2(n_{\mathrm{X}})}$$

where:
$u(E)$, $u(n)$ - the uncertainty of quantity on which Δ_B depends
c - the corresponding sensitivity coefficients.

Sensitivity coefficients are given by:

$$c_1 = \frac{d\Delta_X}{dE_{SAC}} = \frac{1}{n_S\, E_{SDC}};$$

$$c_2 = \frac{d\Delta_X}{dE_{SDC}} = \frac{E_{SAC}}{n_S}\left(-\frac{1}{{E_{SDC}}^2}\right);$$

$$c_3 = \frac{d\Delta_X}{dn_S} = \frac{E_{SAC} - E_{SDC}}{E_{SDC}}\left(\frac{1}{{n_S}^2}\right);$$

$$c_4 = \frac{d\Delta_X}{dE_{XAC}} = \frac{1}{n_X\, E_{XDC}};$$

$$c_5 = \frac{d\Delta_X}{dE_{XDC}} = \frac{E_{XAC}}{n_X}\left(-\frac{1}{{E_{XDC}}^2}\right);$$

$$c_6 = \frac{d\Delta_X}{dn_X} = \frac{E_{XAC} - E_{XDC}}{E_{XDC}}\left(\frac{1}{{n_X}^2}\right);$$

9.4. References

[1] Klonz M.: CCE Comparison of AC-DC Voltage Transfer Standards at the Lowest Attainable Level of Uncertainty. IEEE Trans. on Instr. And Meas. 1997, vol. 46, no 2, pages 342-346.

[2] Laiz H., Klonz M., Kessler E., Kampik M., Lapuch R.: Low- Frequency AC-DC Voltage Transfer Standards with New High- Sensitivity and Low-Power Coefficient Thin-Film Multijunction Thermal Converters IEEE Trans. on Instr. And Meas. 2003, vol. 52, no 2, pages 350-354.

[3] Hermach LF.: Thermal Converters as AC-DC Transfer Standards for Current and Voltage Measurements at Audio Frequencies Journ. Of Res. Of the NBS, vol. 48, no. 2 1952, pages 317-334.

[4] Barański A., Podemski A.: Etalon napięcia przemiennego w zakresie do 1000V i częstotliwo ci do 100 kHz. Przegl. Elektrotech. 1991, pages. 68-71.

[5] Filipski P., van Mullem C., Janik D., Klonz M., Kinard R., Lipe T., Waltrip B.: Comparison of High-Frequency AC-DC Voltage Transfer Standards at NRC, VSL, PTB and NIST. IEEE Trans. on Instr. and Meas. 2001, vol. 50, no 4, pages 349-352.

[6] Kürten W.G., Mohns E.: AC-DC transfer measurements of highest accuracy with synchronous analogue-to-digital conversion. Metrologia 41, 2004, pages. 111-115.

[7] EA Interlaboratory Comparison EL25. AC-DC Voltage Transfer Difference COFRAC/LCIE Paris, 2002.

[8] 792A AC-DC Transfer Standard Instruction Manual, rev. 1 12/92.

[9] www.fluke.com

[10] Barański A., Ratajczak J., Zawadzki P.: Przetworniki termoelektryczne AC-DC jako wzorce napięcia przemiennego", PAK 2007 no 9bis, pages 38-41.

10. COMPARISON OF THE THERMAL AND QUANTUM/DIGITAL CALIBRATION METHODS

10.1. Objective

Thermal method is widely used technique for measurement AC voltage and current at highest level of accuracy. Recently developed Programmable Josephson Voltage Standards (PJVS) and Josephson Arbitrary Waveform Synthesizer (JAWS) combined with digital technology are increasingly used in AC voltage measurements with a clear perspective to become primary standards in this field.

This chapter summarizes the comparison of the quantum & digital and thermal techniques in AC measurements. Work includes comparison of the PJVS and thermal voltage converter (TVC) at AC voltage using a digitizer, comparison of the digitizer-divider combination to the TVC at AC voltage and comparison of digitizer-shunt combination to TVC-shunt combination at AC current.

10.2. Comparison of the PJVS to TVC Using a Digitizer

10.2.1. Devices Used in Comparison

10.2.1.1. Transfer Standard

Comparison of the PJVS to TVC was performed by using a Keysight 3458A multimeter as transfer standard. Device was used in DCV sampling mode with external triggering [1].

10.2.1.2. 10 V PJVS System

TÜBİTAK UME PJVS is a helium free system built in a customized pulse tube cryocooler with an array of 10 V produced by Supracon AG, Fig. 10.1. The array (SNS technology) contains 69632 Josephson junctions grouped in 18 segments having nearly binary sequence and can produce maximum output of ±10.08 V at 70 GHz operating frequency with a resolution of 145 µV.

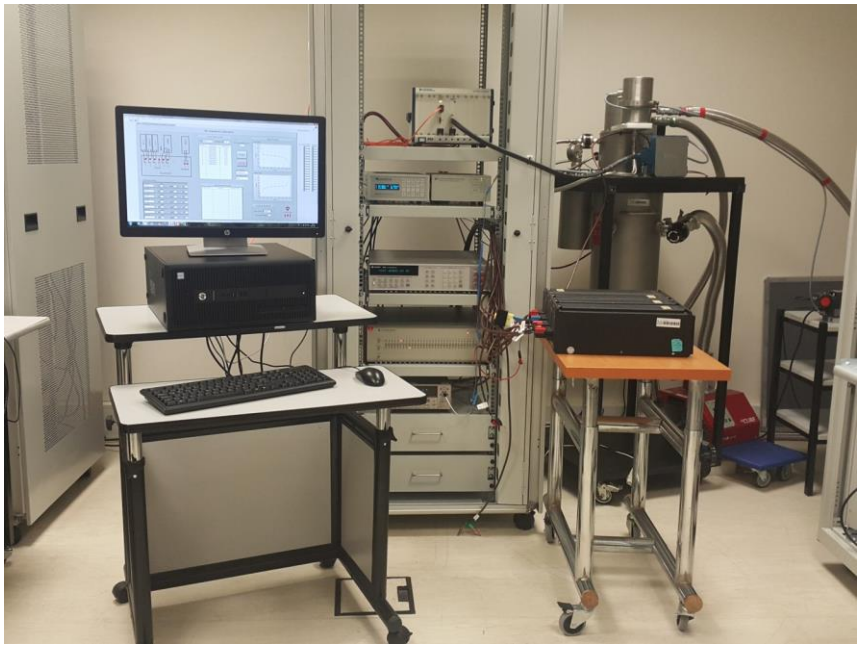

Fig. 10.1. *TÜBİTAK UME 10 V Programmable Josephson Voltage Standard.*

The array is biased with the National Instruments PXIe-6738 32-channel board, mounted in the NI 1082DC PXI chassis. Complete synchronization of all channels is performed on the board. In order to provide electrical isolation from ground, bias source is operated by a battery and controlled by a PC via fibre-optic link [2].

Microwave bias is provided by a compact synthesizer locked at 10 MHz to a frequency standard and controlled by the PC via isolated RS 232 link.

System is controlled by software written in LabVIEW. Software is capable to measure and calculate optimum bias currents and RF power of the array, has options to calibrate DC standards, linearity of high precision voltmeters and can produce quantum based stepwise approximated waveforms.

10.2.1.3. Thermal Voltage Converter

Multi-Junction Thermal Converter (MJTC) of nominal value of 10 V was used as reference standard for thermal technique. It consists of a planar MJTC of 90 Ω heater resistance [15] and a 900 Ω range resistor. Calibration of the standard was performed as described in [3] and [13].

10.2.2. Measurement Procedure

Comparison of PJVS to TVC was realized in two steps; first, digitizer's gain was measured with PJVS [5][7], then digitizer was compared to the reference TVC by measuring AC voltage simultaneously.

10.2.2.1. Calibration of the Digitizer with PJVS

Measurement system is shown in Fig. 10.2. In order to provide synchronization between digitizer and PJVS an external Arbitrary Waveform Generator (AVG) was used. Isolation between PJVS and AVG was realized using an auxiliary opto-isolation [6] of jitter about 300 ps. AWG CH2 was set in burst mode with number of cycles equal to the total samples of one measurement. Each single measurement consists of 10 period cycles while each period contains 1000 samples. Measurements were repeated 15 times and measured voltage was calculated using both, basic RMS formula and four parameter sine fit methods. Uncertainty of the measurements was calculated as presented in [6] and [7].

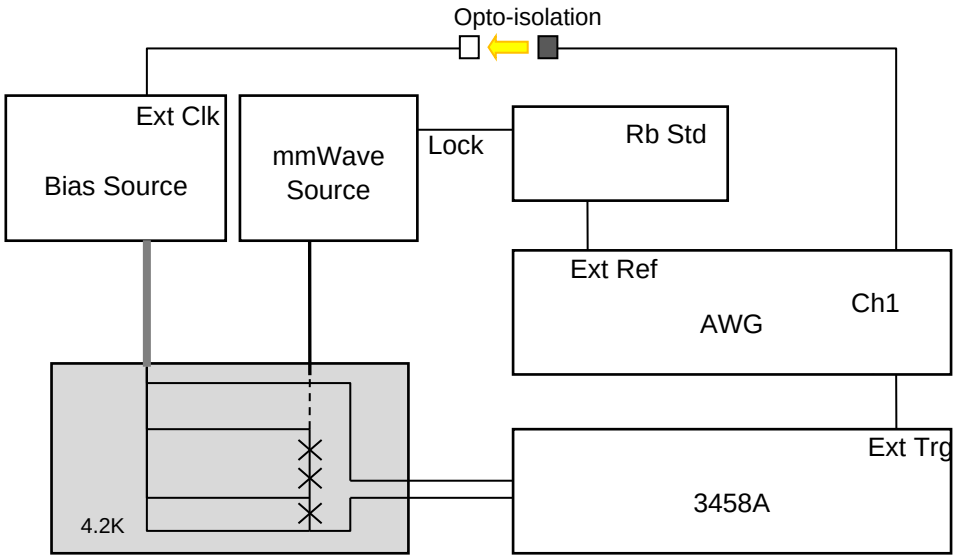

Fig. 10.2. *PJVS – digitizer comparison setup.*

10.2.2.2. TVC – Digitizer Comparison

Measurement Setup is shown in the Fig. 10.3. Triggering of the digitizer was provided, as in 10.2.2.1, externally with an AWG which was locked to the calibrator to provide coherent sampling for RMS method. Digitizer was also used in internal Timer sampling mode, to investigate how sampling mode affects the results.

AC-DC transfer measurements were performed automatically with TÜBİTAK UME control software [4]. Thermal method requires measurements to be performed taking the middle of the tee as reference plane for AC voltage. In the setup calibrator was used as a basic source and AC voltage at the centre of the tee was actually measured with both, TVC and digitizer. The digitizer was also used as the reference for DC voltage.

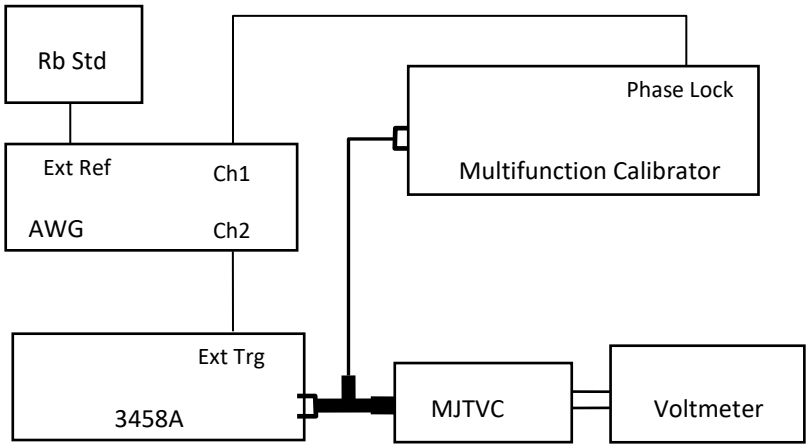

Fig. 10.3. *TVC – digitizer comparison setup.*

Measurement process starts by applying AC voltage to the TVC-digitizer and adjusting calibrator to produce DC voltage as close as possible (min 50 ppm) on the output of the TVC to those produced by test AC voltage. Then, each measurement cycle beginning by applying AC and DC voltages in sequence: AC, DC-, AC, DC+, AC.

The applied DC and AC voltages were measured with the digitizer while at the same time the output of the TVC was measured with a monitoring voltmeter.

AC voltage measured with TVC is calculated by the following equation:

$$V_{ac} = V_{dc}\left(1 + \frac{E_{ac} - E_{dc}}{n \cdot E_{dc}} + \delta_s + C_d\right)$$

where:

V_{dc} Average of absolute forward and reversed DC voltages measured by digitizer

E_{ac}, E_{dc} Output emf of the TVC when applied AC and DC voltage respectively

n Input-output sensitivity parameter of TVC, close to 2 for MJTVC

δ_s AC-DC transfer difference of the reference AC-DC transfer standard

C_d Correction to the measured DC voltage

Uncertainty of the measurements is calculated according to the TÜBİTAK UME calibration procedure for AC voltage source using TVC. Uncertainty budget includes the following components:

- A type uncertainty, standard deviation of the repeated measurements
- Uncertainty of the reference TVC

- Uncertainty of the reference TVC due to drift
- Uncertainty of the DC voltage measurement
- Uncertainty of the DC voltage due to drift

AC voltage was measured with digitizer three times during each measurement sequences. Similarly to PJVS measurements, each measurement consists of 10 samples per period, total 100 periods and repeated 10 times. Then, AC voltage was calculated by both, RMS formula and four parameter sine fit to check consistency of the measurement. Difference of the two algorithms, no matter which sampling mode is used (Ext or Timer) was order of ppb and had no influence on the results. Gain of the digitizer and sinc corrections for particular aperture times were included to calculated data. Uncertainty of the measurements was calculated as presented in [6] and [7] and combined with DC gain drift uncertainty since its last DC gain calibration with PJVS in addition to short time stability of the measurement.

It should be stress out here that while thermal method gives only RMS value of the AC voltage, digital method offer complete list of the waveform parameters. TÜBİTAK UME software for digitizer measurement which was used during comparison beside RMS value could calculate harmonics, offset, phase, SINAD, SNR and THD of the applied voltage, which clearly shows huge advantage of digital method.

10.2.3. Measurement Result

Results of the digitizer measured with PJVS are given in Table 10.1, while results of the digitizer - TVC comparison are given in Table 10.2. Relative difference between two measurements is shown in Fig. 10.4.

Table 10.1. *Gain of the digitizer measured with PJVS.*

Frequency (Integration Time)	DC (1 s)	60 Hz (1.6 ms)	110 Hz (850 µs)	400 Hz (220 µs)
Gain	1.0000033	1.0000033	1.0000034	1.0000073
Uncertainty	0.035 µV/V	0.50 µV/V	0.85 µV/V	2.0 µV/V

Table 10.2. *AC voltage measured with digitizer and TVC.*

Frequency	60 Hz		110 Hz		400 Hz	
	Measured	Uncertainty	Measured	Uncertainty	Measured	Uncertainty
TVC	6.999734 V	5.3 µV/V	6.999740 V	5.3 µV/V	6.999732 V	5.3 µV/V
Digitizer	6.999739 V	2.2 µV/V	6.999743 V	2.4 µV/V	6.999716 V	3.5 µV/V
$\Delta_{TVC\text{-}Digitizer}$	-0.7 µV/V	5.7 µV/V	-0.4 µV/V	5.8 µV/V	2.3 µV/V	6.4 µV/V
E_n	0.2		0.1		-0.4	

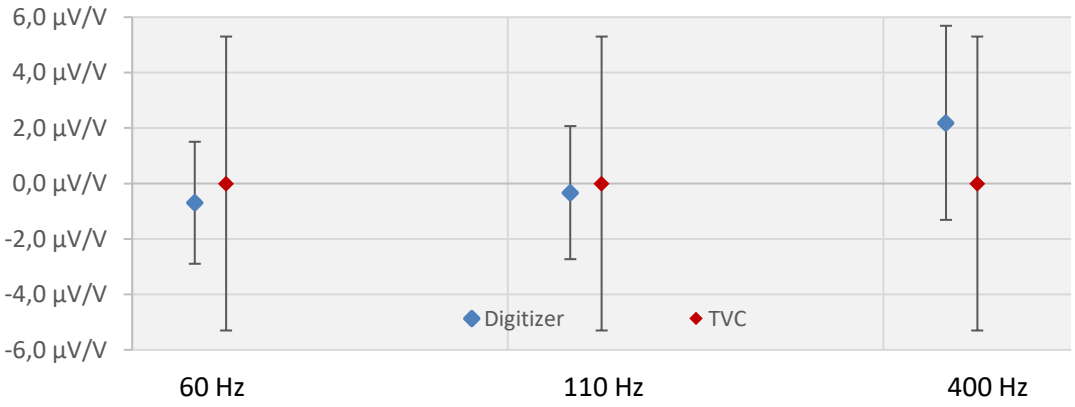

Fig. 10.4. *Relative difference between digitizer and TVC measurement of AC voltage.*

10.3. Comparison of the Digitizer-Divider combination to the TVC

10.3.1. Devices used in Comparison

10.3.1.1. Digitizer - Divider

Keysight 3458A was used as digitizer in a combination with a TÜBİTAK UME 50V 5:1 divider [8][10]. Digitizer was used in DCV sampling mode with both external triggering and Timer function [1]. Gain of the digitizer was calibrated by using PJVS as described in 10.2.2.1. AC-DC transfer difference of the divider was calibrated with thermal converters as described in [10].

10.3.1.2. Thermal Voltage Converter

Multi-Junction Thermal Converter with nominal value of 100 V was used as reference standard for thermal technique. It consists of a planar MJTC of 90 Ω heater resistance and a 10 kΩ range resistor. Calibration of the standard was performed as described in [3]. Traceability of the thermal voltage techniques in TÜBİTAK UME is described in [13].

10.3.2. Measurement Procedure

Measurement Setup is shown in the Fig. 10.5 and schematic in the Fig. 10.6. Triggering of the digitizer was provided with an AWG which is locked to the calibrator. The divider was connected to digitizer and tee with minimal connection. AC voltage seen to TVC is adjusted to 40 V while digitizer measure approximately 0.8 V at the output of the divider.

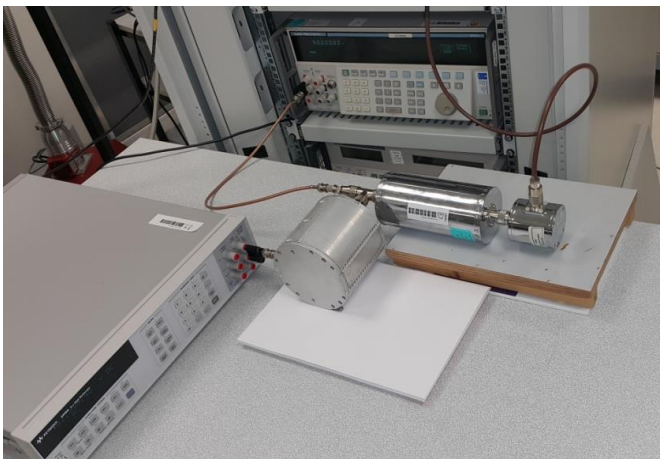

Fig. 10.5. *TVC to digitizer-divider comparison setup.*

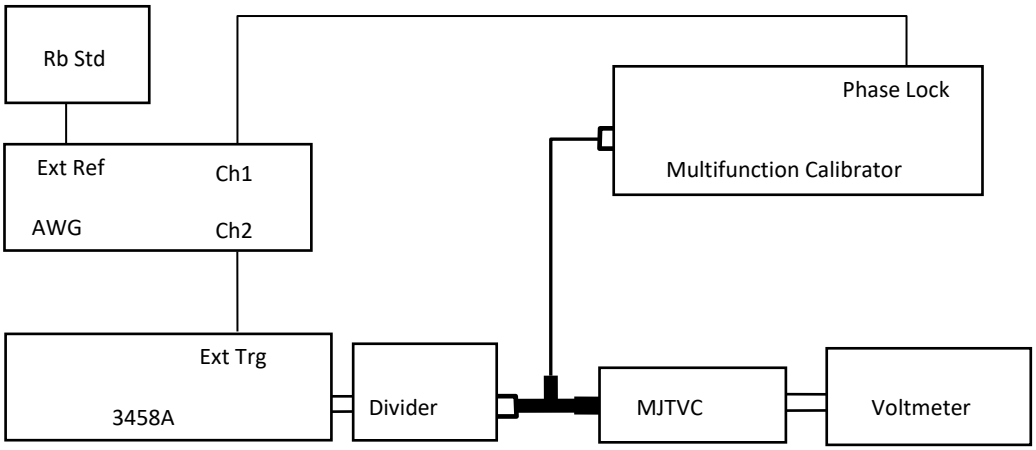

Fig. 10.6. *TVC to digitizer-divider comparison schematic.*

AC-DC transfer measurements were performed automatically with TÜBİTAK UME control software [4]. Thermal method requires measurements to be performed taking the middle of the tee as reference plane for AC voltage. In the setup calibrator was used as a basic source and AC voltage at the centre of the tee was actually measured with both, TVC and digitizer-divider combination. DC voltage applied by the calibrator to the middle of the tee was measured using the digitizer and its DC gain correction and DC ratio of the divider was calibrated according to [10] and [12].

Measurement process starts by applying AC voltage to the tee and adjusting calibrator to produce DC voltage as close as possible (min 50 µV/V) on the output of the TVC to those produced by test AC voltage. Then, each measurement cycle beginning by applying AC and DC voltages to the transfer standard and digitizer in sequence: AC, DC-, AC, DC+, AC. The applied DC and AC voltages were measured with the digitizer-divider combination while at the same time the output of the converter was measured with a monitoring voltmeter.

AC voltage measured with TVC is described in 10.2.2.2. Uncertainty of the measurements is calculated according to the TÜBİTAK UME calibration procedure for AC voltage source using TVC. Uncertainty budget includes the same components as in 10.2.2.2.

AC voltage was measured with digitizer three times during measurement sequences. Each measurement consists of 10 samples per period, total 100 periods and repeated 10 times. Then, AC voltage is calculated by both, RMS formula and four parameter sine fit. AC Gain of the digitizer and sinc corrections for particularly aperture times were included to calculated data. Finally, AC voltage at the input of the divider was calculated by combining digitizer voltage with the AC voltage ratio of the divider calculated according to measurements carried out according to [10]. Uncertainty of the measurements was calculated as presented in [7] and [8] for the digitizer and combined with the AC ratio calibration uncertainty of the divider. Additionally, AC loading error of the divider was calculated and combined to the uncertainty.

10.3.3. Measurement Results

Measurement results and total uncertainty of the AC voltage measured with TVC are listed in the Table 10.3. Relative difference between two measurements is shown in Fig. 10.7.

Table 10.3. *AC voltage measured with digitizer-divider and TVC.*

Frequency	60 Hz		110 Hz		400 Hz	
	Measured	Uncertainty	Measured	Uncertainty	Measured	Uncertainty
TVC	39.99810 V	7.4 µV/V	39.99818 V	7.4 µV/V	39.99810 V	7.4 µV/V
Digitizer-Divider	39.99802 V	5.0 µV/V	39.99807 V	5.0 µV/V	39.99788 V	5.6 µV/V
$\Delta_{TVC-Digitizer}$	2.2 µV/V	8.9 µV/V	2.7 µV/V	8.9 µV/V	5.6 µV/V	9.3 µV/V
E_n	-0.3		-0.4		-0.8	

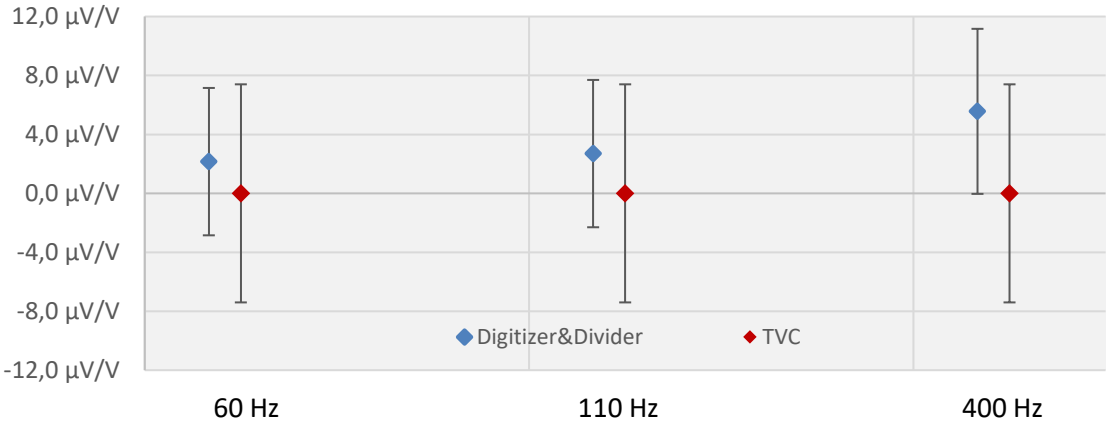

Fig. 10.7. *Relative difference between digitizer-divider and TVC measurement of AC voltage.*

10.4. Comparison of the Digitizer-Shunt to the TVC-Shunt

10.4.1. Devices used in Comparison

10.4.1.1. Digitizer & Shunt

Keysight 3458A was used as the digitizer in a combination with a TÜBİTAK UME 20 mA shunt. Digitizer was used in DCV mode sampling with external triggering and Timer function [1]. Gain of the digitizer was calibrated by using PJVS as described in 2.2.1. TÜBİTAK UME made current shunt attached to the digitizer was calibrated at DC with reference resistance standards while its AC values were calibrated by reference AC-DC shunts of TÜBİTAK UME.

10.4.1.2. Thermal Voltage Converter & Shunt

Multi-Junction Thermal Converter with nominal value of 1 V and TÜBİTAK UME current shunt of nominal current of 20 mA was used as reference standard for thermal technique. Traceability of the thermal current techniques in UME is described in [13] and [14].

10.4.2. Measurement Procedure

Measurement Setup and schematic are shown in the Fig. 10.8. Triggering of the digitizer was provided with an AWG which is locked to the calibrator. A special design serial tee was used to connect shunts in order to minimize cabling.

In the setup, calibrator was used as a basic source and applied AC current is measured with both, TVC-shunt and digitizer-shunt combination. DC current applied by the calibrator was measured using the

digitizer and shunt attached to. AC-DC transfer measurements were performed automatically with TÜBİTAK UME control software [4].

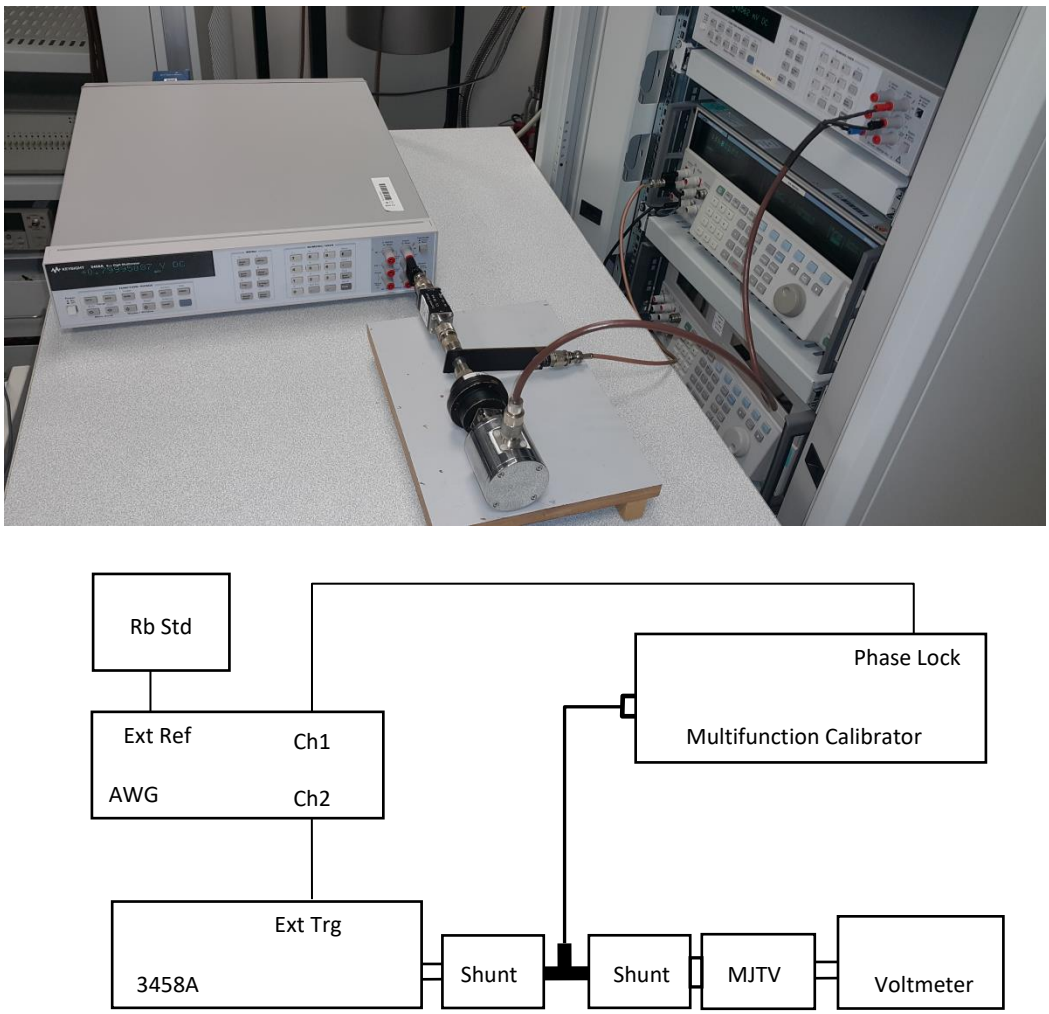

Fig. 10.8. *TVC-shunt – digitizer-shunt comparison setup and schematic.*

Measurement process starts by applying AC current and adjusting calibrator to produce DC current as close as possible (min 50 ppm) on the output of the TVC to those produced by test AC current. Then, each measurement cycle beginning by applying AC and DC currents to the transfer standard and digitizer in sequence: AC, DC-, AC, DC+, AC. The applied DC and AC currents were measured with the digitizer-shunt combination while at the same time the output of the TVC was measured with a monitoring voltmeter.

AC current measured with TVC-shunt combination is calculated by the following equation:

$$I_{ac} = I_{dc}\left(1 + \frac{E_{ac} - E_{dc}}{n \cdot E_{dc}} + \delta_s + C_d\right)$$

where:

I_{dc}	Average of absolute forward and reversed DC Current measured by digitizer-shunt
E_{ac}, E_{dc}	Output emf of the TVC when applied AC and DC current respectively
n	Input-output sensitivity parameter of TVC, close to 2 for MJTVC
δ_s	AC-DC transfer difference of the reference TVC-shunt combination
C_d	Correction of the DC current

Uncertainty of the measurements was calculated according to the TÜBİTAK UME calibration procedure for AC current source using TVC and shunt. Uncertainty budget includes the following components:

- A type uncertainty, standard deviation of the repeated measurements
- Uncertainty of the reference TVC / Shunt
- Uncertainty of the reference TVC / Shunt drift
- Uncertainty of the DC current measurement
- Uncertainty of the DC current measurement due to drift

AC voltage was measured with digitizer three times during measurement sequences. Each measurement consists of 10 samples per period, total 100 periods and repeated 10 times. AC voltage was calculated by both, RMS formula and four parameter sine fit. AC Gain of the digitizer and sinc corrections for particularly aperture times were included to calculated data.

Finally, AC current was calculated by Ohm low, dividing voltage with shunt's AC resistance. Uncertainty of the measurements was calculated as presented in [7] for the digitizer and combined with AC resistance calibration uncertainty of the current shunt.

10.4.3. Measurement Results

Measurement results and total uncertainty of the AC current measured with TVC & shunt are listed in the Table 10.4. Relative difference between two measurements is shown in Fig. 10.9.

Table 10.4. *AC current measured with digitizer-shunt and TVC-shunt.*

Frequency	60 Hz		110 Hz		400 Hz	
	Measured	Uncertainty	Measured	Uncertainty	Measured	Uncertainty
TVC-shunt	19.99907 mA	6.2 µA/A	19.99907 mA	6.2 µA/A	19.99908 mA	6.2 µA/A
Digitizer-shunt	19.99907 mA	7.5 µA/A	19.99907 mA	7.6 µA/A	19.99907 mA	8.0 µA/A
$\Delta_{TVC\text{-}Digitizer}$	0.1 µA/A	9.7 µA/A	0.0 µA/A	9.8 µA/A	0.5 µA/A	10.1 µA/A
E_n	0.0		0.0		-0.1	

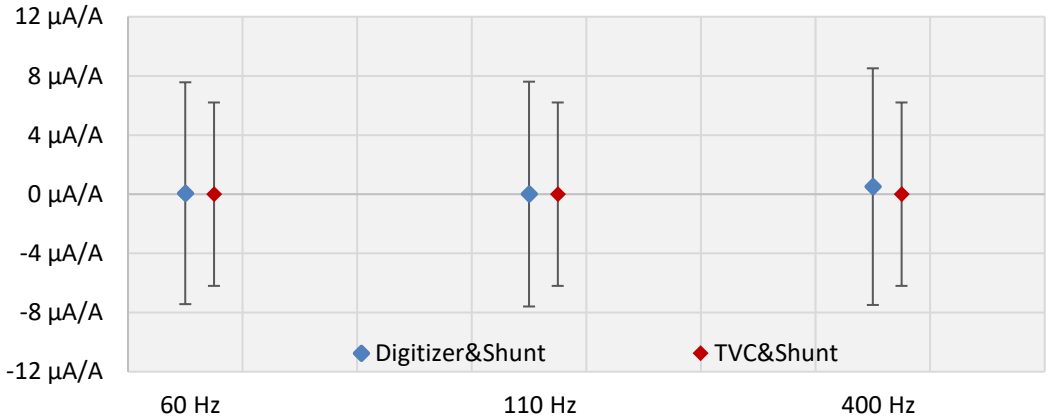

Fig. 10.9. *Relative difference between digitizer-shunt and TVC - shunt measurement of AC Current.*

10.5. Conclusions

Comparison between digital and thermal techniques has been performed and described with three common examples. The most accurate instruments currently on both sides, 3458A digitizer and MJTVC, have been used in the comparisons.

The measurements are made at frequencies that are suitable for both systems to highlight their full potential. As can be seen from the measurement results both methods are in good agreement at the points measurement made at.

The intention of this comparison was not focused on comparison points but on the methodology and potential of digital measurements. During the comparison, it was once again confirmed how fast, flexible and comprehensive the digital method is than the thermal method for measuring AC voltage. The only advantage of the thermal method currently is its applicability to a wider frequency range, up to 1 MHz, while for digital method it is about several kilohertz, with the existing technology at accuracy comparable to thermal method. This seems to be the only drawback of the digital method as auxiliary equipment like current shunts and voltage dividers, which are combined with digitizers, are already capable for possible extending of the frequency band. It should be noted that shunts and dividers are still calibrated at highest level of accuracy by using thermal method.

Having in mind the speed of measurements, the amount of information that can be obtained from digital measurements and the possibilities of their analysis, this method can be recommended whenever its uncertainty is sufficient to measure AC voltage.

10.6. References

[1] 3458A Multimeter User's Guide, 2021 Keysight Technologies
[2] M.Arifovic, R.Orhan, N.Kanatoğlu, "10V Programmable Josephson Voltage Standard Established in TÜBİTAK UME", CPEM 2018, Paris-France
[3] M. Arifovic, M. Klonz, "AC-DC Voltage Transfer at UME", CPEM 2002, Ottawa-Canada
[4] M. Arifovic, N.Kanatoğlu, "Automation of the ac-dc transfer measurements in UME", XX IMEKO, Busan- Korea
[5] N.Kanatoğlu, R.Orhan, M.Arifovic, "Linearity Testing of High Precision Digital Voltmeters with Programmable Josephson Voltage Standard", CPEM 2018, Paris-France
[6] Coskun Ozturk, T., Erturk, S., Tangel, A., Gedik, A., Yogun, M., Celep, M. "Establishing Programmable Josephson Voltage Standard and Maintaining its Quantum Accuracy", International Journal of Electrical and Electronic Engineering and Telecommunications, 8:1 (2019): 19-25
[7] Coskun Ozturk, T., Erturk, S., Tangel, A., Arifovic, M. "Using Programmable Josephson Voltage Standard for Static and Dynamic Gain Characterization of Integrating ADC", IEEE Transactions on Instrumentation and Measurement, 69:7 (2020): 4425-4435
[8] "Report on Uncertainty Estimation for Digital Measurements of Voltage Waveforms", TÜBİTAK UME Internal Report of 17RPT03 DIG-AC, October 2021
[9] Coskun Ozturk, T., Erturk, S., Tangel, A., Arifovic, M., Celep, M. "Towards Wideband Voltage Scaling to Quantum Standards at the Accuracy of the Stability ", CPEM 2018), Paris-France
[10] Coskun Ozturk, T ,Arifoviç Mehedin, Turhan Enis "Deliverable D7:Report including an uncertainty budget on a voltage divider suitable to scale 100 V:1 V target uncertainty of 25 µV/V for frequencies up to 100 kHz", QuADC Project Deliverable
[11] "Activity A2.2.6: Evaluating Dividers' Performances Suitable to be Used for Waveform Scaling", TÜBİTAK UME Internal Report of 17RPT03 DIG-AC, April 2022
[12] Coskun Ozturk T, Turhan S., Yilmaz, O. "An Improvement of Dc Voltage Ratio Measururements by Characterization of the Dc Voltage Divider at UME", XX IMEKO, Busan-Korea
[13] A.Sasso et al.," Overview of scaling methods in use" DIG-AC Project, Internal Report of 17RPT03 DIG-AC
[14] Arifovic, M., Kanatoglu, N., Uzun, S. "Extending AC-DC Current Transfer to 100 A, 100 kHz in UME ", CPEM 2016, Canada
[15] M. Klonz and T. Weimann, "Accurate thin film multijunction thermal converter on a silicon chip (AC-DC standard)," IEEE Trans. on Instrum. Meas., vol. 38, no. 2, pp. 335-337, April 1989

11. PROTOCOL FOR A FUTURE INTERCOMPARISON OF DIGITAL AC VOLTAGE AND CURRENT STANDARDS BETWEEN EUROPEAN NMIs

11.1. Introduction

Intercomparisons support mutual recognition agreements between members of the European Community. Regarding ongoing comparisons involving DIG-AC project topic, AC-DC voltage transfer at 3 V, 10 Hz to 1 MHz, 500 V to 1000 V, 10 Hz to 100 kHz (CCEM-K6.a/K9) has been organized under the auspices of the Consultative Committee of Electromagnetism, CCEM, with measurements expected to be completed by May 2022 [2][1]. BIPM onsite comparison covering Josephson Voltage Standards (BIP.EM-K10.a/b) has been going on for some time. Concerning future comparisons, ten laboratories have showed interest on a BIPM onsite Programmable Josephson Voltage Standard (PJVS) AC voltage comparison [1].

At the beginning of DIG-AC project, the analysis carried out between participants showed that a rather small part of AC calibrations is based on sampling and almost none on digital techniques for voltage/current scaling [2]. An intercomparison on these areas is therefore of great importance since it could support future CMCs claims. Digital techniques will allow high accuracy dissemination for complex waveforms that vary with time or have a decent amount of harmonic content. At the same time a digital traceability chain will simplify and shorten calibration procedures.

This intercomparison consists in the measurement of AC voltage and current for different frequencies, voltage/current amplitudes and single/combined waveforms.

The comparison will be carried out in accordance with the CCEM Guidelines for Planning, Organizing, Conducting and Reporting Key, Supplementary and Pilot Comparisons [3].

All participants to this comparison accept the general instructions and commit themselves to follow the procedures described in this technical report.

Once the protocol and the list of participants have been agreed, no change to the protocol or to the list of participants may be accepted without prior agreement of all the participants.

11.2. Travelling standard

11.2.1. General requirements

The quantity to be reported is the calibration error of the travelling standard when measuring current and when measuring voltage, defined as the difference between the measured quantity by the travelling standard and the quantity applied to it, and divided by the applied current/voltage. The calibration error will be expressed in µV/V and µA/A, respectively.

The current travelling standard is a digitiser Keysight 3458A working in DCV mode together with a 20 mA current shunt.

The same Keysight 3458A digitiser working in DCV mode together with a 4 V resistive voltage divider (RVD) is chosen as voltage travelling standard.

A laptop with the software to be used and connectors are also provided.

The pilot laboratory is responsible for decision about the suitability of the travelling standard for use in the comparison based on its experience and expectation (in some cases a study of the long-term stability and the transport behaviour of the standards will be necessary).

11.2.2. Description of the standard

The equipment transferred during the intercomparison is shown in Fig. 11.1. Technical details about the digitiser can be found in [4].

The range used in the digitiser is ±1 V. The maximum voltage in the digitiser is 0.8 V_{RMS}.

Fig. 11.1. *Components transferred in the intercomparison: digitiser, current shunt and RVD.*

11.2.3. Quantities to be measured

Three AC voltage and three AC current signals at three different frequencies are sampled by the combination digitiser + shunt. Signals are inputted one by one and in combination (three signals at the same time) as indicated in Fig. 11.2.

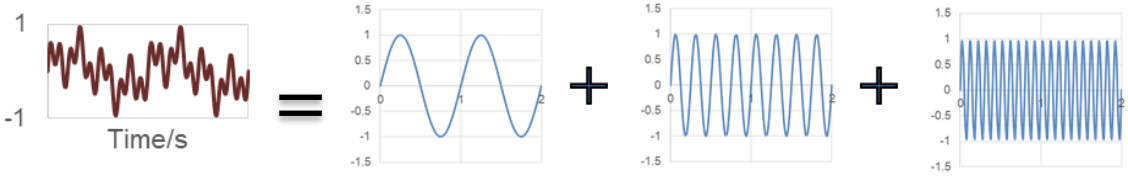

Fig. 11.2. *Signal inputs: three waves inputted at the same time and three waves inputted one by one.*

The combined waveforms are, in turn, combined in three different ways:

- Same amplitude, same phase
- Different amplitude, same phase
- Same amplitude, different phase

In total, six waveforms are inputted for current and six for voltage as is summarized in Table 11.1 and 11.2.

The participating laboratory should report a single measurement result and its uncertainty for each of the testing points represented in the second column of Table 11.1 and Table 11.2. In total, the amount of testing points is 12 values for current and 12 for voltage.

Measurements should be performed with the environmental/test conditions as follow:

- Voltage: 230 V
- Frequency: 50 Hz ± 0.05 Hz
- Temperature: (23 ± 1) °C
- Humidity: 30% rh to 60% rh

Table 11.1. *Parameters of the current source.*

Input #	Testing point	Current source		
		Current RMS/mA	**Frequency/Hz**	**Phase/°**
1	**1.1**	11.00	100	-
2	**2.1**	11.00	400	-
3	**3.1**	11.00	1000	-
4	**4.1**	3.70	100	α
	4.2	3.70	400	α
	4.3	3.70	1000	α
5	**5.1**	5.55	100	α
	5.2	3.70	400	α
	5.3	1.85	1000	α
6	**6.1**	3.70	100	α
	6.2	3.70	400	α + 45
	6.3	3.70	1000	α + 90

Table 11.2. *Parameters of the voltage source.*

Input #	Testing point	Voltage source		
		Voltage RMS/V	**Frequency/Hz**	**Phase/°**
1	**1.1**	4.000	100	-
2	**2.1**	4.000	400	-
3	**3.1**	4.000	1000	-
4	**4.1**	1.330	100	α
	4.2	1.330	400	α
	4.3	1.330	1000	α
5	**5.1**	1.995	100	α
	5.2	1.330	400	α
	5.3	0.665	1000	α
6	**6.1**	1.330	100	α
	6.2	1.330	400	α + 45
	6.3	1.330	1000	α + 90

11.2.4. Method of computation of the reference value

The reference value will be set by the pilot laboratory.

11.3. Organisation

11.3.1. Co-ordinator

The co-ordinator and pilot laboratory have to be defined.

11.3.2. Participants

Participants should express their interest and could be NMI or DI.

11.3.3. Time schedule

Participants have 3 weeks for conducting measurements and one week for sending the travelling standard to the next laboratory.

In the case of unexpected delays, the coordinator of the comparison and the next participant should be notified by fax or by e-mail.

11.3.4. Transportation

The aim for the time between shipment and reception is one week. Both, standard shipment (road) and expedited transport (plane) are allowed.

11.3.5. Unpacking, handling, packing

The travelling standard will be transported in a container, which is designed for safe transportation of the standard. Upon arrival, participants will check the container for external damage, take photos if possible and make sure that all parts are present according to the list.

Opening the corpus of the standards is strictly prohibited.

After the measurements travelling standards will be carefully packed back into the container, in which it arrived. Linear dimensions of container are approximately: 800 mm x 600 mm x 200 mm. The shipping weight is approximately 20 kg.

If damage on the container is detected, the travelling standard will be packed in a new container, which will provide the necessary protection during transportation.

11.3.6. Failure of the travelling standard

If any defects are found in the travelling standard, the participating laboratory will inform the pilot laboratory immediately. If repair of the travelling standard is needed, the participant will send a travelling standard to the pilot laboratory.

11.3.7. Financial aspects, insurance

Each participant is responsible for paying the cost for measurements. Each participant is also responsible for arranging shipment to the next participant on his own responsibility and cost, including customs formalities.

11.4. Measurement instructions

11.4.1. Test before measurements

Before performing measurements, it is necessary to understand the working principles of travelling standards. Digitiser manual can be found online [4].

Participants will check the standard for external damage, will connect it to mains and will verify that no errors are displayed. If an error appears, it should be easily corrected. If this is not the case the participant will act as indicated in 11.11.3.6.

There are no performance tests on the reference standard to be performed before measurements at the participant’s laboratory.

11.4.2. Measurement performance

The standard should be kept at test conditions temperature at least 24 h after arrival. Warm up time is at least 4 h.

Components will be connected through provided coaxial cables.

11.4.3. Method of measurement

The measurement method is that used by the participating laboratory for the provision of a digital calibration.

Make sure that testing voltage and current are within at least 0.2 % of the values shown in Table 11.1 and Table 11.2.

At every testing point shown in Table 11.1 and Table 11.2, make as many independent measurements as stated on the calibration procedures of your laboratory.

Record the data from travelling standard using the software provided in the provided laptop. Calculate current/voltage from recording data with algorithm included in laptop.

Calculate the calibration error of the travelling standard for current/voltage at the testing points shown in Table 11.1 and Table 11.2. The calibration error is defined as the difference between the measured quantity calculated by the reference standard and the quantity applied to it and divided by the applied quantity. The calibration error should be expressed in μA/A or μV/V. The error is positive if the reference standard's indication is more positive than the applied quantity.

The total estimated expanded uncertainty quoted in the laboratory's report should encompass the Type A and Type B uncertainties of the corresponding NMI calibration service. The expanded uncertainty should be estimated for a level of confidence of 95.45 %.

Report the mean value and spread of the ambient temperature and relative humidity of the laboratory.

11.5. Uncertainty of measurement

11.5.1. Main uncertainty components, including sources and typical values

Participant laboratories are requested to report the main uncertainty components of their measurement systems, identifying all the pertinent uncertainty sources and quantifying their contribution to the expanded uncertainty.

As a guide, uncertainty components can be calculated from DIG-AC Task 3.3 "Report on Uncertainty Estimation for Digital Measurements of Voltage Waveforms".

11.5.2. Scheme to report the uncertainty budget

Measurement uncertainty is calculated according to the JCGM 100:2008 (Evaluation of measurement data - Guide to the expression of uncertainty in measurement) [5].

All influencing quantities, their distributions, estimated values, standard uncertainties, degrees of freedom, sensitivity coefficients and components of uncertainty should be given in the uncertainty budget according to the Guide for the Expression of Uncertainty in Measurement [5].

Participant laboratories are requested to report the main uncertainty components of their measurement systems, identifying all the pertinent uncertainty sources and quantifying their contribution to the expanded uncertainty.

11.6. Measurement report

Each participating laboratory will submit a report with measurements results to the pilot laboratory within six weeks after the completion of the measurements. The report should be sent to the pilot laboratory by e-mail.

11.7. Report of the comparison

Pilot laboratory will prepare draft A report and will send it to the participating laboratories for comments.

Participating institutes will send back their comments to the pilot laboratory within 6 weeks.

After that, pilot laboratory will prepare the final report.

The participating laboratory will be informed if the significant difference between its results of measurements and preliminary reference value is found.

11.8. References

[1] Consultative Committee for Electricity and Magnetism (CCEM), Report of the 32nd meeting (14-15 April 2021) to the International Committee for Weights and Measures

[2] 17RPT03 DIG-AC, Digital techniques for quantum-traceable AC scaling, A. Sosso, Activity A2.1.4, February 2022

[3] CCEM Guidelines for Planning, Organizing, Conducting and Reporting Key, Supplementary and Pilot Comparisons, Version 2.1 (June 2017)

[4] Keysight 3458A Multimeter, Quick Reference Guide, August 2017, https://www.keysight.com/es/en/assets/9018-14517/quick-start-guides/9018-14517.pdf

[5] Guide to the Expression of Uncertainty in Measurement, 1999. International Organization of Standards, Geneva, Switzerland. ISO ENV 13005:1999.

12. CONCLUSION AND FUTURE COLLABORATION AMONG EUROPEAN NMIs AND DIs

This Good Practice Guide is the result of activities carried out within EMPIR JRP 17RPT03 DIG-AC “A digital traceability chain for AC voltage and current” project aimed at developing new digital traceability chains for AC voltage and current metrology in Europe by making cutting-edge knowledge accessible to all EURAMET National Metrology Institutes (NMIs) and establishing a basis for future cooperation. It gives the guidelines in the establishment of such chain for dynamic electrical measurements, having the quantum standard for alternating voltage based on the Josephson effect (PJVS or JAWS) as the reference, and the digitizer as the core measuring instrument. This also includes scaling of AC voltages and AC currents, as even wider range, and field of applications, together with the software for measurement and uncertainty calculations.

With the knowledge acquired in the project, each NMI partner developed an individual strategy covering at least the next five years, which covers the development of either individual or collaborative quantum standards (or an agreement to the future use of other NMI standards), scaling procedures and transfer standards, research collaborations, quality schemes and accreditation. All the individual strategies were revised to ensure a coordinated development of the European research and measurement infrastructure from the early beginning.

Several points are in common in these strategies, and the fields of interest for possible research and collaboration in the future are as follows:

- Characterization of analog-to-digital converters
- Direct traceability to the future SI definition for digital voltage and current metrology
- Progressively replacement of the thermal converters as AC standards
- Traceability of current shunts and voltage dividers, amplitude and phase
- Underpinning of new power and energy traceability using a digital measurement chain based on quantum standards
- Digital impedance bridges
- Wider frequency ranges of Josephson impedance bridges
- Characterization of components for use in quantum computing, in-situ at low temperature

In Section 11 is described the “Protocol for a future intercomparison of digital ac voltage and current standards between European National Metrology Institutes (NMIs)”. Such a planned intercomparison brings many advantages. It ensures a future collaboration / guest working in this specific area, and besides partners of the project other EURAMET NMIs/DIs will be informed for possible involvement. The comparison protocol will also include detailed uncertainty calculations for the establishment of appropriate quality schemes and accreditation.

Finally, a successful proof-of-principle study has already been carried out within the frame of this project (a publication is in preparation). Furthermore, the standards for such an intercomparison are widespread, they are available in most NMIs and they can easily be replaced if better ones are on disposal.